UNIVERSITY OF NOVA GORICA
GRADUATE SCHOOL

PERSISTENCE, DEGRADATION AND TOXICITY OF TRANSFORMATION PRODUCTS OF SELECTED INSECTICIDES

DISSERTATION

Romina Žabar

Mentor: prof. dr. Polonca Trebše

Nova Gorica, 2012

TABLE OF CONTENTS

ABSTRACT

This work describes for the first time the stability of three different insecticides' transformation products - 2-isopropyl-6-methyl-4-pyrimidinol (IMP), 3,5,6-trichloro-2-pyridinol (TCP) and 6-chloronicotinic acid (6CNA) in aqueous solutions. Stability studies were assessed by exposing aqueous samples to different temperatures, different pH (4, 7, and 10), presence or absence of sunlight within 90 days and the results showed that TCP is a photolabile compound while IMP and 6CNA are stable compounds.

The toxicity study with luminescent bacteria *Vibrio fischeri* indicated that IMP and 6CNA do not act like toxic chemicals; however the TCP can be classified as harmful to aquatic organisms within 30 min EC_{50} of 15.1 mg L^{-1}.

Photolytic experiments were performed with three polychromatic fluorescent lamps with broad maximum at 355 nm and with a low-pressure mercury monochromatic germicidal lamp at 254 nm. Finally, the photolytic experiments under simulated sunlight conditions using SUNTEST apparatus were assessed. All experiments resulted in the relatively high stability of 6CNA under all conditions, while IMP showed little degradation under polychromatic fluorescent lamps. Alternatively, TCP again showed to be a photolabile compound which underwent transformation into other compounds which were further identified with GC-MS and LC-MS. However, the toxicity experiments revealed significant luminescence inhibition for *V. fischeri* after photolytic degradation of TCP, probably due to the formation of more toxic by-products.

Photocatalytic experiments were performed using immobilised titanium dioxide (TiO_2) on six glass slides in the spinning basket inside a photocatalytic quartz cell under similar irradiation conditions as photolytic experiments. Results indicated a high disappearance rate for all three transformation products as well as high mineralization. The formation of chloride and nitrate ions was observed as well as the formation of by-products with GC-MS, LC-MS and even with ^1H NMR. The luminescence inhibition for *V. fischeri* revealed an increase of toxicity within 120 minutes of photocatalysis and again this can be probably attributed to the formation of more toxic by-products.

Furthermore, the toxicity toward non-target terrestrial isopods *Porcellio scaber* was assessed through food experiments. After two weeks of exposure to contaminated food, endpoints for example, mortality, weight change, assimilation efficiency, consumption rate and defecation, were investigated and compared with the control group. Lipid

peroxidation, a biomarker of effect for oxidative stress was assessed via TBA-MDA reaction.

POVZETEK

Moje delo prvič opisuje stabilnost treh različnih razgradnih produktov insekticidov - 2-izopropil-6-metil-4-pirimidinola (IMP), 3,5,6-trikloro-2-piridinola (TCP) in 6-kloronikotinske kisline (6CNA) v vodnih raztopinah. Stabilnostne študije so bile izvedene tako, da sem vodne vzorce v 90-ih dneh izpostavila različnim temperaturam, različnim pH (4, 7, 10) in sončni svetlobi. Rezultati so pokazali, da je TCP dokaj fotolabilna spojina, medtem ko sta IMP in 6CNA v vodni raztopini stabilni spojini.

Študije strupenosti z luminiscenčnimi bakterijami *Vibrio fischeri* so pokazale, da IMP in 6CNA nista strupeni, TCP pa lahko opredelim kot škodljivo za vodne organizme, saj je bila izračunana vrednost EC_{50} pri 30 min izpostavitvi 15,1 mg L^{-1}.

Fotolizni poskusi so bili izvedeni s tremi polikromatskimi fluorescenčnimi sijalkami s širokim spektrom in maksimumom pri 355 nm ter z nizkotlačno živosrebrno germicidno monokromatsko sijalko pri 254 nm. Študirala sem tudi obnašanje izbranih spojin pri simulirani sončni svetlobi z uporabo SUNTEST aparata. Vsi eksperimenti so pokazali razmeroma visoko stabilnost 6CNA, medtem ko je bila opažena majhna stopnja razgradnje IMP pri uporabi polikromatskih fluorescenčnih sijalk. Po drugi strani pa so nekateri poskusi zopet pokazali na dejstvo, da je TCP fotolabilna spojina, pri čemer pride do pretvorbe v druge produkte, ki sem jih uspešno karakterizirala z uporabo GC-MS in LC-MS. Strupenostne študije z *V. fischeri* so pokazale visoko inhibicijo luminiscence med razgradnjo vodne raztopine TCP, verjetno zaradi tvorbe bolj strupenih razgradnih produktov tekom reakcije.

Fotokatalitski eksperimenti so bili izvedeni z uporabo imobiliziranega titanovega dioksida (TiO_2) na šestih steklenih nosilcih, vpetih v posebno košarico znotraj celice. Rezultati so pokazali visoko stopnjo razgradnje za vse tri produkte kot tudi zadovoljivo stopnjo mineralizacije. Med poskusi sem z uporabo ionske kromatografije zaznala nastajanje kloridnih in nitratnih ionov. Z uporabo GC-MS, LC-MS in ^{1}H NMR pa sem identificirala novonastale stranske produkte. Inhibicija luminiscence za *V. fischeri* je pokazala na povečanje strupenosti po uporabi katalizatorja, verjetno zopet zaradi tvorbe bolj strupenih razgradnih produktov tekom fotokatalitske razgradnje.

Ocenila sem tudi strupenost razgradnih produktov na neciljne enakonožne kopenske rake *Porcellio scaber*. V dveh tednih izpostavljenosti kontaminirani hrani sem spremljala umrljivost, maso živali, listov in iztrebkov, nato pa izračunala asimilacijsko učinkovitost, stopnjo potrošnje in iztrebljanje. Lipidno peroksidacijo kot biomarkerja

učinka za oksidativni stres pa sem ocenila z uporabo tiobarbiturne kisline, ki reagira z malondialdehidom kot produktom oksidacije lipidov.

Ključne besede: razgradni produkti, stabilnost, fotokataliza, strupenost, *Porcellio scaber*

LIST OF TABLES

LIST OF FIGURES

10 for 50 µg/g; N = 8 for 100 µg/g). Red longer lines indicate median values.

Figure 72: Lipid peroxidation in hepatopancreas of adult *P. scaber* after two weeks of exposure to uncontaminated food (C) and leaves contaminated with 1, 10, 50 and 100 µg IMP/g dry food (N = 10 for C; N = 10 for 1 µg/g; N = 10 for 10 µg/g; N = 10 for 50 µg/g; N = 8 for 100 µg/g). Red longer lines indicate median values.

Figure 73: Mortality of adult *P. scaber* during two weeks of exposure to uncontaminated food (C) and leaves contaminated with 1, 10, 50 and 100 µg TCP/g dry food (N = 12 for each group).

Figure 74: Body weight change (in mg fresh weight) of adult *P. scaber* after two weeks of exposure to uncontaminated food (C) and leaves contaminated with 1, 10, 50 and 100 µg TCP/g dry food (N = 10 for C; N = 11 for 1 µg/g; N = 11 for 10 µg/g; N = 8 for 50 µg/g; N = 11 for 100 µg/g). Red longer lines indicate median values.

Figure 75: Faecal pellets production (in mg dry weight/mg fresh body weight/day) of adult *P. scaber* after two weeks of exposure to uncontaminated food (C) and leaves contaminated with 1, 10, 50 and 100 µg TCP/g dry food (N = 10 for C; N = 11 for 1 µg/g; N = 11 for 10 µg/g; N = 8 for 50 µg/g; N = 11 for 100 µg/g). Red longer lines indicate median values and the asterisk indicates significant difference in relation to control according to Mann-Whitney statistics.

Figure 76: Consumption rate (in mg food consumed/mg fresh body weight/day) of adult *P. scaber* after two weeks of exposure to uncontaminated food (C) and leaves contaminated with 1, 10, 50 and 100 µg TCP/g dry food (N = 10 for C; N = 11 for 1 µg/g; N = 11 for 10 µg/g; N = 8 for 50 µg/g; N = 11 for 100 µg/g). Red longer lines indicate median values.

Figure 77: Assimilation efficiency of adult *P. scaber* after two weeks of exposure to uncontaminated food (C) and leaves contaminated with 1, 10, 50 and 100 µg TCP/g dry food (N = 10 for C; N = 11 for 1 µg/g; N = 11 for 10 µg/g; N = 8 for 50 µg/g; N = 11 for 100 µg/g). Red longer lines indicate median values and the asterisk indicates significant difference in relation to control according to Mann-Whitney statistics.

Figure 78: Lipid peroxidation in hepatopancreas of adult *P. scaber* after two weeks of exposure to uncontaminated food (C) and leaves contaminated with 1, 10, 50 and 100 µg TCP/g dry food (N = 10 for C; N = 11 for 1 µg/g; N = 10 for 10 µg/g; N = 8 for 50 µg/g; N = 11 for 100 µg/g). Red longer lines indicate median values and the asterisk indicates significant difference in relation to control according to Mann-Whitney statistics.

Figure 79: Mortality of adult *P. scaber* during two weeks of exposure to uncontaminated food (C) and leaves contaminated with 1, 10, 50 and 100 µg 6CNA/g dry food (N = 12 for each group).

Figure 80: Body weight change (in mg fresh weight) of adult *P. scaber* after two weeks of exposure to uncontaminated food (C) and leaves contaminated with 1, 10, 50 and 100 µg 6CNA/g dry food (N = 11 for C; N = 10 for 1 µg/g; N = 9 for 10 µg/g; N = 11 for 50 µg/g; N = 10 for 100 µg/g). Red longer lines indicate median values.

ABBREVIATIONS AND SYMBOLS

6CNA	6-chloronicotinic acid
AChE	acetylcholinesterase
AE	assimilation efficiency
amu	atomic mass unit
AOPs	advanced oxidation processes
APCI	atmospheric pressure chemical ionization
CI	chemical ionization
COD	chemical oxygen demand
CR	consumption rate
DNA	deoxyribonucleic acid
DOM	dissolved organic matter
EC	European Commission
EC_{50}	median effect concentration
EFSA	European Food Safety Authority
EI	electro ionization
EID	electro ionization detector
ELISA	enzyme-linked immunosorbent assay
ESI	electro spray ionization
EU	European Union
FAO	Food and Agriculture Organization of the United Nations
FID	flame ionization detector
FPIA	fluorescence polarization immunoassay
FPP	faecal pellets production
GST	glutathione S-transferaze
GC-MS	gas chromatography coupled with mass spectrometry
^{1}H NMR	proton nuclear magnetic resonance
HPLC-DAD (UV-Vis)	high pressure liquid chromatography coupled with diode array detector operating in the range from ultraviolet to visible light
IMP	2-isopropyl-6-methyl-4-pyrimidinol
LC-MS	liquid chromatography coupled with mass spectrometry
LP	lipid peroxidation
MDA	malondialdehyde
MRLs	maximum residue limits
MSDS	material safety data sheet

MTBSTFA	N-($tert$-buthyldimethylsilyl)-N-methyltrifluoroacetamide
M_W	molecular weight
nAChR	nicotinic acetylcholine receptor
NOEC	non-observed effect concentration
OCs	organochlorine pesticides
$\cdot$OH	hydroxyl radical
OPs	organophosphorus pesticides
PIF	photochemically induced fluorescence
POPs	persistent organic pollutants
P_{OW}	partition coefficient octanol-water
PPPs	plant protective products
ROS	reactive oxygen species
SD	standard deviation
SIM	selected ion monitoring
SPE	solid phase extraction
TBA	thiobarbituric acid
TCP	3,5,6-trichloro-2-pyridinol
TIC	total ion chromatogram
TLC	thin layer chromatography
TN	total nitrogen
TOC	total organic carbon
TPs	transformation products
UV	ultraviolet
UV-A	ultraviolet A
UV-B	ultraviolet B
UV-C	ultraviolet C
WC	weight change
wt	weight

1   INTRODUCTION

Synthetic pesticides have been used for more than six decades and their consumption increases constantly worldwide. In the past, several different types of pesticides were synthesised and put into application; from organochlorine insecticides at the beginning, to organophosphorus type of pesticides. Over the past 15 years neonicotinoids have gained increasing interest in the agricultural sector across Europe (European Union Council Directive 91/414/EEC and European Commission Directive EC 1107/2009). Pesticides present one of the greatest problems, as the world population is expected to continue increasing during the 21st century, the requirement for a continued increase in agricultural productivity will also be an unavoidable necessity. Associated with this is a proportionally, or even greater increase, in the production and consumption of agrochemical products and pesticides (Fernandez-Alba *et al.*, 2002).

Previously, the legislation concerning food safety, for example, vegetables and fruits, focused only on the monitoring of parent insecticides, however recently, the European Commission has focused on this problem with regulation EC 1107/2009 (European Commission Directive EC 1107/2009). However, the most important and critical concern is the fact, that little attention and almost no control is paid to the presence of metabolites or transformation products (TPs) which can be formed after applications within the environment and later during processing. There is a quantity of literature available regarding pesticides, but on the other hand, not many studies have been conducted on metabolites and degradation products with regard to their properties, degradation, bioaccumulation and toxicity.

My research focused on three different TPs from two different groups of insecticides. From the group of organophosphorus pesticides two TP were chosen; **2-isopropyl-6-methyl-4-pyrimidinol** (IMP) - the TP of diazinon and **3,5,6-trichloro-2-pyridinol** (TCP) - the TP of chlorpyrifos. From the group of neonicotinoid insecticides, **6-chloronicotinic acid** (6CNA) has been chosen - the common TP of acetamiprid and imidacloprid.

Stability of selected TPs under different conditions was tested and compared. The role of several parameters was investigated, such as temperature, natural sunlight and simulated sunlight. Moreover, varieties of simulated light sources were used, i.e. simulated sunlight using Suntest apparatus, monochromatic low-pressure mercury germicidal lamps (25 nm) and polychromatic low-pressure mercury lamps (355 nm).

As every year more and more xenobiotics are released into the environment, a pathway for their efficient degradation or removal should be implemented. Since many of them still exhibit high stability toward different environmental conditions, many new techniques for their removal were introduced. A promising method for decreasing pesticides' concentration, or even complete removal from the environment, is the application of the advanced oxidation processes (AOPs). Lately, photocatalytic degradation with application of TiO_2 has shown to be of great importance, where the production of highly reactive oxygen species – mainly the hydroxyl radicals has taken place. It is well known, that the hydroxyl radical, after fluorine, is the most powerful oxidant (Litter, 2005) and therefore, can attack virtually all organic compounds and consequently mineralize them into CO_2 and H_2O.

Extended studies showed that the identification of possible intermediates, toxicity measurements and risk assessment is more than required, since more toxic substances than the parent ones could be formed during the photocatalytic treatment. Therefore, several analytical methods, as well as toxicity tests, were applied to assess the efficiency of AOPs.

Moreover, the paucity of literature regarding properties, degradation and bioaccumulation of pesticides transformation products (TPs) generated the interest to also measure the toxicity of selected TPs. Since they can act completely differently in comparison to their parent compounds, several toxicological tests should be implemented. Two different species which proved to be sensitive enough to the presence of pesticides were selected for TPs toxicity testing. As shown from the literature, the simplest is the toxicity test with aquatic luminescent bacteria *Vibrio fischeri*. Since pesticides are mostly applied in the terrestrial environment additional attention is paid to terrestrial organisms as crucial indicator for risk assessment. Therefore, the terrestrial isopod *Porcellio scaber* was selected for toxicity measurements of selected TPs through feeding exposure experiments. Finally, the effect on *P. scaber* hepatopancreatic cells via lipid peroxidation as an oxidative stress parameter was assessed.

2   THEORETICAL BACKGROUNDS

2.1   Pesticides – general overview

As the Food and Agriculture Organization of the United Nations (FAO) defined, pesticide is any substance or mixture of substances intended for preventing, destroying, repelling or mitigating any pest, including vectors of human or animal disease, unwanted species of plants or animals causing harm during or otherwise interfering with the production, processing, storage, transport or marketing of food, agricultural commodities, wood and wood products or animal feedstuffs, or substances which may be administered to animals for the control of insects, arachnids or other pests in or on their bodies. A pesticide may be a chemical substance, biological agent (such as a virus or bacteria), antimicrobial, disinfectant or device used against any pest (Saravi and Shokrzadeh, 2011). Basically, agricultural pesticides are divided into five categories, depending on the target pest: insecticides, herbicides, fungicides, rodenticides, and fumigants (Saravi and Shokrzadeh, 2011).

Recently, the European Food Safety Authority (EFSA) tried to replace the expression "pesticide" due to its negative connotation, with the new the term - "plant protective product - PPP".

For more than six decades synthetic pesticides or PPPs have been used and their consumption increases constantly worldwide. In the past, several different types of insecticides were synthesized and put into application; starting with organochlorine insecticides at the beginning of the last century, through organophosphorus pesticides after the Second World War. However, over the past twenty five years, neonicotinoids have gained increasing interest in the agricultural sector.

Organochlorine pesticides (OCs) are chlorinated hydrocarbons used extensively from the 1940s through the 1960s in agriculture and in mosquito control. Representative compounds in this group include DDT, aldrin, dieldrin and lindane. It is generally known, that organochlorine pesticides accumulate in the environment (Meleiro Porto *et al.*, 2011). Prior to the mid-1970s, organochlorines resulted in widespread reproductive failure among birds because birds laid eggs with thin shells that cracked before hatching (Meleiro Porto *et al.,* 2011).

Organophosphorus compounds (OPs) are a massive and highly diverse family of organic chemicals. Representative compounds in this group include the most known compounds such as; malathion, chlorpyrifos, diazinon, and methyl-parathion. The term, organophosphorus insecticides, means all insecticides that have the phosphorus atom in their structure. The toxicity of OP pesticides plays a key role in their market registration worldwide. It is well known, that toxic effect of OPs can be attributed primarily to their ability to inhibit acetylcholinesterase (AChE), an enzyme vital for normal nerve function (Chambers and Levi, Eds., 1992).

Neonicotinoids are a group of insecticides derived from nicotine. Nicotine, isolated from the tobacco plant, possesses insecticidal activity and has been used extensively as commercial insecticide. Their physicochemical properties render them useful for a wide range of application techniques, including foliar, seed treatment, soil drench, and stem application (Millar and Denholm, 2007). They are generally low toxic to mammals, birds, and fish (Tomizawa and Casida, 2005). Neonicotinoid insecticides are strong selective agonists of insect nicotinic acetylcholine receptors (nAChRs) so they exhibit specific activity against the insect nervous system. This unique mode of action makes these pesticides highly applicable for controlling the biological effect of insects in cases when these developed resistance to organophosphate, carbamate and pyrethroid insecticides (Jeschke *et al*., 2001). Imidacloprid, the representative of the first generation neonicotinoid insecticides, was patented in 1985 by Bayer and was placed on the market in 1991. Today it has been made commercially available by Bayer AG and Nihon Tokushu Noyaku Seizo KK. Imidacloprid demonstrates selective toxicity for insects over vertebrates (Matsuda *et al*., 2001) and it is the highest selling insecticide worldwide used to control insects on crops or for seed treatment as well as veterinary medicine against parasites in dogs and cats. Other important neonicotinoids are acetamiprid, clothianidin, dinotefuran, thiacloprid and thiamethoxam.

2.1.1 Legislation and use of pesticides in European Union

In the European Union, the pesticides market (approval, label instructions and their application) has been regulated by the European Union Council Directive 91/414/EEC since 1992. Lately, this directive has been replaced by European Commission Directive EC 1107/2009.

The use of OCs is completely banned by the European Union Council Directive 79/117/EEC. Furthermore, according to the European Union regulation EC 850/2004 which implements the Persistent Organic Pollutants (POPs) or Stockholm Convention in Europe, some of OCs are also banned for export.

On the other hand, on the basis of the European Commission Implementing Regulation EU 540/2011, some OPs are banned in EU while others are still in use. To conclude, chlorpyrifos and malathion, for example, are still allowed while diazinon is banned.

The use of neonicotinoids i.e. imidacloprid, acetamiprid, thiacloprid, thiamethoxam and clothianidin have been approved in the EU and they are currently in use.

2.1.2 Legislation and use of pesticides in Slovenia

In Slovenia, as part of the European Union, the OCs are also not registered anymore and consequently not in use.

The OPs, such as diazinon and malathion, are banned as plant protective products, while on the other hand, chlorpyrifos and chlorpyrifos-methyl are in use and they will continue in use till 2014 and 2017, respectively (Phytosanitary Administration, Republic of Slovenia; FITO-INFO browser, November 2011). It was estimated that in the year 2004 approximately 14,700 kg of diazinon and 2,100 kg of chlorpyrifos was sold in Slovenia (Phytosanitary Administration of the Republic of Slovenia, personal communication, 2005).

Neonicotinoids, i.e. imidacloprid, thiamethoxam, acetamiprid and thiacloprid are registered on the Slovenian market. However, since May 2008, the insecticides thiamethoxam, clothianidin and imidacloprid were banned for treatment of corn seeds (*Zea mays*), oilseed rape seeds (*Brassica napus*) and sugar beet seeds (*Beta vulgaris*) (The Official Gazette of the Republic of Slovenia No. 50/2008). Moreover, in August 2008, the Phytosanitary Administration of Republic of Slovenia withdrew the restriction for oilseed rape seeds (*Brassica napus*) for treatment with imidacloprid, thiamethoxam and clothianidin (The Official Gazette of the Republic of Slovenia No. 80/2008). Despite all the precautions taken in order to avoid the poisoning of bees, a large number of bees' colonies died in the eastern part of Slovenia during April 2011 (Pomor čebel v Pomurju dobiva nove razseznosti, 2011). Due to these repetitive events, the Phytosanitary Administration of Slovenia completely banned clothianidin, imidacloprid and thiamethoxam for any seed treatment. Therefore, clothianidin is now

completely banned in Slovenia for any use (The Official Gazette of the Republic of Slovenia No. 31/2011). It was estimated that in Slovenia approximately 2,400 kg of neonicotinoids was sold in the year 2004 (Phytosanitary Administration of the Republic of Slovenia, personal communication, 2005).

2.2 Pesticides' transformation products - general overview

A quantity of literature is available on OCs and OPs pesticides regarding their stability, fate and behaviour in different matrices (Burrows *et al.*, 2002; Meallier, 1999) such as water, soil and food. On the other hand, there is relatively little data available on neonicotinoids. Nowadays, the pesticides are widely applied and their consumption and variety constantly increases. Moreover, these pesticides can be transformed in the environment, crops, animals and finally humans, into large numbers of different products, called transformation products (TPs). It is widely known that TPs may have different properties which enable them to occur in the environmental areas which cannot be reached by a pesticide itself. Due to their higher polarity and mobility in the soil-water environment, TPs may reach groundwater more easily than the parent compound (Hernández *et al.*, 2008a). Furthermore, TPs can be more toxic (Bavcon Kralj *et al.*, 2007a) and more persistent than the parent compound (Kolpin *et al.*, 2009). Moreover, the legislator, in our case the European Union, recognised this concern and the necessity to implement TPs in legislation concerning pesticides and, therefore, the maximum residue limits (MRLs) have been established for several TPs, i.e. for the malathion transformation product - malaoxon.

In order to track the TPs in the environment and in different matrices, sensitive techniques for their monitoring should be developed. In the literature, the most widely applied method is the mass spectrometry technique, coupled with GC or LC, due to its intrinsic characteristics, such as selectivity, sensitivity and identification-confirmation capability. Depending on the TPs volatility and polarity, the gas chromatography coupled with mass spectrometry (GC-MS) or liquid chromatography coupled with mass spectrometry (LC-MS) is further selected (Martínez Vidal *et al.*, 2009; Hernández *et al.*, 2008b; del Mar Gómez-Ramos *et al.*, 2011). Despite all the advantages, that the mass spectrometry techniques provide, the differentiation between the isomers cannot be performed. In these specific, but not so rare cases, their identification with nuclear magnetic resonance (NMR) plays an important role (Topalov *et al.*, 2001).

My research focused on three different TPs from two different groups of insecticides. From the group of organophosphorus pesticides two TP were chosen; 2-isopropyl-6-methyl-4-pyrimidinol (IMP) - the TP of diazinon and 3,5,6-trichloro-2-pyridinol (TCP) - the TP of chlorpyrifos. From the group of neonicotinoid insecticides 6-chloronicotinic acid (6CNA) has been chosen - the common TP of acetamiprid and imidacloprid.

2.2.1 Properties of diazinon and its transformation product - 2-isopropyl-6-methyl-4- pyrimidinol

2.2.1.1 Properties of diazinon

Diazinon (*O,O*-diethyl *O*-[2-isopropyl-4-methyl-6-pyrimidinyl]phosphorotioate) with CAS number 33-41-5 and M_w 304.4 g mol^{-1} is an organophosphorus insecticide, which belongs to the group of phosporothioates. It is a colourless to dark brown liquid with water solubility of 40 mg L^{-1} and the log P_{0W} of 3.3 (Diazinon MSDS Sigma-Aldrich; Milne, 2004). Diazinon is a non systemic organophosphate insecticide used to control a wide range of sucking and chewing insects and mites in a very wide range of crops and is also used as a veterinary ectoparasiticide. Diazinon, shown in Figure 1, was commercially introduced in 1952 and nowadays it is well studied insecticide (Zhang and Pehkonen, 1999).
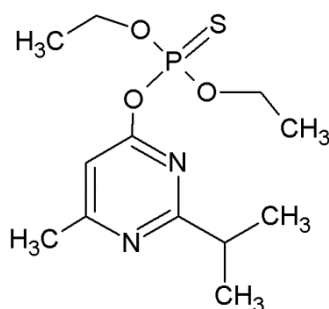
Figure 1: Chemical structure of diazinon.

A variety of toxicity studies on diazinon were conducted and many studies are available. To briefly precise, diazinon inhibits deoxyribonucleic acid (DNA) synthesis in primary cultures of rat cortical astrocytes and in human 1321N1 astrocytoma cells (Guizzetti *et al.*, 2005). Moreover, toxicity studies were performed on a non-target terrestrial organism, *Porcellio scaber,* by determining several different parameters as AChE activity, lipid and protein content, weight change, feeding activity and mortality and the results indicated negative effect of diazinon on isopods (Stanek *et al.*, 2006).

2.2.1.2 Properties of 2-isopropyl-6-methyl-4-pyrimidinol (IMP)

It has been reported in the literature (Bavcon *et al.*, 2003) that IMP (2-isopropyl-6-methyl-4-pyrimidinol), with CAS number 2814-20-2 and M_W 152.1 g mol^{-1}, is the main product of diazinon hydrolysis as well as a main photodegradation product of diazinon (Shemer and Linden, 2006; Čolović *et al.*, 2010). The chemical structure of IMP is

shown in Figure 2 (IMP MSDS, Sigma-Aldrich). Extended study on diazinon stability was performed on different matrices under environmental conditions - water, soil and chicory were treated with certain amounts of diazinon and the degradation and formation of new by-products (i.e. IMP) was monitored during the period of 21 days.
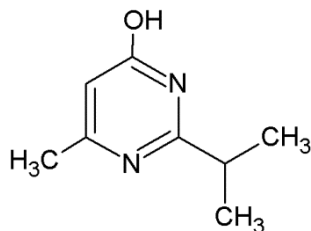
Figure 2: Chemical structure of IMP.

During the 21 days of experiment under environmental conditions 90 % of the initial amount of diazinon was degraded and about 40 % of IMP was formed. The difference between the degraded amount of diazinon and the formed IMP is a result of natural effects such as runoff, soil humidity, microbiological and photochemical degradation. The results showed the presence of IMP in water and in soil on the sunlight (Bavcon *et al.*, 2003).

The variety of analytical methods, including gas chromatography coupled with mass spectrometry (GC-MS) and high pressure liquid chromatography (HPLC) for the detection of IMP in different matrices is summarized in Table 1.

Table 1: Some of the methods for the detection of IMP in different samples.

Matrix	*Method*	*Sample treatment*	*Column*	*Mobile phase*	*Detector*	*Reference*
deionised water	LC	none	C-18 (7.5 mm x 150 mm)	15 % CH_3CN (gradient)	UV-Vis (234 nm)	Shemer and Linden, 2006
air	LC	SPE	C_6-phenly column (150 mm x 2 mm; 3 µm)	60 % 0.1 % formic acid 40 % CH_3OH	MS	Raina and Sun, 2008
rat plasma, urine	HPLC	extraction C_{18} cartridges, CH_3CN	C-18 µBondpak (3.9 mm x 300 mm; 10 µm, 125 nm)	water (pH 3.00 with CH_3COOH) CH_3CN	UV-Vis (230 nm)	Abu-Qare and Abu-Donia, 2001a
deionised water	HPLC	none	Zorbax C_8 (250 mm x 4.6 mm, 5 µm)	75 % water (pH=3.00 CH_3COOH) 15 % CH_3CN (gradient)	UV-Vis (242 nm)	Žabar *et al.*, 2011a
deionised water	UPLC	none	Acquity UPLC BEH C_{18} (50 mm x 2.1 mm; 1.7 µm)	10 % (0.1 % formic acid) 90 % CH_3CN (gradient)	UV-Vis (230 nm)	Čolović *et al.*, 2010
ditch water	GC	extraction with hexane	HP-5-MS (30 m x 0.25 mm x 0.25 µm)	He (0.7 mL min^{-1})	EID	Li *et al.*, 2002
water soil chicory	GC	extraction with ethyl acetate	non-polar SPB-1 (30 m x 0.53 mm; 3 µm)	not defined	FID	Bavcon *et al.*, 2003
sludge soils	GC	extractions, derivatization (MTBSTFA)	HP-5-MS (30m x 0.25 mm I.D., 0.25 µm)	He (1 mL min^{-1})	MS (SIM)	Díaz-Cruz and Barceló, 2006
deionised water	GC	not defined	not defined	not defined	MS	Lee *et al.*, 2003

2.2.2 Properties of chlorpyrifos and its transformation product - 3,5,6-trichloro-2-pyridinol

2.2.2.1 Properties of chlorpyrifos

Chlorpyrifos is an organophosphorus insecticide with the IUPAC name *O,O*-diethyl *O*-3,5,6-trichloro-2-pyridyl phosphorothioate, a CAS number of 2921-88-2 and with M_w of 350.6 g mol^{-1}. The chemical structure of chlorpyrifos is presented in Figure 3 (Chlorpyrifos Safety Data Sheet, Sigma-Aldrich).
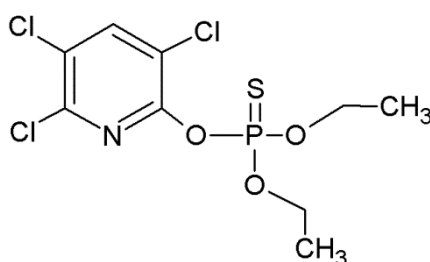
Figure 3: Chemical structure of chlorpyrifos.

Chlorpyrifos is a broad-spectrum insecticide, widely used in our environment. Its insecticidal property comes from a bioactivation to chlorpyrifos-oxon in organisms and the ability to inhibit acetylcholinesterase (AChE), an enzyme crucial for normal nerve function (Chambers and Levi, Eds., 1992). The chemical structure of chlorpyrifos-oxon is presented in Figure 4.
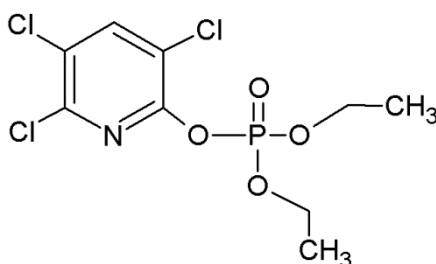
Figure 4: Chemical structure of chlorpyrifos-oxon.

The acute toxicity depends on the level of exposure to chlorpyrifos, the rate of transformation to chlorpyrifos-oxon and the ability to hydrolyze it to TCP. Chlorpyrifos-oxon is about three orders of magnitude more potent as an inhibitor of AChE as chlorpyrifos (Chambers and Levi, Eds., 1992). The acute toxicity of chlorpyrifos expressed as LD_{50} (oral, male rat) is 82-155 mg kg^{-1} (Kousba *et al.*, 2004).

2.2.2.2 Properties of 3,5,6-trichloro-2-pyridinol (TCP)

The fate of chlorpyrifos is described and major degradation products are known. The primary degradation product of chlorpyrifos and chlorpyrifos-oxon, by both hydrolysis and photolysis, is TCP (3,5,6-trichloro-2-pyridinol) (Liu *et al.*, 2001; Kale *et al.,* 1999; Duirk *et al.*, 2008) with CAS number 6515-38-4 and M_W of 198.4 g mol^{-1} (TCP MSDS, Sigma-Aldrich). The chemical structure of TCP is shown in Figure 5. The formation of TCP was confirmed by many different pathways, such as photodegradation of chlorpyrifos (Bavcon Kralj *et al.*, 2007b), via microbial degradation of chlorpyrifos (Robertson *et al.*, 1998) and via natural occurring hydrolysis of chlorpyrifos-oxon (Chambers and Levi, Eds., 1992).
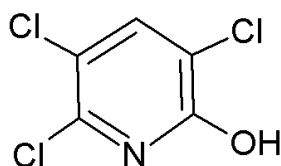
Figure 5: Chemical structure of TCP.

Studies showed that TCP was found in green golf course leachates, where chlorpyrifos was applied, in concentrations from 0.15 to 1.77 mg L^{-1} (Shemer *et al.*, 2005). A study on food was performed and TCP was found in several agriculture crops such as spinach, cauliflower and potato and the concentration was found in the range of mg kg^{-1} (Randhawa *et al.*, 2007), however derivatization with *N*-(*tert*-buthyldimethylsilyl)-*N*-methyltrifluoroacetamide (MTBSTFA) was performed. Moreover, TCP has been found also in the urine of the United States population (Barr *et al.*, 2005).

The variety of analytical methods for the detection of TCP in different matrices is summarized in Table 2.

Table 2: Some of the methods for the detection of TCP in different samples.

Matrix	Method	Sample treatment	Column	Mobile phase	Detector	Reference
deionised water	HPLC	none	Zorbax C_8 (250 mm x 4.6 mm, 5 μm)	75 % water (pH=3.00 CH_3COOH) 15 % CH_3CN (gradient)	UV-Vis (242 nm)	Žabar *et al.*, 2011a
rat plasma, urine	HPLC	extraction C_{18} cartridges, CH_3CN	C-18 μBondpak (3.9 mm x 300 mm; 10 μm, 125 nm)	water (pH 3.2 ; CH_3COOH) CH_3CN CH_3OH	UV-Vis (260 nm)	Abu-Qare and Abou-Donia, 2001b
air	LC-ESI	SPE	C_6-phenly column (150 mm x 2 mm; 3 μm)	60 % 0.1 % formic acid 40 % CH_3OH	MS	Raina and Sun, 2008
human urine	LC-ESI weak anion exchange	extraction acidic hydrolysis	Kromasil 3-thiopropyl (100 mm x 4 mm; 5 μm)	20 mM HAc in ACN/water (30:70 v/v; pH 6.45) 20 mM HAc in ACN/water (80:20 v/v; pH 7.45	MS	Bicker *et al.*, 2005
spinach cauliflower potato eggplant tomato	capillary GC	extraction ethyl acetate cyclohexane derivatization (MTBSTFA)	DB-5MS capillary column	not defined	MS	Randhawa *et al.*, 2007
sludge soils	GC	extractions, derivatization (MTBSTFA)	HP-5-MS (30m x 0.25 mm I.D., 0.25 μm)	He (1 mL min^{-1})	MS (SIM)	Díaz-Cruz and Barceló, 2006
soil fruit	ELISA	heating extraction CH_3COCH_3	/	/	ELISA plate reader	Velasco-Arjona *et al.*, 1997

2.2.3 Properties of imidacloprid, acetamiprid and their transformation product - 6-chloronicotinic acid

2.2.3.1 Properties of imidacloprid

Imidacloprid with the IUPAC name (*E*)-1-(6-chloro-3-pyridylmethyl)-*N*-nitroimidazolidin-2-ylideneamine is neonicotinoid insecticide with CAS number 138261-41-3 and M_W of 255.7 g mol^{-1}. Its chemical structure is presented in Figure 6 (Imidacloprid MSDS Sigma-Aldrich; Milne, 2004). It acts differently than other insecticides presented and it is chemically related to the nicotinic acetylcholine receptor (nAChR) antagonist nicotine and epibatidine (Roberts and Huston, 1999). The hydrolysis and photodegradation of imidacloprid in an aqueous buffer solution were investigated under laboratory conditions (Moza *et al.,* 1998). At environmentally relevant pH (4-9) in the absence of light under sterile conditions, imidacloprid is stable in water (Krohn and Hellpointner, 2002). Imidacloprid expresses contact and ingestion activity. The target pest's feeding activity ceases within minutes to hours and death occurs within 24 to 48 hours (Roberts and Huston, 1999).
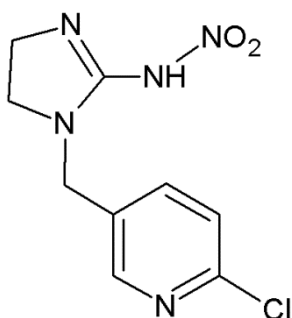
Figure 6: Chemical structure of imidacloprid.

Acute toxicity of imidacloprid was tested on several organisms. For *Daphnia magna*, the EC_{50} values within 48 h ranged from 10 to 85 mg L^{-1} (Jemec *et al.*, 2007b). Another study tested the potential hazards of imidacloprid and its commercial product Confidor SL 200 to aquatic environment were identified by the acute and chronic toxicity assessment using bacteria *Vibrio fischeri*, algae *Desmodesmus subspicatus*, crustacean *D. magna*, fish *Danio rerio* and the ready biodegradability determination. Among the organisms tested, water flea *D.magna* proved to be the most sensitive species after a short-term (48 h EC_{50} = 56.6 mg L^{-1}) and long term exposure (21 d NOEC = 1.25 mg L^{-1}) (Tišler *et al.,* 2009). Toxicity of imidacloprid was also tested to the terrestrial isopods *Porcellio scaber* with observing the decrease in GST (glutathione S-transferase) activity at concentrations of 25 μg of imidacloprid/g of dry food (Drobne *et al.*, 2008). It has

also been reported, that imidacloprid can bind to human serum albumin (Mikhailopulo *et al.,* 2008).

2.2.3.2 Properties of acetamiprid

Acetamiprid with the IUPAC name (*E*)-N^1-[(6-chloro-3-pyridyl)methyl]-N^2-cyano-N^1-methylacetamidine, CAS number 135410-20-7 and M_W of 222.7 g mol^{-1} is a systemic and contact insecticide. Acetamiprid also belongs to the chloronicotine class and has a broad insecticidal spectrum. Its chemical structure is shown in Figure 7 (Acetamiprid MSDS Sigma-Aldrich).
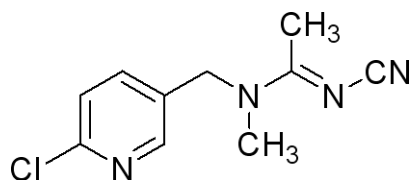
Figure 7: Chemical structure of acetamiprid.

Acetamiprid shows excellent efficacy against aphids, leafhoppers, whiteflies, thrips, leaf beetles, leafminer moth, termites, etc. in various crops. It has been reported, that acetamiprid can be toxic to honey bees *Apis mellifera*, and the observed LD$_{50}$ value was 7.1 μg bee^{-1} (Iwasa *et al.,* 2004). A similar study was performed on bees' behavioural response and the study showed adverse effects after acetamiprid treatment (El Hassani *et al.,* 2008). However, the authors did not confirm whether the effects were due to acetamiprid or 6CNA which were both present in the head of bees at significant levels over a 72-h observation period. Little work has been done on acetamiprid, the photocatalytic degradation with TiO$_2$ has been described (Khan *et al.*, 2010; Guzsvány *et al.*, 2009) and photolytic stability in different solvents was investigated (Guohong *et al.*, 2009).

2.2.3.3 Properties of 6-chloronicotinic acid (6CNA)

As neonicotinoid insecticides are recently introduced group of chemicals, not so many data about environmental fate is available as in the case of organophosphorus compounds.

Based on few published papers, the common transformation product of two neonicotinoids, imidacloprid (Garrido Frenich *et al.*, 2000; Segura Carretero *et al.*, 2003) and acetamiprid (Marin *et al.*, 2004) is 6-chloronicotinic acid (6CNA). Its chemical structure is shown in Figure 8.
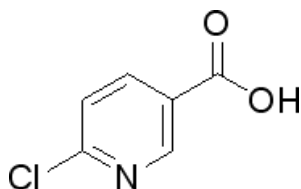
Figure 8: Chemical structure of 6CNA.

The formation of 6CNA was also observed during photo-Fenton reaction of acetamiprid (Žabar *et al.*, 2012a, in preparation) as well as within photocatalytic degradation with immobilized TiO_2 of imidacloprid aqueous solution (Žabar *et al.*, 2012b, in preparation) and within photocatalytic degradation with TiO_2 of acetamiprid (Guszvány *et al.*, 2009). The presence of 6CNA was also confirmed in soil (de Erenchun *et al.*, 1997). Additionally, imidacloprid residues were found in fruits and vegetables (Daraghmeh *et al.*, 2007), but the authors did not distinguish between imidacloprid and 6CNA concentration in crops due to pre-oxidation of all samples into 6CNA and subsequent derivatization into 6-chloronicotinic acid trimethylsilyl ester before analysis with gas chromatography–mass spectrometry (GC–MS). The large varieties of analytical methods for the detection of 6CNA in different matrices are summarized in Table 3.

Table 3: Some of the methods for the detection of 6CNA in different samples.

Matrix	Method	Sample treatment	Column	Mobile phase	Detector	Reference
honeybees	LC	extraction	Luna C_{18} (150 mm x 4.6 mm; 5 μm)	90 % water (pH = 3.00 CF_3COOH) 10 % CH_3OH	MS	Totti *et al.*, 2006
soil	LC	extraction CH_3CN and CH_3OH	Spherisorb CN (250 mm x 4.1 mm; 5 μm)	NaH_2PO_4 H_3PO_4	amperometric detection	de Erenchun *et al.*, 1997
dd water	LC	none	Premier C_{18} (100 mm x 4.6 mm; 3 μm)	0.4 % penthanol in water with 0.2 % CH_3COOH	PDA-MS	Lavine *et al.*, 2010
greenhouse air	HPLC	SPE	C_{18} Column (15 cm x 0.46 cm; 5 μm)	25 % CH_3CN 75 % 0.01 M phosphate buffer	UV-Vis (227 nm)	Garrido Frenich *et al.*, 2000
water	HPLC	extraction CH_2Cl_2	C_{18} (100 mm x 4.6 mm; 3 μm)	15 % CH_3CN 75 % 0.01 M phosphate buffer	UV-Vis (220 nm)	Martínez Galera *et al.*, 1998
honeybees	HPLC	extraction with acetone and ultrasound	Aquasil C18 (50 mm × 4.6 mm; 5 μm)	90 % CH_3CN 10 % dd water	PIF-FD	Gil García *et al.*, 2007
deionised water	HPLC	none	Zorbax C_8 (250 mm x 4.6 mm; 5 μm)	75 % water (pH = 3.00 CH_3COOH) 15 % CH_3CN (gradient)	UV-Vis (242 nm)	Žabar *et al.*, 2011a
honeybee bees product	UPLC	extraction	Acquity HSS T3 (10 cm x 2.1 mm; 1.8 μm)	H_2O; CH_3OH (95/5); formic acid H_2O; CH_3OH (5/95); formic acid	MS	Kamel, 2010
urine soil water	FPIA	extraction	polyclonal antibody	antiserum from immunized rabbit	fluorescence	Shim *et al.*, 2009

.....continuation of Table 3: Some of the methods for the detection of 6CNA in different samples.

Matrix	Method	Sample treatment	Column	Mobile phase	Detector	Reference
green beans roasted beans freeze coffee	GC	extraction derivatization (MTBSTFA)	DB-17 MS (30 m x 0.25 mm; 0.25	He (5 psi)	MS	Lodevico and Li, 2002
deionised water	GC	extraction preconcentration	DB-5-MS (30 m x 0.25 mm; 0.25 µm)	He (1.1 mL min^{-1})	MS (EI and CI)	Agüera *et al.*, 1998
apples, grapes, bananas, maize, potatoes	GC-MS	extraction derivatization	DB-5 capillary column (30 m x 0.25 mm x 0.25 µ	He (1 mL min^{-1})	MS	Daraghmeh *et al.*, 2007
deionised water	GC-MS	preconcentration	CP-Sil 8 CB MS column (30 m x 0.25 mm;	He (1 mL min^{-1})	MS	Žabar *et al.*, 2011b

2.2   Methods for pesticides degradation

According to the work published by Chiron *et al.* (1997), there are four major causes of pesticide water pollution:

- Pesticide treatment as a consequence of agricultural practices (in concentration range of few ppb),
- Rinse water from containers and spray equipment (10-100 ppm),
- Wastewater from agricultural industries (10-100 ppm),
- Wastewater from formulating or manufacturing pesticide plants (1-1000 ppm).

As every year more and more xenobiotics are released into the environment, a pathway for their efficient degradation or removal should be implemented. Various techniques are reported, such as microbial degradation of pesticides (Arbeli and Fuentes, 2007), constructed wetlands (Budd *et al.*, 2011), biological waste water treatment plants (Oller *et al.*, 2011) and sonochemical degradation (Chowdhury and Viraraghavan, 2009). Moreover, photodegradation studies were efficiently used for various pesticide degradation sequences during last decade and revealed diverse kinetics, mechanisms and the formation of by-products (Burrows *et al.*, 2002).

A promising way for decreasing pesticides' concentration, or even complete removal, is the application of advanced oxidation processes (AOPs) (Badawy *et al.*, 2006; Konstantinou and Albanis, 2003). Heterogeneous TiO_2 photocatalysis (Burrows *et al.*, 2002) and photo-Fenton's reagent (Ballesteros *et al.*, 2009) are the most intensively applied techniques. However, the efficiency of applied AOPs was mostly evaluated through the mineralisation rate and the degradation of an initial compound (Černigoj *et al.*, 2007a).

2.2.1   Photodegradation of pesticides

According to the literature (Burrows *et al.*, 2002; Ray *et al.*, 2006; Chiron *et al.*, 2000; Litter, 2005) the degradation of pesticides can be classified into a few broad categories such as:

- Direct photodegradation,
- Photosensitized degradation,
- Advanced Oxidation Processes (AOPs).

Most of the photodegradation experiments under natural conditions or laboratory conditions are performed in water (natural waters or deionised water) and in soil. Some of them are carried out in field while others are performed under laboratory conditions. The main procedure for these methods is to prepare a known concentration of selected pesticides in a certain matrix and within defined time intervals the sampling was carried out. The time intervals varying from 21 days (Bavcon *et al.*, 2003) to 30 days (Mouvet *et al.*, 1997) and also time intervals up to 40 or 60 days are reported (Kale *et al.*, 1999; Sarkar *et al.*, 1999). In some experiments, analysis with variable temperature and presence of light were carried out – simulating seasonal variations during the summer and winter (Lartiges and Garrigues, 1995). Some of the analyses were carried out in amber glass bottles in order to avoid possible influence from light or sunlight. However, this parameter (presence of light) is not well defined in all cases.

In the following paragraphs photodegradation processes will be presented in general with some examples of degradation of parent compounds, i.e. diazinon, chlorpyrifos, imidacloprid and acetamiprid. More detailed information about degradation procedure of selected TPs (i.e. IMP, TCP and 6CNA), reactors applied, kinetics, and identification of formed products are given in Table 4.

2.2.1.1 Direct photodegradation

Almost all pesticides show absorbance in UV-Vis spectrum, however at short wavelengths. On the other hand, light from the Sun reaches the Earth' surface, but with the small amount of UV irradiation, mostly UV-A and the small part of UV-B. Therefore, the direct photodegradation of the pesticides was expected to be very limited. In the literature, the direct photodegradation was mostly studied through laser-pulsed UV radiation.

Direct irradiation will, therefore, induce the pesticides excited singlet states and as a consequence they may cross to produce triplet states. Such excited states can then undergo i.e. homolysis, heterolysis or photoionization, as shown in Figure 9 (Burrows *et al.*, 2002).
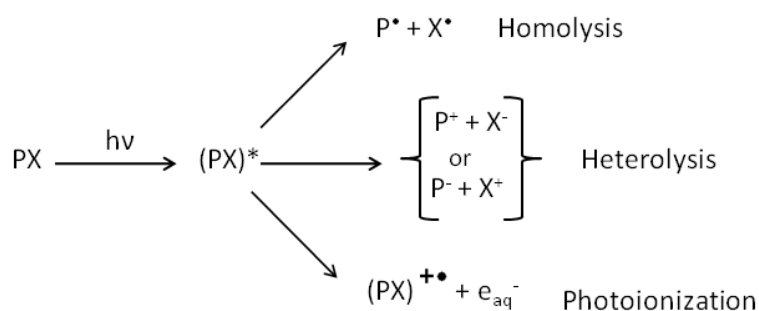
Figure 9: Possible chemical events taking place during direct photolysis (Burrows et al., 2002).

An important parameter to characterize the photo susceptibility of a molecule is the photo-transformation quantum yield (Φ). This parameter Φ can be defined as the ratio between the number of moles, which are transformed, and the number of Einsteins (mole of photons), which are absorbed. For solutions of low absorbance and with monochromatic light sources it can be calculated from the following relationship (Meallier, 1999) explained further (1):

$$\Phi \, I_m = \frac{-dC_A}{dt} \tag{1}$$

    C_A = concentration of the organics

    Φ = quantum yield of the reaction

    I_m = average number of Einsteins absorbing species per unit volume and unit time (at the monochromatic light)

    t = time

Recently, ultraviolet irradiation as a food preservation tool has gained application interest (Allende and Artés, 2003; Geveke, 2008) and this is an important consideration. The most effective and widely used is the UV-C germicidal lamp with emission at wavelengths around 254 nm. The wavelength of 253.7 nm is most efficient in terms of germicidal effect since photons are mostly absorbed by the micro-organisms' DNA (Koutchma, 2009).

Mansour *et al*. (1997) studied the photolysis of diazinon by UV light of different wavelengths in water and water/soil suspensions. Diazinon degraded faster in river water than in distilled water, and this rate enhancement was higher upon exposure to sunlight. The effect of added humic acids was lower than that of river water components.

The photodegradation of chlorpyrifos by simulated sunlight in water/methanol was studied (Barcelo *et al.*, 1993). The major photoproduct was 3,5,6-trichloro-2-pyridinol.

Photolytic degradation of imidacloprid or formulated product called Confidor is well described in the literature by using various light sources (Wamhoff and Schneider, 1999; Schippers and Schwack, 2008; Lavine *et al.*, 2010; Redlich *et al.*, 2007) showing high susceptibility to photodegradation with first-order decay kinetics resulting in several photoproducts. Photolytic degradation of acetamiprid was studied and reported again as first-order degradation kinetics; however no identification of degradation products was reported (Guohong *et al.*, 2009).

2.2.1.2 *Photosensitized degradation*

This specific degradation depends on the absorption of light by another molecule. Moreover, this process can transfer energy from its excited state to the pesticides and again as a consequence, pesticides can undergo different processes following direct photodegradation (Burrows *et al.,* 2002). A detailed scheme is presented in Figure 10.
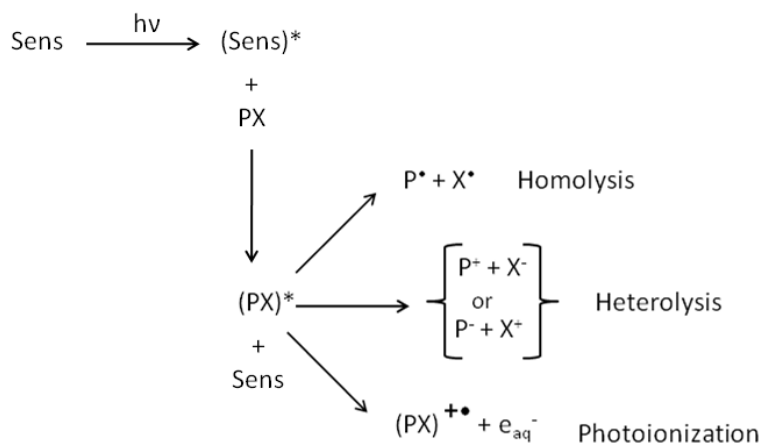
Figure 10: Photosensitized photolysis with involved energy transfer (Burrows et al., 2002).

Kamiya and Kameyama (1998) studied the photochemical effects of humic materials on the degradation of various OPs including diazinon and chlorpyrifos. The authors suggested that the sensitization effect of humic substances depends on the binding affinity of pesticides to the radical source of the humic material.

On the other hand, the photodecomposition of neonicotinoid insecticides thiamethoxam and thiacloprid in presence of dissolved organic matter (DOM) revealed more rapid disappearance (Peña *et al.*, 2011).

2.2.1.3 Advanced oxidation processes (AOPs)

The various currently used chemical oxidation processes for pesticide elimination are reported. Heterogeneous TiO_2 photocatalysis, ozonation and photo-Fenton's reagent are the most intensively applied technologies. A promising way for decreasing pesticides' concentration, or even complete removal, is the application of the so called advanced oxidation processes (AOP) (Badawy *et al.*, 2006; Konstatinou and Albanis, 2003).

Within the photocatalytic experiments with TiO_2, the production of highly reactive oxygen species – mainly the hydroxyl radicals – took place. It is well known, that the hydroxyl radical, after fluorine, is the most powerful oxidant and therefore can attack virtually all organic compounds. Several other reactive oxygen species, for example, the superoxide radical ($O_2^{\bullet-}$) and its conjugate acid form, the hydroperoxyl radical ($HO_2^{\bullet}$) can be also generated within AOP, but they are far less active than the hydroxyl radical (Litter, 2005).

In the AOP, the organic compounds can be completely mineralised to carbon dioxide and water mostly by hydroxyl radicals ($OH^{\bullet}$) and these radicals can be generated by following methods (Litter, 2005; Chiron *et al.*, 2000):

Addition of hydrogen peroxide undergoes homolysis upon irradiation (H_2O_2/UV) (2-6):

$$H_2O_2 + h\nu \rightarrow 2\ HO\cdot \tag{2}$$

However, hydrogen peroxide also reacts with hydroxyl radicals and this limits the efficiency of process.

$$^{\bullet}OH + H_2O_2 \rightarrow H_2O + HO^{\bullet}_2 \tag{3}$$

$$HO^{\bullet}_2 + H_2O_2 \rightarrow {^{\bullet}OH} + H_2O + O_2 \tag{4}$$

$$2\ HO^{\bullet}_2 \rightarrow H_2O_2 + O_2 \tag{5}$$

$$HO^{\bullet}_2 + {^{\bullet}OH} \rightarrow H_2O + O_2 \tag{6}$$

Photolysis of water with irradiation of wavelength lower than UV-C can also result in hydroxyl radical formation (Litter, 2005) (7):

$$H_2O + h\nu \rightarrow {^{\bullet}OH} + H^{\bullet} \tag{7}$$

Homogeneous photocatalysis with most known Fenton's oxidation is one of the best known metal catalyzed oxidation reactions of water-miscible organic compounds. The mixture of $FeSO_4$ or any other ferrous complex and H_2O_2 (Fenton's reagent) at low enough pH, results in Fe^{2+} catalytic decomposition of H_2O_2 and proceeds via a free radical chain process that produces hydroxyl radicals, which have extremely high oxidizing ability and can oxidize very stable organic compounds in a short time. The Fenton's reagent does not have only oxidation function but also coagulation by the formation of ferric-hydroxo complexes. The reaction for Fenton's oxidation is given below (Litter, 2005; Segura $et\ al.,$ 2008) (8-11):

$$Fe^{2+} + H_2O_2 \rightarrow Fe^{3+} + OH^- + HO^\bullet \tag{8}$$

$$Fe^{3+} + H_2O_2 \Leftrightarrow FeOOH^{2+} + H^+ \tag{9}$$

$$Fe–OOH^{2+} \rightarrow HO_2^\bullet + Fe^{2+} \tag{10}$$

$$Fe^{3+} + HO_2^\bullet \rightarrow Fe^{2+} + O_2 + H^+ \tag{11}$$
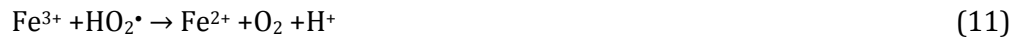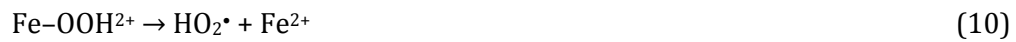
The crucial step in Fenton's oxidation is maintaining the low pH due to the formation of the ferric-hydroxo complexes which consequently slows the reaction.

Heterogeneous photocatalysis is the most applied technique in last decades regarding organic pollutants removal from water samples. Generally, the photocatalysis can be defined as cyclic photoprocess in which the pesticide degrades and spontaneous regeneration of catalyst occurs. This fact allows the cycle to continue until all the substrate is destroyed. Several catalysts are reported in the literature; however, lately the titanium dioxide (TiO_2) in different states plays a crucial role.

Usually, the semiconductor is excitated by light of energy higher than that of the band gap. Under these conditions, a short living electron-hole pairs are created and meanwhile electrons and holes migrate to the surface and react with adsorbed species, acceptors or donors. In detail, these holes in aqueous solution react with adsorbed water or OH^- ions, generating the hydroxyl radicals. The detailed procedure is given below (Ghezzar $et\ al.,$ 2007) (12-16):

$$TiO_2 + h\nu \rightarrow TiO_2\ (e_{cb}^- + h_{vb}^+) \tag{12}$$

$$O_2 + e_{cb}^- \rightarrow O_2^{\bullet-} \tag{13}$$

$$H_2O + h_{vb}^+ \rightarrow {}^\bullet OH + H^+ \tag{14}$$

$$\cdot OH + RH \rightarrow R\cdot + H_2O \tag{15}$$

$$R\cdot + O_2 \rightarrow R'COO\cdot \rightarrow R'\cdot + CO_2 \tag{16}$$

During the heterogeneous photocatalytic treatment, the organic compounds can be completely mineralized into CO_2 and H_2O and different inorganic ions. High attention should be also paid to the presence of so called "scavengers" of hydroxyl radicals due to their reduction of AOP efficiency evaluated through degradation of the parent compound. Important scavengers are carbonate ions and dissolved organic matter (Chiron *et al.*, 2000).

<u>Ozonation processes</u> are commonly used in water and wastewater applications for disinfection because ozone is a powerful oxidant and reacts with most toxic organics. Direct ozonation of organic molecules may act in different ways, such as breaking a double bond to form aldehydes and ketones, insertion of an oxygen atom into a benzene ring and reacting with alcohol to form organic acids (Ray *et al.*, 2006). While direct ozonation is not an effective process in many cases, ozone decomposes in water at high pH (about 10) to create a large number of hydroxyl radicals. Ozone decomposition occurs according to the following equations (Ray *et al.*, 2006) (17-19):

$$O_3 + H_2O \rightarrow HO_3^+ + OH^- \tag{17}$$

$$HO_3^+ + OH^- \rightarrow 2HO_2\cdot \tag{18}$$

$$HO_2\cdot + O_3 \rightarrow OH\cdot + 2O_2 \tag{19}$$
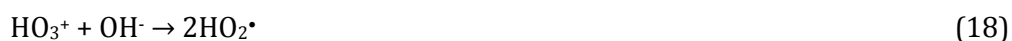
The critical issue in case of ozonation is removal of ozone that has not been consumed by the reaction. In most cases it needs to be eliminated and this process can suggest additional cost and consumption of time (Chiron *et al.*, 2000).

The involvement of AOPs in pesticides degradation processes is well studied and heterogeneous TiO_2 photocatalysis (Burrows *et al.*, 2002) and photo-Fenton's reagent (Ballesteros *et al.*, 2009) are the most intensively applied technologies.

A study by Doong and Chang (1997) reported the photocatalytic degradation of diazinon in water, assisted by TiO_2 and using the UV radiation supplied by a medium pressure mercury lamp. The TiO_2 apparently enhances the photodegradation of diazinon. Furthermore, Kouloumbos *et al.* (2003) conducted photocatalytic degradation of diazinon aqueous solution and showed IMP as a by-product within the reaction.

In addition, the chlorpyrifos degradation including AOP was investigated with TiO_2 showing first-order disappearance kinetics (Bavcon Kralj *et al.*, 2007b). Moreover, chlorpyrifos-oxon was detected by GC–MS in photodegradation of chlorpyrifos as the main photoinduced compound, whereas TCP was detected only in minor amounts (0.4 %) by HPLC analysis.

Photocatalytic degradation of imidacloprid is well described in the literature using different forms of the catalyst TiO_2 and again showing the first-order degradation kinetics along with the study of degradation products (Agüera *et al.*, 1998; Kitsiou *et al.*, 2009; Malato *et al.*, 2001). Nevertheless, within all photocatalytic studies reported on imidacloprid (Agüera *et al.*, 1998; Kitsiou *et al.*, 2009; Malato *et al.*, 2001; Guzsvany *et al.*, 2010), the 6CNA was reported as the final (oxidation) by-product of the pyridyl ring after the cleavage of the bond between the pyridyl ring and the imidazole ring. As reported by Kitsiou *et al.* (2009), linear oxo-compounds have been detected; however there is an erratum among the reported by-products since the carbon in one molecule possesses six bonds. However, it was not clearly indicated, if the shown linear oxo-compounds can be generated after the cleavage of the pyridyl ring from 6CNA or after the cleavage of the imidazole ring. Therefore, the appearance of 6CNA in the mixture is probably tightly related with the duration of the treatment of the initial compound (i.e. imidacloprid, acetamiprid). The photocatalytic degradation of acetamiprid and the study of its degradation products were reported with the first-order degradation kinetics (Khan *et al.*, 2010). A separate study investigated the reactivity of hydroxyl radicals with imidacloprid and acetamiprid as well detection of degradation products where again 6CNA showed as a final degradation product (Dell'Arciprete *et al.*, 2009). Reactivity of acetamiprid and imidacloprid with singlet oxygen was also investigated and again, the 6CNA has been reported as a final by-product during reaction (Dell'Arciprete *et al.*, 2010).

The degradation processes, kinetics and photoreactors involving IMP, TCP and 6CNA are presented in Table 4.

Table 4: Degradation processes, kinetics and photoreactors involving IMP, TCP and 6CNA.

Compound	System	Photoreactor	Kinetics	Mineralization/ by-products	Toxicity	Reference
IMP	UV-A/TiO$_2$	Pyrex photoreactor High-pressure mercury lamp λ_{max} = 360 nm	first-order degradation k_c = 13.3 – 19.0 10^{-3} min^{-1}	not defined	not defined	Oh *et al.*, 2007
IMP	UV/TiO$_2$	Pyrex photoreactor High-pressure mercury lamp 700 W	not defined	formation of CO_2	not defined	Lee *et al.*, 2005
IMP	UV/TiO$_2$	Pyrex photoreactor High-pressure mercury lamp 700 W	first-order degradation	GC-MS (no names or structures)	not defined	Lee *et al.*, 2003
IMP	UV-C	monochromatic low-pressure mercury lamp λ = 254 nm 4.86×10^{14} photons s^{-1} cm^{-2}	aerated dC/dt = 9.662x10^{-9} [mol L^{-1} s^{-1}] deoxygenated dC/dt = 1.000x10^{-8} [mol L^{-1} s^{-1}]	UV-Vis	not defined	Žabar *et al.*, 2011a
TCP	biodegradation	*Bacillus pumilus* strain C2A1	not defined	HPLC only	not defined	Anwar *et al.*, 2009
TCP	biodegradation	*Burkholderia cepacia* strain KR100	not defined	UV-Vis	not defined	Kim and Ahn, 2009
TCP	UV	medium mercury-pressure lamp λ = 200-400 nm (dose 310 mJ cm^{-1})	pseudo first-order	HPLC UV-Vis	not defined	Shemer *et al.*, 2005

...continuation of Table 4: Degradation processes, kinetics and photoreactors involving IMP, TCP and 6CNA.

Compound	System	Photoreactor	Kinetics	Mineralization/by-products	Toxicity	Reference
TCP	UV/H_2O_2	medium mercury-pressure lamp λ = 200-400 nm, dose 310 mJ cm^{-1} C (H_2O_2) = 5 mg L^{-1}	pseudo first-order	HPLC	not defined	Shemer *et al.*, 2005
TCP	UV-C	germicidal lamp λ = 254 nm 30 W 0.5 W/sq ft at 1 ft	not defined	radioactive labelling chlorine conc. HPLC, GC-MS, NMR	not defined	Feng *et al.*, 1998
TCP	microbial	*Pseudomonas* sp. ATCC 700113	not defined	radioactive labelling chlorine conc. HPLC, GC-MS, NMR	not defined	Feng *et al.*, 1998
TCP	UV-C	monochromatic low-pressure mercury lamp λ = 254 nm 4.86×10^{14} photons s^{-1} cm^{-2}	aerated dC/dt = 2.620x10^{-8} [mol L^{-1} s^{-1}] deoxygenated dC/dt = 3.330x10^{-8} [mol L^{-1} s^{-1}]	UV-Vis	not defined	Žabar *et al.*, 2011a
6CNA	UV-C	monochromatic low-pressure mercury lamp λ = 254 nm 4.86×10^{14} photons s^{-1} cm^{-2}	aerated dC/dt = 2.620x10^{-8} [mol L^{-1} s^{-1}] deoxygenated dC/dt = 3.330x10^{-8} [mol L^{-1} s^{-1}]	UV-Vis	not defined	Žabar *et al.*, 2011a
6CNA	UV-A/TiO_2	polychromatic low-pressure mercury lamp (λ_{max} = 355 nm) immobilized TiO_2 on glass slides	first-order kinetics. k = 0.011 ± 0.001 min^{-1} t$_{1/2}$ = 63.1 ± 5.5 min	UV-VIS, TOC, TN HPLC-DAD, GC-MS NMR	*Vibrio fischeri*	Žabar *et al.,* 2011b

2.2.2 Identification of by-products within the degradation processes

Extended studies showed that the identification of possible intermediates is essential as well as the assessment of the mineralisation rate (Konstantinou and Albanis, 2003; Chiron *et al.*, 2000; Chiron *et al.*, 1997). During the photocatalytic treatment of pesticides, the process does not instantaneously release carbon dioxide – but it is generated through formation of usually long-living intermediates. Detection and furthermore, identification, therefore plays crucial role for better determination and understanding what kind of chemical structures are still present in the solution at the end of the oxidation process.

In the literature, various analytical techniques for extraction of these organic intermediates are reported, but mostly liquid-liquid extraction and solid phase extraction are applied (Konstantinou and Albanis, 2003). Moreover, the separation techniques coupled with a variety of detectors such as GC-MS and LC-MS and also ^{1}H NMR proved wide range of application within AOPs (Žabar *et al.*, 2011b; Kitsiou *et al.*, 2009; Lambropoulou *et al.*, 2011). Identification of the by-products is the key to maximizing the overall process efficiency. The identification with GC-MS is limited with the volatility of compounds and therefore the requirement of the derivatization with i.e. MTBSTFA has arisen. The identification non-volatile compounds can be performed via the LC-MS technique with different ionization sources such as electro spray ionization (ESI) or atmospheric pressure chemical ionization (APCI). Many of the by-products often have similar chemical structures and molecular masses and this, therefore, renders their identification difficult. A useful tool for the isomers or positional isomers identification is the appliance of ^{1}H NMR or ^{13}C NMR studies (Žabar *et al.*, 2011b; Topalov *et al.*, 2001). Finally, when by-products are not commercially available for the confirmation, some authors undertook the laboratory synthesis of degradation products for better confirmation.

Several studies showed that the efficiency of AOPs cannot be evaluated just through HPLC and total organic carbon (TOC) measurements. Crucial investigation in AOPs is also the assessment of the mineralization rate and this is usually performed via TOC, chemical oxygen demand (COD) and total nitrogen (TN) measurements (Kitsiou *et al.*, 2009). Additionally, of great importance is the monitoring of so called end-products, such as CO_2, Cl^-, SO_4^{2-}, NH_4^+, NO_3^- etc., mostly with ion chromatography, spectrophotometry and titrations. Many studies revealed the conversion of organic nitrogen to NH_4^+ and NO_3^- (Kitsiou *et al.*, 2009; Chiron *et al.*, 1997).

2.3 Toxicity testing of pesticides

For understanding the pesticides' ecotoxicity and consequently the influence on biota, the pesticides' fate should be well understood. Most of the OCs and OPs are non polar molecules; therefore they are poorly soluble in water. However, the producers tend to make the commercial product more water soluble by adding many different additives. Neonicotinoids, on the other hand, are mostly polar molecules; therefore no difficulties with solubility arise. Nevertheless, the commercial products contain several additives to improve solubility and other properties necessary for efficient action.

After the application of the pesticides in the form of diluted commercial products, this can be with spraying through sprinkling or by wetting the seeds or crops; the pesticides can influence many organisms, as it is shown in Figure 11.
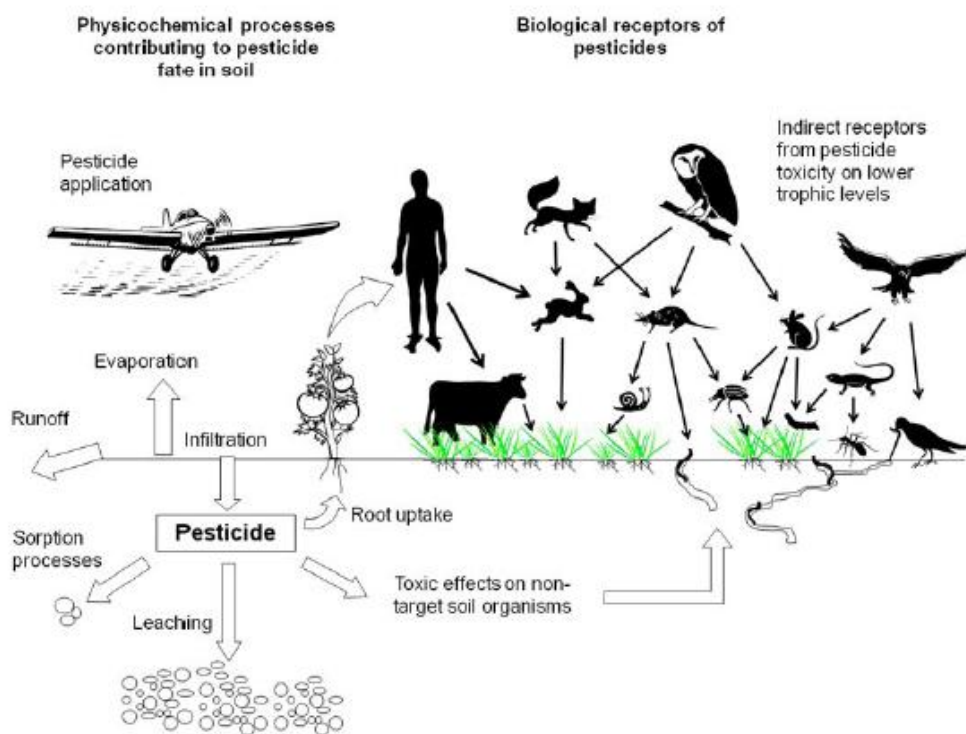
Figure 11: The general scheme of pesticides fate in the environment (Sanchez-Hernandez, 2011).

Most important processes in pesticide fate are: leaching into soil and water, atmospheric deposition, runoff and uptake by plants (Sanchez-Hernandez, 2011). However, the indirect influence of pesticides to non-target organisms should not be neglected. Mostly, the toxicity of pesticides is assessed from aquatic organisms but lately more and more attention is also paid to terrestrial organisms' toxicity measurements. All of these are considered to be so called non-target organisms.

For the toxicity measurements of pesticides, short and long term effects can be evaluated with acute or chronic toxicity bioassays. Usually, the acute bioassays last for a shorter period of time, while chronic exposure is longer. However, the exposure time depends on the life cycle of the tested organisms. In the case of *Vibrio fischeri* acute exposure can be accounted for in only 30 minutes while with *Porcellio scaber*, the acute exposure takes longer periods, for example, 14 days.

The toxicity endpoints can be very different, depending on organisms, and on the assessed chemical. Mortality and changes in growth, reproduction, and mobility are the simplest endpoints; however they can give a rapid estimation of toxicity. Moreover, different biomarkers are used to estimate toxicity through sublethal endpoints where no change in physiological parameters is observed. Over recent decades, great importance has been placed on the measurements of different enzymatic activities as an important sublethal endpoint. The most frequently used enzymes are acetylcholinesterase (AChE), glutathione S-transferase (GST), superoxide dismutase (SOD) and catalase (CAT) (Jemec *et al.*, 2007a; Jemec *et al.,* 2011) which can be affected by the different xenobiotics. Moreover, lipid peroxidation (LP) measurements are also often applied (Valant *et al.,* 2011).

2.3.1 Toxicity of TPs – in general

Much information is available on the adverse effects of parent chemicals (pesticides) and almost none about the possible adverse effects of TPs. However, as mentioned above, the TPs may be more toxic than the parent compound, as it was in a case of OP insecticides (Bavcon Kralj *et al.*, 2007a). They can be more persistent and more mobile than their parent compounds (Bavcon Kralj *et al.*, 2007a).

Understanding the toxicity of TPs is, therefore, crucial and essential for accurate assessment of environmental risks of synthetic chemicals. Many authors used the data on pesticides and TPs to explore the relationship between parent and TPs toxicity and sometimes describe the potential higher toxicity of TPs than the toxicity of parent compounds (Sinclair and Boxall, 2009). In addition, the prediction of ecotoxicity with the QSAR modelling system is also on the rise (Sinclair and Boxall, 2009; Sinclair *et al.*, 2006). Recently, risk assessment studies of TPs are of great importance and several studies were performed, indicating that TPs may possess greater toxicity than the parent compound (Sinclair *et al.*, 2006; Sinclair and Boxall, 2003). Moreover, the risk assessment of each TP in comparison to its parent pesticide was created on the basis of

their physico-chemical properties (Belfroid *et al.*, 1998) and they highlighted the lack of measured log P_{OW} for TPs. Not to be neglected, the log P_{OW} plays an important role in a compound's water solubility. Therefore, on the basis of this parameter, toxicity testing on aquatic or terrestrial organisms could be evaluated.

Significant differences in toxicity of parent compounds and TPs can be further explained by the facts reported by Sinclair and Boxall (2003):

- Active moiety of the parent compound is still present in the TP and hence the TP has the same toxic mechanism as the parent compound,
- the TP is the active component of a propesticide, where the applied substance is designed to be absorbed by an organism and once absorbed it is metabolized to an active substance that elicits the desired effect,
- the bioconcentration factor for the TP is greater than that for the parent,
- the TPs pathway results in a product with a different and more potent mode of action than the parent compound.

In the literature, little data is available on IMP, TCP and 6CNA toxicity testing. Few papers are published and more details, including species and exposure time, are presented in Table 5.

Table 5: Toxicity of IMP, TCP and 6CNA involving different methods and organisms.

Compound	Test organisms	Endpoint/application	EC$_{50}$ or similar toxicity data	Reference
IMP	electric eel acetylcholinesterase (AChE)	inhibition of AChE 20 min IC$_{50}$	no inhibition	Čolović *et al.*, 2011
IMP	cultivated human blood cells (lymphocytes and erythrocytes)	Incidence of micronuclei (MN)	statistically significant increase of micronuclei frequency (p = 0.008)	Čolović *et al.*, 2010
IMP	*Vibrio fischeri*	luminescence inhibition after 30 min of exposure	cannot be calculated due to the low inhibition of luminescence	Žabar *et al.*, 2011a
TCP	fetal rat astrocytes human astrocytoma cell line (132N1)	inhibition of [^{3}H]thymidine incorporation	no effects observed	Guizzetti *et al.*, 2005
TCP	human placental choriocarcinoma (JAR)	induced apoptosis TNF	24h IC$_{50}$ greater than 250 μM.	Saulsbury *et al.*, 2008
TCP	*Daphnia carinata*	survival tests immobility	48 h LC$_{50}$ = 0.2 μg L^{-1}	Cáceres *et al.*, 2007
TCP	rats rabbits	evaluation of foetuses feed consumption body weight gain	no clinical signs of toxicity in both species.	Hanley *et al.*, 2000
TCP	electric eel acetylcholinesterase (AChE)	inhibition of AChE 20 min IC$_{50}$	no inhibition	Čolović *et al.*, 2011
TCP	*Vibrio fischeri*	luminescence inhibition after 30 min of exposure	cannot be calculated due to the low inhibition of luminescence	Žabar *et al.*, 2011a

Compound	Test organisms	Endpoint/application	EC_{50} or similar toxicity data	Reference
6CNA	*Honey bee (Apis mellifera)*	colony health – mortality and adult abundance	no statistical difference was found	Maiue-Pierre *et al.*, 2009
6CNA	*Honey bee (Apis mellifera)*	acute toxicity LC_{50}	no significant toxicity was observed	Suchail *et al.*, 2001
6CNA	*Honey bee - Apis mellifera L var carnica*	Acute oral and contact toxicity tests	$LD_{50} > 121\,500$ ng per bee	Nauen *et al.*, 2001
6CNA	*Honey bee (Apis mellifera)*	contact toxicity	no mortality at 50 mg bee^{-1}	Iwasa *et al.*, 2004
6CNA	*Vibrio fischeri*	luminescence inhibition after 30 min of exposure	30 min $EC_{50} = 15.1$ mg L^{-1}	Žabar *et al.*, 2011a

2.3.2 Toxicity testing of by-products within the degradation processes

An important issue in degradation processes is formation of by-products and their toxicity. The degradation products formed during the AOPs of hydrophobic pesticides are often more polar and more bio available than the original contaminants. If the formed by-products are more toxic then initial compound (Bavcon Kralj *et al.*, 2007a), there is a need to couple AOPs to biodegradation or other suitable processes to completely eliminate the contaminants (Chiron *et al.*, 2000).

Still, many reported studies on pesticides' AOPs does not include their toxicity testing, therefore, the complete removal of the parent compound could be observed, but as a consequence, incomplete mineralization may result in the formation of more toxic intermediates. To avoid this drawback, AOPs are expected to be carefully operated and monitored.

In order to prove that AOPs are efficient, certain toxicity tests need to be performed. Numerous bioassay procedures are available and reported; however, as toxicity is a biological response, a universal monitoring device is unlikely to be available. Therefore, in order to increase confidence in the measurements of their toxicity, it is necessary to use a battery of different organisms from different taxonomic groups (Fernandez-Alba *et al.*, 2002).

However, some of the tests could be time-consuming, demanding and additionally, the sample preparation plays an important role. Therefore, toxicity testing with luminescence marine bacteria *Vibrio fischeri* seems to be the most applied toxicity test for the evaluation of AOPs efficiency. Different commercial kits are available, most frequently described are Microtox® (Lapertot *et al.*, 2008) and Lumistox® (Dell'Arciprete *et al.*, 2009, 2010; Kitsiou *et al.*, 2009; Žabar *et al.*, 2011b). Moreover, the procedure with *V. fischeri* is standardized, as described in the ISO-Guideline No. 11348-Part 1–3 (2007).

2.3.3 Toxicity testing with luminescent the bacteria *Vibrio fischeri*

Bacteria are important members of the aquatic ecosystem. The number and characteristics of ecotoxicological test methods with bacteria are large. For nearly 25 years the luminescent bacteria test with the marine bacterium *Vibrio fischeri* (formerly *Photobacterium phosphoreum*) has become a basic test for ecotoxicological testing of chemicals, waste water and eluates from soil and sediment. *V. fischeri* is a Gram-

negative bacterium with most distinguishing characteristic, bioluminescence, controlled by a small set of genes known as the *lux* operon. *V. fischeri* in presented in Figure 12.
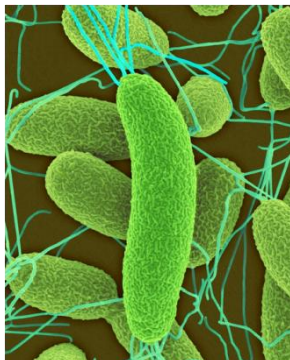
Figure 12: A photo of Vibrio fischeri *bacteria (Dr. Dennis Kunkel Microscopy, Inc./Visuals Unlimited, Inc.).*

Luminescence is a chemical reaction in which the enzyme, luciferase, oxidizes organic compounds, such as long chain aldehyde and reduces flavin mononucleotide, so as to release free energy in the form of blue-green light at 490 nm. The reaction that takes place in *V. fischeri* is as follows (20):

$$FMNH_2 + RCHO + O_2 \text{ --> } FMN + RCOOH + H_2O + h\nu \text{ (490nm)} \tag{20}$$
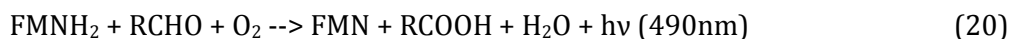
This is a rapid method for the determination of the toxicity of an aqueous solution of known or unknown samples. The inhibition of the luminescence emitted by *V. fischeri* after a given exposure time is determined, usually after 30 min. The luminescent bacteria test can be carried out by using freshly prepared bacteria, as well as liquid-dried or freeze-dried samples.

The test measures the inhibition of the light emission of *V. fischeri* according to the ISO-Guideline No. 11348-Part 1–3 (2007) as part of the basic test battery it was described in a Standard Operation Procedure (SOP). Measurements can be carried out using freshly prepared bacteria (Part 1), as well as liquid-dried (Part 2) or freeze-dried (Part 3) bacterial preparations. Specified volumes of the diluted test sample are combined with the luminescent bacteria suspension in a test tube. The test criterion is the luminescence, measured after a contact time of 30 min taking into account a correction factor (C_f), which is derived from the intensity changes of control samples during the exposure time.

The inhibitory effect of the sample on the light emission of *V. fischeri* can be determined as a 30 min EC_{50} value. The ISO guideline 11348 (2007) recommends testing at least one of the three reference substances (3,5-dichlorophenol, potassium dichromate and zinc sulphate heptahydrate) parallel to each testing. For each reference substance and the different bacteria, a defined concentration is given, which has to cause 20–80 % inhibition after 30 min contact time. The evaluation of the toxicity test is ensured by the reference substance, where the check on the bacteria batch before experimentation is performed.

The effect of imidacloprid on *V. fischeri* was assessed by Tišler *et al.* (2009) and the results showed that 30 min IC_{50} for imidacloprid was 61.9 mg L^{-1}. Another study performed by Dell'Arciprete *et al.* (2009) reports the inhibition of *V. fischeri* bacteria 28 ± 6 % at concentration 80 mg L^{-1} for acetamiprid and 32 ± 7 % at concentration 80 mg L^{-1} for imidacloprid.

The toxicity of chlorpyrifos on *V. fischeri* was performed by Palma *et al.* (2008) and the 30 min EC_{50} value was 2.84 mg L^{-1}.

2.3.4   Toxicity testing with terrestrial isopods *Porcellio scaber*

Terrestrial isopods *Porcellio scaber* live in the upper layers of the soil and surface leaf litter in urban and natural habitats. Their biology and physiology is well known due to their important ecological role as decomposers of organic materials. Their role is in fragmentation of dead plant material and making it available for other decomposing invertebrates. They prefer moist habitat but on the other hand they also need places with lower humidity for excretion (Drobne, 1997). The *P. scaber* is presented in Figure 13.

Figure 13: A photo of a **Porcellio scaber** *(Wikipedia, January 2012).*

Terrestrial isopods are well accepted organisms of choice in terrestrial ecotoxicology (Drobne, 1997) due to their appropriateness to the criteria in ecotoxicological studies. The criteria are size, abundance, simple identification and simple aging. Good knowledge of biology is more than necessary to assess the sublethal responses of chemicals (Drobne, 1997). Therefore, the terrestrial isopods *P. scaber* do mach the criteria, however, the biggest challenge is still their low growth rates and long reproductive cycle. Even at 25 °C it takes a minimum of 6 months for newly hatched juveniles to reach reproductive age (Walker *et al.*, 2001).

2.3.4.1 Biomarkers in ecotoxicology with terrestrial isopods

The most widely used ecotoxicological endpoints are mortality, growth and reproduction. However, mortality (as endpoint) is sometimes not appropriate due to its interpretation – it is very hard to estimate if the animal died due to the chemical or due to the other impacts. Moreover, the other responses such as growth or reproduction are sometimes inconvenient due to long duration in the exposure time (Drobne, 1997). Feeding activity is a very good approach for assessing the food quality and consequently measuring the wide range of stressors. The feeding assay is based on the consumption of the food mass (leaf mass) (Stanek *et al.,* 2006).

Biochemical biomarkers play an important role in pesticides toxicity testing with isopods. Several studies reported measuring the activity of specific enzymes, for example, glutathione-S-transferase (GST) and catalase (CAT) (Stanek *et al.*, 2006; Jemec *et al.,* 2011). Furthermore, energy reserves evaluation, such as protein, glycogen and lipid content, were also investigated in order to obtain a better insight into energy depletion reserves upon exposure to xenobiotic (Stanek *et al.,* 2006). Moreover, lipid peroxidation (LP) assessment in *P. scaber* toxicity testing is also reported (Valant *et al.,* 2011).

Lipid peroxidation (LP) is a free radical chain reaction and an attractive general mechanism of xenobiotic stress. This cascade reaction is primarily an outcome of oxidation and the formation of free radicals by reactive oxygen species (ROS) such as peroxides and superoxide's which are continuously generated in the living cells due to environmental stress (Wheatley, 2000). LP alters the normal structure and functional properties of the cell leading to cytotoxic manifestations mediated by dismantling of the cell membrane structure along with various adaptive reactions (Linden *et al.*, 2008). Many xenobiotics, when undergoing metabolisation, can form intermediate

reactive forms of the oxygen molecule, but ROS are also the result of incomplete oxygen reduction during normal aerobic processes. LP occurs when the natural antioxidant defences are overcome and fatty acid hydroperoxides are formed with the consequence of membrane and membrane-bound enzymes destabilisation (Porter *et al.*, 1995). One of the consequences of oxidative stress is the peroxidation of lipids. Lipid peroxides, derived from polyunsaturated fatty acids, are unstable and decompose to form a complex series of compounds. These include reactive carbonyl compounds, of which the most abundant is malondialdehyde (MDA). A detailed scheme of peroxidation is presented in Figure 14.
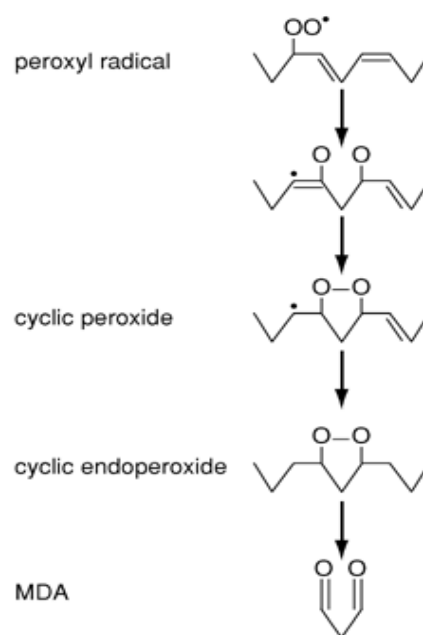
Figure 14: Schematic illustration of lipid peroxidation with MDA as final by-product.

The simplest and the most frequently used assay for lipid peroxidation determination is the thiobarbituric acid (TBA) assay. MDA as final lipid peroxidation product in biological samples reacts with TBA under strong acidic condition and heating. This reaction is actually the formation of a pink-colour product (TBA-MDA) which can consequently be measured by the colorimetric method (Lykkesfeldt, 2007). The detailed reaction is shown in Figure 15.
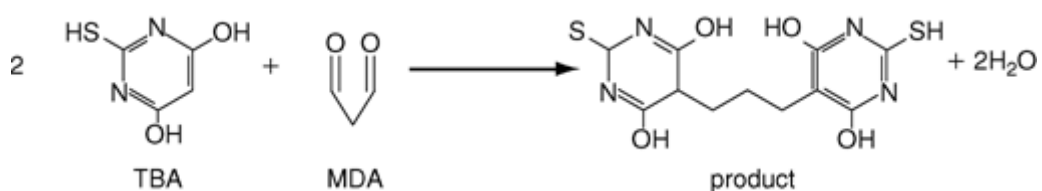
Figure 15: Schematic illustration of MDA-TBA reaction and formation of a colour product.

The effect of several pesticides to isopods was investigated in the past. The sublethal effects of diazinon on *P. scaber* were studied by several authors. Widianarko and Van Straalen (1996) studied the mortality of *P. scaber* when exposed for different periods of time to different concentrations of diazinon in soil. The results clearly indicated the high mortality for concentrations 8.00 µg/g and 11.31 µg/g soil and the LC_{50} value was 4.4 µg of diazinon/g dry weight of soil.

On the other hand, Stanek *et al.* (2006) studied the linkage along levels of biological complexity in juvenile and adult diazinon fed *P. scaber.* They assessed the effects of diazinon on AChE activity, lipid, protein and glycogen content, weight change, feeding activity and mortality of juvenile and adult terrestrial isopods. The non-observed effect concentration (NOEC) for AChE activity after exposure within two weeks was below 5 µg/g diazinon. Glycogen and lipid content, feeding activity and weight change were not affected during two weeks of exposure up to 100 µg/g diazinon.

Furthermore, in the study performed by Stanek *et al.* (2003), the *P. scaber* were fed with diazinon dosed food. Juveniles were exposed for four weeks to concentrations of 50, 100, 150, 200 and 300 µg diazinon/g dry weight of food and the adults were exposed to lower concentrations (0.1, 1, 10 and 50 µg diazinon/g dry weight of food). Finally, the mortality, growth, feeding rate and AChE activity were measured. The results showed that AChE inhibition in juvenile and adults proved to be a more sensitive parameter in respect to mortality, growth and feeding rate.

A study performed by Achuthan Nair *et al.* (2002) reports the effects of chlorpyrifos to *P. scaber*. Adult animals were exposed for different periods of time to a known quantity of dry lemon leaves, soaked with a known concentration of chlorpyrifos. Unfortunately, the detailed procedure was not clearly explained. The growth, feeding rate, assimilation rate and assimilation efficiency were calculated after 14 days of experimentation. Chlorpyrifos was found to be highly toxic to *P. scaber* and the 24 h LD_{50} was observed to be 27.5 µg g^{-1}. Significant difference in feeding rate, assimilation rate and assimilation efficiency was observed for all applied concentrations.

Additionally, the toxicity of imidacloprid to the terrestrial isopod *P. scaber* was also investigated (Drobne *et al*., 2008) and the authors suggested, that weight gain, feeding rate, total protein contents, GST and digestive gland epithelial thickness in juveniles and adults were most affected. Moreover, an estimate of actual intake rates suggests that imidacloprid affect isopods at similar exposure concentrations as insects. Moreover, the results showed that toxicity testing with *P. scaber* provides relevant,

repeatable, reproducible and comparable toxicity data that is useful for the risk assessment of pesticides in the terrestrial environment.

An interesting study on *P. scaber* hepatopancreas epithelial thickness and lipid droplets in stress conditions was performed by Lešer *et al.* (2008). The results highlighted the involvement of hepatopancreatic function into stress management in different physiological conditions. During the test, the abundance, the distribution, and the size of lipid droplets in the hepatopancreatic epithelium were recorded. Authors proposed that in animals exposed for two weeks, the epithelial thickness and the abundance of lipid droplets were significantly reduced.

Finally, a study with LP assessment was performed by Valant *et al.* (2011), where the authors studied whether ingested TiO_2 nanoparticles damaged the cell membrane of digestive gland cells in *P. scaber* either mechanically or by means of oxidative stress.

3   RESEARCH GOALS

The research goals could be divided in the following parts:

- Development of a fast HPLC-DAD method for simultaneous determination of IMP, TCP and 6CNA in aqueous solutions without additional time-requiring sample preparation. This step was crucial for the research, since the monitoring of selected analytes was involved in all further experiments applied. The proper method therefore enabled easier monitoring of initial compounds and transformation products throughout the experiments.

- Investigation of the behaviour of IMP, TCP and 6CNA aqueous solution under various conditions; such as different pH (4, 7, 10), temperature (4 °C *vs.* 22 °C), presence of natural sunlight, presence of simulated sunlight within different seasons of the year and finally, behaviour under germicidal light (245 nm - in aerated in deoxygenated conditions), which is often used as a tool for food sterilisation.

- The application of AOPs techniques (photocatalysis with immobilised TiO_2) for the possible degradation and removal of the substances IMP, TCP, 6CNA from an aqueous solution.

- Toxicity testing using luminescence marine bacteria *Vibrio fischeri* for standard solutions of IMP, TCP and 6CNA in an aqueous solution as well as for monitoring the evolution of toxicity during the applied AOPs.

- Toxicity testing of IMP, TCP and 6CNA using non-target terrestrial isopods - *Porcellio scaber* via feeding experiments and evaluation of the sublethal endpoints such as: mortality, growth, assimilation efficiency, consumption rate and faecal pellets production. In addition, the investigations of selected TPs on levels of hepatopancreatic lipid peroxidation in *P. scaber* were performed.

4 MATERIALS AND METHODS

4.1 Chemicals

Analytical standards of TPs were as fol

- 6CNA, 97.0 % pure, was provided by Fluka,
- IMP, 99 % pure, was provided by the Aldrich Chemical Company Inc.,
- TCP, analytical standard, was provided by Fluka.

Chemicals for the synthesis of standards were:

- trifluoroacetic acid from Sigma Aldrich Company Ltd,
- 30 % hydrogen peroxide from Sigma Aldrich Company Ltd..

Chemicals for HPLC-DAD analyses were:

- acetic acid glacial 100 % p.a. from Merck,
- acetonitrile, Chromasolv for HPLC, from Sigma Aldrich Company Ltd,
- double deionised water (< 18 MΩ cm) was prepared through the NANOpure water system (Barnstead, USA).

Chemical for ^{1}H NMR was:

- Methanol-d$_4$ from Eurisotop.

Chemicals for TOC and TN analyses were:

- Potassium hydrogen phthalate was purchased from Alfa Aesar GmbH,
- ammonium sulphate from Fluka,
- hydrochloric acid 37 % puriss. p.a. from Sigma Aldrich Company Ltd..

Chemicals for ion chromatography (IC) were:

- sodium carbonate from Fluka,
- sodium bicarbonate from Fluka,
- Multivalent Ion Chromatography Standard Solution from Fluka.

Chemicals for actinometry were purchased as follows:

- sodium acetate from Fluka,
- potassium oxalate monohydrate from Fluka,
- sulphuric acid from Fluka,
- iron(III) sulphate hydrate from Riedel-de Haen,
- 1,10-phenanthroline from Sigma Aldrich.

Chemicals for photocatalytic thin films preparations were:

- titanium(IV) isopropoxide from Acros Organics,
- ethyl acetoacetate from Riedel-de Haen,
- 2-methoxyethanol from Fluka,
- copolymer Pluronic F-127 from Sigma-Aldrich Company Ltd..

Chemicals for the *Vibrio fischeri* toxicity test were:

- Sodium hydroxide p.a. from AppliChem,
- sodium chloride from Carlo Erba Reagenti,
- hydrochloric acid 37 % puriss. p.a. from Sigma Aldrich Company Ltd..

Chemicals for lipid peroxidation determination for *Porcellio scaber* were:

- trichloroacetic acid from Calbiochem,
- thiobarbituric acid from Merck,
- diethyl ether from Merck,
- butylhydroxytoluene from Merck,
- hydrochloric acid 37 % puriss. p.a. from Sigma Aldrich CompanyLtd.,
- ethanol absolute p.a. from Sigma Aldrich CompanyLtd.,
- 1-buthanol p.a. from from Sigma Aldrich CompanyLtd..

4.2   Stability studies under laboratory conditions

Stability of IMP, TCP and 6CNA aqueous solution was assessed by exposing aqueous samples to different temperatures, different pH (4, 7, and 10) and presence or absence of sunlight. Samples containing selected transformation products were dissolved in double deionised water and stored under different laboratory conditions in 100 mL SCHOTT DURAN flasks, with an initial concentration of 13.5 mg L^{-1} for IMP, 15.4 mg L^{-1} for TCP and 16.8 mg L^{-1} for 6CNA. One set of flasks was kept on the laboratory desktop exposed to sunlight at room temperature 22 °C and the second set of flasks was refrigerated in the dark, at a temperature of 4 °C. During the period of 90 days, the concentration of solutions was monitored with a high pressure liquid chromatography coupled with a diode array detector operating in the range from ultraviolet to visible light (HPLC-DAD (UV–Vis)) and the pH was also monitored.

4.3 Stability studies under simulated sunlight using SUNTEST apparatus

Stability study experiments under simulated sunlight were performed in a Suntest CPS+ solar simulator (Atlas MTT, Illinois, US), equipped with a xenon arc lamp (1500 W) and Special UV Glass (Suprax) filter restricting the transmission of wavelength below 290 nm. The 250 mL of aqueous solutions of IMP, TCP and 6CNA with concentrations 50.3 ± 0.1 mg L^{-1} for IMP and 6CNA and 50.5 ± 0.4 mg L^{-1} for TCP were prepared daily in double deionised water and put in special sealed cylinders made of borosilicate glass with an area of 79 cm^2. Experiments were carried out at different intensities; 250 W m^{-2}, 500 W m^{-2} and 750 W m^{-2} and therefore, simulating sunlight irradiation on a winter day, autumn day and summer day in Nova Gorica, Slovenia (45° 57' 25"N, 13° 38' 53"E) (ARSO - Slovenian Environment Agency). The total dosage within 6 h at intensity 250 W m^{-2} was 5383 kJ m^{-2}, at intensity 500 W m^{-2} was 10684 kJ m^{-2} and at intensity 750 W m^{-2} was 16015 kJ m^{-2}. The irradiance and temperature (20 ± 1.7 °C) were maintained constantly throughout the experiments by an internal radiometer and chiller. Aqueous solutions of all three analytes were put separately in special sealed cylinders in order to prevent evaporation and afterwards exposed for 6 hours to the irradiation under the same conditions. At selected time intervals (0, 1, 2, 3, 4, 5, 6 h) samples from all cylinders were collected. Every time the pH of the solution was measured and a part of the sample was quantitatively analysed directly by HPLC–DAD (UV-Vis). For the evaluation of the mineralisation rate, TOC instrument was used, and for the monitoring of UV-Vis spectra evolution UV-Vis spectrophotometer was applied. Sample toxicity was evaluated with luminescent bacteria, *V. fischeri.* Samples were further analysed by LC-MS and GC-MS for the identification of photodegradation by-products. In order to evaluate the thermal degradation of samples, a control black experiment was run where one cylinder per experiment was covered with aluminium film and exposed to simulated sunlight.

4.4 Photodegradation studies with a monochromatic low-pressure mercury lamp (245 nm)

A quartz cell (10 mm × 10 mm× 40 mm) was filled with an aqueous solution of each chemical separately in concentration of 18.0 ± 0.1 mg L^{-1} for IMP, 21.6 ± 0.2 mg L^{-1} for TCP and 21.2 ± 0.1 mg L^{-1} for 6CNA. Afterwards, the solutions were placed in front of the monochromatic low-pressure mercury germicidal lamp emitting at a wavelength of

254 nm. The photon flux was evaluated by actinometry using potassium ferrioxalate (Murov *et al.*, 1993) and the value obtained was 4.86×10^{14} photons s^{-1} cm^{-2}. The solutions were stirred and irradiated for a given period of time (0, 5, 10, 20 and 30 min) then analysed by the HPLC-DAD (UV-Vis) as well as by UV-Vis spectrophotometer with time intervals of 0, 5, 10, 20, 30, 45, 60, 80 and 100 min. After each sample collection, a fresh sample was irradiated in order to retain the same sample volume. All the samples were irradiated in aerated and oxygen free solutions. In the latter case, prior to irradiation, the samples were purged for 10 minutes with argon. In order to obtain a better insight into possible degradation behaviour, the additional experiments were performed in order to estimate the degradation quantum yields under various conditions. Adequate values were calculated according to the Meallier (1999) with some modifications, by employing the following expression (21);

$$\Phi = \frac{\left(-\frac{dC}{dt}\right)(N \, l \, 10^{-3})}{[I_0(1-10^{A_0})]} \qquad (21)$$

dC/dt: the slope of the initial linear part of the kinetic curve (concentration as a function of irradiation time) [mol L^{-1} s^{-1}],

N: Avogadro number [molecules mol^{-1}],

l: optical path length [cm],

I_0: photonic flux evaluated to 4.68×10^{14} [photons s^{-1} cm^{-2}],

A_0: the initial absorbance of the studied solution at the excitation wavelength 254 nm.

4.5 Photodegradation studies with three polychromatic low-pressure mercury lamps (355 nm)

The experimental reactor consisted of a glass tube (240 mm, inner diameter 40 mm) with the effective volume of 250 mL (Černigoj *et al.*, 2007b). The cell was placed in the centre in-between the lamps at a distance of 10 cm. Three low-pressure mercury fluorescent lamps were used as UV-A (315–400 nm) radiation source (CLEO 20 W, 438 mm x 26 mm, Phillips; broad maximum at 355 nm). The photon flux in the cell was evaluated by potassium ferrioxalate actinometry (Murov *et al.*, 1993), and determined to be 2.3×10^{-5} Einstein L^{-1} s^{-1}. The temperature was kept constant at 28 ± 2 °C during the experiment. Aqueous solutions of IMP, TCP and 6CNA were prepared daily in double deionised water in concentrations of 53.0 ± 1.5 mg L^{-1} for IMP, 54.3 ± 2.1 mg L^{-1} for TCP and 50.7 ± 1.6 mg L^{-1} for 6CNA. The solutions were irradiated for fixed periods of time. The aliquots were taken periodically (0, 5, 10, 20, 30, 45, 60, 80, 120 min) and

analysed with HPLC-DAD (UV–Vis), UV–Vis spectrophotometer, TOC analyzer, ion chromatography and pH meter. Samples were further analysed by LC-MS and GC-MS for the identification of photodegradation by-products. The conductivity during the photodegradation studies and toxicity of selected samples with the luminescent bacteria *V. fischeri* were tested as well.

4.6 Photocatalytic studies with polychromatic three low-pressure mercury lamps (355 nm) and immobilised TiO₂

The photocatalytic experiments were performed in an experimental reactor as already described in Chapter 4.5. An additional spinning basket made entirely of Teflon was inserted into the cell. Six glass slides with the immobilised catalyst TiO$_2$ were fastened around the axis of the spinning basket. A detailed scheme of the Teflon spinning basket inside the photocatalytic cell is presented in Figure 16.
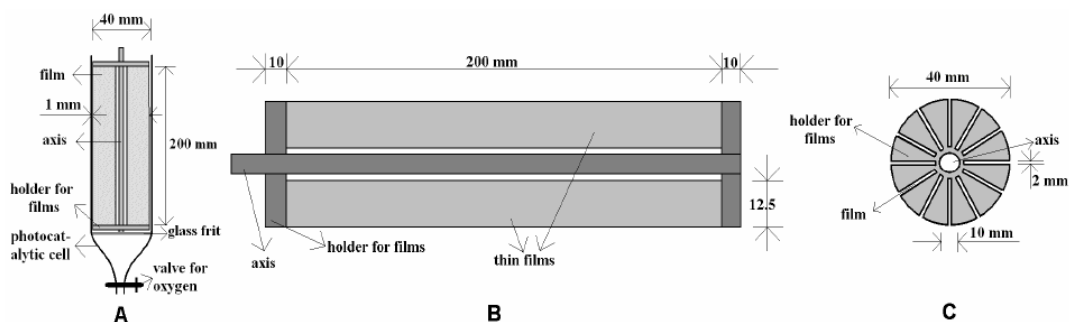
Figure 16: The photocatalytic cell (A), its longitudinal profile with thin films position (B) and Teflon holder with twelve notches for film fastening (C) developed by Černigoj et al. (2007b).

Transparent TiO$_2$-anatase films deposited on both sides of SiO$_2$-precoated soda-lime glass slides (175 mm x 12.5 mm x 2 mm) were produced by sol-gel processing as already described by Černigoj *et al.* (2006). The total surface area covered with TiO$_2$ was 262 cm² and the average amount of TiO$_2$ on each slide, determined by weighing (Černigoj *et al.*, 2006), was approximately 10 mg. The motor on the top of the reactor was rotating the spinning basket at the speed of 100 rpm. The photon flux in the cell was evaluated by potassium ferrioxalate actinometry (Murov *et al.*, 1993), and determined to be 2.3 x 10^{-5} Einstein L^{-1} s^{-1}. The temperature was kept constant at 28 ± 2 °C during the experiment. Aqueous solutions of IMP, TCP and 6CNA were prepared daily in double deionised water in concentrations of 53.8 ± 0.7 mg L^{-1} for IMP, 52.0 ± 1.5 mg L^{-1} for TCP and 51.2 ± 0.2 mg L^{-1} for 6CNA. The solutions were irradiated for fixed periods of time. The aliquots were taken periodically (0, 5, 10, 20, 30, 45, 60, 80,

120 min) and analysed with HPLC-DAD (UV–Vis), UV–Vis spectrophotometer, TOC analyzer, ion chromatography and pH meter. Samples were further analysed by LC-MS, GC-MS and ^{1}H NMR for the identification of photodegradation by-products. The conductivity during photocatalytic studies and toxicity of selected samples with luminescent bacteria *V. fischeri* were tested as well.

4.6.1 Preparation of immobilised TiO_2 films by the sol-gel procedure

According to the literature (Černigoj *et al.*, 2006), the titania sols were made from a modified precursor (titanium(IV) isopropoxide) by the addition of ethyl acetoacetate (ethyl acetoacetate/titanium(IV) isopropoxide = 1.0). The resulting exothermic reaction gave rise to a stable solution into which the solvent 2-methoxyethanol was added (titanium(IV) isopropoxide/2-methoxyethanol = 0.075) with surfactant triblock copolymer (Pluronic F-127, Sigma) (9.7 wt. %, sol C). The surfactant weight percentage is given with respect to the total weight of solution. The resulting solution was stirred at room temperature for at least three hours. Coatings were made in the dip-coating unit with pulling speeds of up to 10 cm min^{-1}. The supporting soda–lime glass plates coated with SiO_2 had been cleaned with ethanol and dried. The xerogel films were calcinated at 500 °C for 60 min (Černigoj *et al.*, 2006).

4.7 Analytical procedures

4.7.1 HPLC-DAD method

Aqueous solutions of 6CNA, IMP and TCP were analysed by HPLC consisting of an Agilent 1100 Series chromatograph, coupled with a DAD (UV–Vis) detector. The separation was achieved using a Zorbax C8 column (250 mm x 4.6 mm) filled with a stationary phase Chromasil 100 (pore size 5 μm) produced by BIA Separations d.o.o., Slovenia, maintained at 25 °C. The injection volume was 75 μL. The eluents consisted of acetonitrile (A) and acetic acid 1.5 % v/v (B); flow rate was 1 mL min^{-1} and the wavelength 242 nm. The gradient elution was as follows: 0–16 min 15 % A, 75 % B; 16–20 min 70 % A, 30 % B. For quantification purposes a calibration curve in the range from 0.1–100 mg L^{-1} was prepared.

4.7.2 LC–ESI–MS/MS analyses

Mass spectrometry analyses of irradiated samples were performed using a LC Perkin Elmer Series 2000 (Schelton, CT, USA) linked to a 3200 Q TRAP MS system equipped with an electro spray ionization (ESI) source from Applied Biosystems/MDS Sciex (Foster City,CA, USA). The separation was achieved using a monolith C_{18} column Merck, Purospher STAR (250 mm x 4.6 mm, pore size 5 μm) produced by Merck and kept at 25 °C. The injection volume was 20 μL and the flow rate 1 mL min^{-1}. The eluents consisted of acetonitrile (A) and acetic acid 1.5 % v/v (B).

The gradient for **IMP** was as follows: 0-4 min 15 % A, 16-23 min 70 % A, 23-28 min 85 % A. Mass spectrometric scans were performed in negative Q1 mode, scanning from *m/z* 60 to *m/z* 400 amu in 1 s. An ESI source voltage of -4500 V was applied; declustering potential of -60 V and Turbo Ion Spray temperature was maintained at 400 °C.

The gradient for **TCP** was as follows: 0-4 min 15 % A, 14-20 min 70 % A, 22-28 min 85 % A. Mass spectrometric scans were performed in negative Q1 mode, scanning from *m/z* 60 to *m/z* 400 atomic mass unit (amu) in 1 s. An ESI source voltage of - 4500 V was applied; declustering potential of -77 V and Turbo Ion Spray temperature was maintained at 400 °C. Prior to analyses, 150 mL of the water sample was evaporated to dryness in a rotary evaporator and the residue was again dissolved in 1.5 mL of double deionised water.

The gradient for **6CNA** was as follows: 0-4 min 15 % A, 16-23 min 70 % A, 23-28 min 85 % A. Mass spectrometric scans were performed in positive Q3 mode, scanning from *m/z* 60 to *m/z* 400 amu in 1 s. An ESI source voltage of 5000 V was applied; declustering potential of 50 V and Turbo Ion Spray temperature was maintained at 400 °C. Prior to analyses, 150 mL of the water sample was evaporated to dryness in a rotary evaporator and the residue was again dissolved in 1.5 mL of double deionised water.

4.7.3 GC–MS analyses

Gas chromatography analyses of **non aqueous samples** were performed with a Varian, Saturn 3900 chromatograph, coupled to a Saturn 2100T mass spectrometer on a CP-Sil 8 CB low bleed/MS column (5 % phenyl–95 % methylpolysiloxane, 30 m x 0.25 mm; film thickness 0.25 μm). Prior to analyses, 150 mL of the water sample were evaporated to dryness on a rotary evaporator and the residue was again dissolved in

1.5 mL of methanol. The injector was held at 270 °C, oven started at 100 °C, and then temperature was increased with a gradient of 5 °C min^{-1} till 320 °C and maintained constant for 5 min. The carrier gas was helium with a constant column flow of 1 mL min^{-1} and the injection volume was 5 μL. The mass spectrometer operated in electron ionisation mode with 35 μA filament current, the temperature of transferline was 173 °C and the scanning range of m/z from 35 to 300 amu with acquisition frequency of 0.5 scans s^{-1}.

Gas chromatography analyses of **aqueous samples** were performed with the same machine, but on a CP-WAX-57 CB wall-coated open-tubular (WCOT) fused silica column (1.2 μm polyethylene glycol phase, 25 m x 0.32 mm). The injector was held at 80 °C, oven started at 50 °C, and the temperature was increased with a gradient of 5 °C min^{-1} till 200 °C and maintained constant for 5 min. The carrier gas was helium with a constant column flow of 1 mL min^{-1} and the injection volume was 5 μL. The mass spectrometer operated in electron ionisation mode with 35 μA filament current, the temperature of transferline was 173 °C and the scanning range of m/z from 35 to 300 amu with acquisition frequency of 0.5 scans s^{-1}.

4.7.4 ^{1}H NMR spectroscopy

Extra analyses with ^{1}H NMR spectroscopy were performed in order to obtain complete information on the structure of products formed. 150 mL of irradiated aqueous solution was evaporated to dryness on a rotary evaporator and the residue was dissolved in 650 μL of methanol d$_4$. ^{1}H NMR spectra were recorded on a Bruker Avance DPX 300 spectrometer (300 MHz). Chemical shifts are reported against the tetramethylsilane standard.

4.7.5 Ion chromatography

The anions were determined on a Dionex IonPac AS4A separation column (250 mm x 4 mm). A mixture of sodium carbonate and sodium bicarbonate in water (1.8 mM: 1.7 mM) with a flow rate of 2 mL min^{-1} was used as the mobile phase. The injection volume was 100 μL. For quantification purposes a calibration curves for chloride and nitrate(V) ions was prepared and the r^2 value of the regression line for chloride was 0.998 and 0.997 for nitrate(V) ions.

4.7.6 TOC and TN analyses

TOC and TN concentration were analysed by TOC Analitik Jena AG multi N/C 3100, calibrated with potassium hydrogen phthalate and ammonium sulphate. Before analyzing, samples were acidified to pH 2–3 with hydrochloric acid. Mineralisation rate (M_r) was calculated using formula (22);

$$M_r = 100 - 100 \; x \; \left(\frac{TOC_t}{TOC_0}\right) \tag{22}$$

TOC_0: value of TOC in mg L^{-1} at time 0,
TOC_t: value of TOC in mg L^{-1} at time t.

4.7.7 UV-Vis measurements

The absorption spectra of 6CNA, IMP and TCP within all photodegradation experiments were recorded from 200–600 nm with the UV–Vis Hewlett Packard 8453 spectrophotometer and a Varian Cary 300 scan spectrophotometer.

4.7.8 Conductivity and pH measurements

The pH was measured using a pH meter, Hanna Instruments HI 8417, and the conductivity was monitored using a WTW Multi 3500i meter.

4.7.9 Statistical analysis

All experimental results were performed at least in triplicate (n > 3) in order to evaluate the reproducibility of measurements and the data are expressed as means ± standard deviation (SD).

4.8 Toxicity experiments with *Vibrio fischeri*

The toxicity tests with luminescent bacteria were separated into two main experiments:

- Determination of 30 min EC_{50} values for aqueous solutions of 6CNA, IMP and TCP,
- Monitoring of toxicity within different degradation experiments.

The toxicity of IMP, TCP and 6CNA (at initial concentrations of 108 mg L^{-1} for IMP, 104 mg L^{-1} for TCP and 110 mg L^{-1} for 6CNA) was assessed using liquid-dried luminescent bacteria *V. fischeri* NRRL B-11177 with system LUMIStox, Dr.LANGE. Before analyzing the samples, the pH adjustment to 7 ± 0.2 with hydrochloric acid or sodium hydroxide was performed as well as the addition of a proper amount of sodium chloride salt i.e. 2 % w/v in order to avoid possible adverse effects due to an incorrect pH value or inappropriate sodium chloride concentration. An aliquot containing *V. fischeri* was added to each vial in two parallels and luminescence was measured immediately. Afterwards, the selected sample was added to the vial with bacteria and thermostated to 15 ± 1 °C for 30 min. Various dilution levels (2, 4, 8, 16, 64, 128, and 256) were achieved by following ISO 11348-3 standard (ISO 11348-3; 2007). Luminescence was measured with a photomultiplier LUMIStox 300 luminometer and thermostated at 15 ± 1 °C. The luminescence of bacteria within the sample was again measured after 30 min of exposure and the inhibition of luminescence with 95 % confidence limits, according to ISO 11348-2 standard (ISO 11348-2; 2007), was calculated, using a model supported by computer software. The toxicity endpoint was determined as reduced luminescence emission after incubation with the presence of the selected chemical. The blank test was performed with 2 % w/v sodium chloride solution. The results are presented as luminescence inhibition in percentage and consequently, the 30 min EC_{50} values for IMP, TCP and 6CNA were determined.

The toxicity evaluation of irradiated samples within various degradation studies was performed with the same procedure as described above, but with no additional dilution levels. Prior to analyses, all samples were diluted 1:1 with 2 % w/v sodium chloride since the increase of luminescence inhibition during the irradiation processes was expected. The toxicity endpoint was determined as reduced luminescence emission after incubation with the presence of selected chemical or mixture and the results are presented as luminescence inhibition percentage within degradation experiments. This

way of presenting the toxicity results is commonly adopted in the literature (Sakkas *et al.*, 2004; Dell'Arciprete *et al.*, 2009, 2010; Kitsiou *et al.*, 2009).

4.9   Toxicity experiments with *Porcellio scaber*

4.9.1   Test organisms

Terrestrial isopods (*Porcellio scaber*, Isopoda, Crustacea) were collected in uncontaminated woodlands near Nova Gorica (Slovenia). Prior to experimentation, the animals were kept in a terrarium (20 cm x 35 cm x 20 cm) inside the laboratory. The terrarium was filled with a layer of moistened sand and soil (2–5 cm) and a thick layer of partly decomposed hazelnut tree leaves (*Corylus avellana*). The substratum in the terrarium was heated to 80 °C for several hours, in order to destroy predators (spiders) before the introduction of the isopods. Hazelnut tree leaves were collected from uncontaminated woodland near Nova Gorica (Slovenia) and air-dried at room temperature. The terrarium was sprayed daily with water to ensure high humidity and kept at room temperature up to one week before the experiments commenced.

4.9.2   Food preparation

Fallen and brown hazelnut tree leaves were collected in uncontaminated woodland near Nova Gorica (Slovenia) in autumn, dried at room temperature and herbarized. Dry leaves were afterwards cut up into pieces of approximately the same surface area and a weight of 100 ± 2 mg. Solutions of different concentrations of IMP, TCP and 6CNA were prepared from a standard solution diluted with double deionised water. 150 µL of the solution was applied with a pipette to the lower leaf surface as small droplets and evenly spread over the surface with a paintbrush. The treated leaves were left to dry before starting the experiment. The nominal concentrations of IMP, TCP and 6CNA in the leaves were 1, 10, 50 and 100 µg chemical/g dry food. Animals in the control group were fed with hazelnut tree leaves prepared in the same way, yet with double deionised water.

4.9.3   Experimental set-up

Adult animals with a body weight more than 20 mg were collected from the terrarium, precisely weighed and placed into plastic Petri dishes with a diameter of 9 cm and

height of 1.5 cm along with processed hazelnut tree leaves (*C. avellana*). Each animal was placed individually in a Petri dish together with a leaf contaminated with an exact amount of IMP, TCP or 6CNA. Humidity in all Petri dishes was maintained by regular spraying (every third day) with deionised water on the internal side of the upper lids, each time with approximately 1.3 ± 0.1 mL of water. All Petri dishes were put in a large covered glass container, which enabled keeping the relative humidity sufficiently high. Since the lipid peroxidation can be also caused by UV light, the experimental set-up was kept in the dark. The experiments consisted of 5 groups, a blank or unexposed group, and groups with 1, 10, 50, 100 µg chemical/g dry food. Separately, in each group, the total number of 12 animals were exposed. The experiments on isopods were run for 14 days, after which, the animals were weighed again. Faecal pellets and leaves were left for 10 days to dry and then they were carefully separated and weighed.

4.9.4 Determination of physiological parameters

On the basis of gathered data on the mortality, masses of animals, leaves and faeces, assimilation efficiency, consumption rate, faecal pellets production (defecation) as a measure of feeding activity and weight change of each exposed animal separately has been determined. For calculation of these parameters, the following equations were used;

assimilation efficiency (AE) was determined as (23):

$$AE = \frac{food\ consumed\ [mg] - faecal\ pellets\ [mg]}{food\ consumed\ [mg]} \qquad (23)$$

consumption rate (CR) was determined as (24):

$$CR = \frac{food\ consumed\ [mg]}{fresh\ body\ weight\ at\ end\ of\ experiment[mg]\ x\ days\ of\ experiment} \qquad (24)$$

faecal pellets production (FPP) was determined as (25)

$$FPP = \frac{faecal\ pellets\ [mg]}{fresh\ body\ weight\ at\ and\ of\ experiment\ [mg]\ x\ days\ of\ experiment} \qquad (25)$$

weight change (WC) was determined as (26):

$$WC = fresh\ body\ weight\ at\ end\ [mg] - fresh\ body\ weight\ at\ beginning[mg] \qquad (26)$$

4.9.5 Determination of lipid peroxidation

In addition to the physiological parameters, lipid peroxidation as marker of oxidative stress in the digestive glands (hepatopancreas) was determined. Lipid peroxidation (LP) was determined after the formation of a colourful product with malondialdehyde (MDA) and thiobarbituric acid (TBA) with maximum absorbance at 535 nm as already described in the literature (Ortega-Villasante, 2005) but with small modifications.

Animals were anesthetized with diethyl ether and afterwards decapitated with special tweezers. Four digestive glands were carefully removed, collected in an Eppendorf tube and dissolved in 600 μL of buffer solution (15 g CCl_3COOH, 24 mL 1 M HCl, 0,376 g TBA in 100 mL of double deionised water), afterwards, 5 μL of antioxidant solution was added (1.1 g butylhydroxytoluene in 100 mL of ethanol). The homogenisation of the sample was achieved by sonication and the protein denaturation was prevented by cooling down the Eppendorf tubes with ice. Samples were then incubated at 90 °C for 30 minutes in a thermoblock, cooled again on ice and then 1.2 mL of 1-butanol was added. To achieve the extraction of the colourful product, the centrifugation at 12000 rpm for 10 minutes was performed. The supernatant was collected and the absorbance was measured at 535 nm for TBA-MDA product and 600 nm for correction of non-specific turbidity. Detailed procedure is presented in Figure 17.
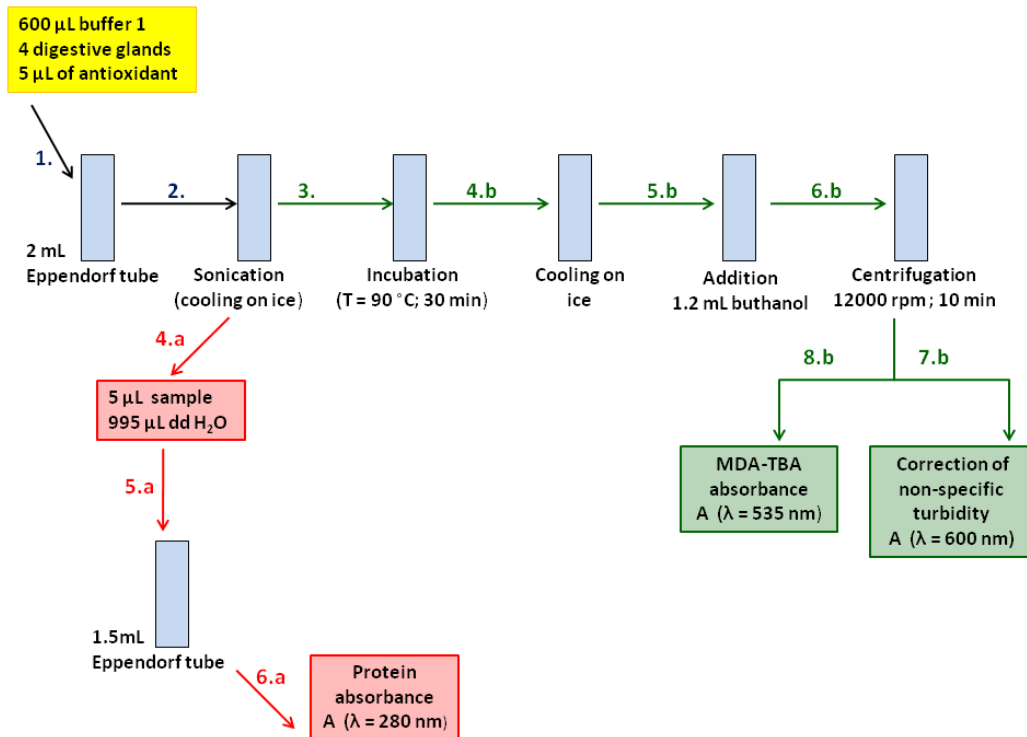
Figure 17: Schematic presentation of lipid peroxidation determination.

Before incubation of the samples at 90 °C, 5 µL of the homogenised sample was transferred into new Eppendorf tube and dissolved in 995 µL of double deionised water. Afterwards, the absorbance was measured at 280 nm in order to determine the protein content.

LP was therefore calculated as a ratio between TBA-MDA product absorbance and protein absorbance, equation (27):

$$LP = \frac{A\,(535\,nm) - A\,(600\,nm)}{A\,(280\,nm)} \tag{27}$$

Lipid peroxidation values are presented without units and were normalised by an average value of the unexposed group. This step enabled us easier comparison of results, since the value for the unexposed group was set as 1 and other values were therefore lower or higher.

4.9.6 Statistical analysis

The difference of measured parameters in the exposed and unexposed group were tested by non-parametric Mann-Whitney test, showing the significant difference when $p < 0.04$. The results are presented as black line for each animal and the red line indicates the median value.

5 RESULTS AND DISCUSSION

5.1 Liquid chromatography (HPLC-DAD) results and calibration curves

The retention times for HPLC-DAD chromatograms were as follows: for 6CNA 12.5 min, for IMP 6.6 min and for TCP 18.4 min. The HPLC-DAD chromatogram for IMP, TCP and 6CNA is presented in Figure 18.
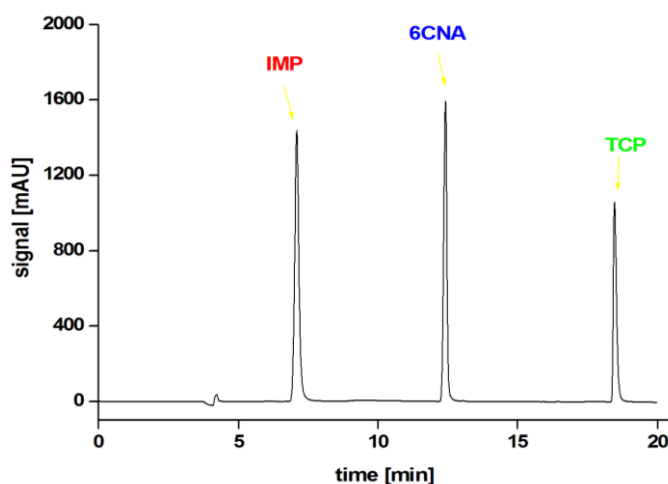
Figure 18: HPLC-DAD chromatogram of IMP, TCP and 6CNA standard solution.

The calibration curves for all three analytes are presented in Figure 19, Figure 20 and Figure 21. Furthermore, the r^2 values of the regression line were calculated and for 6CNA was 0.9985, for IMP 0.9998 and for TCP 0.9998.
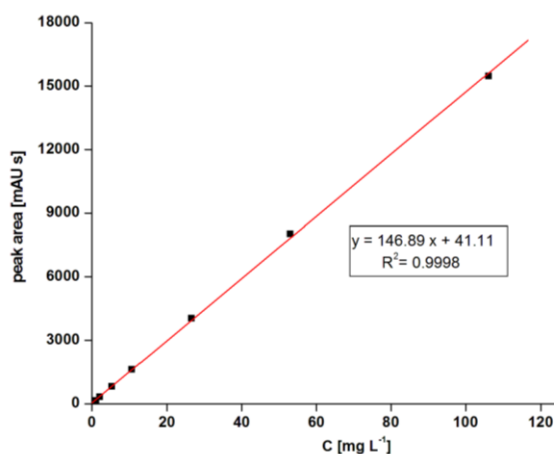
Figure 19: Calibration curve for IMP standard solution.
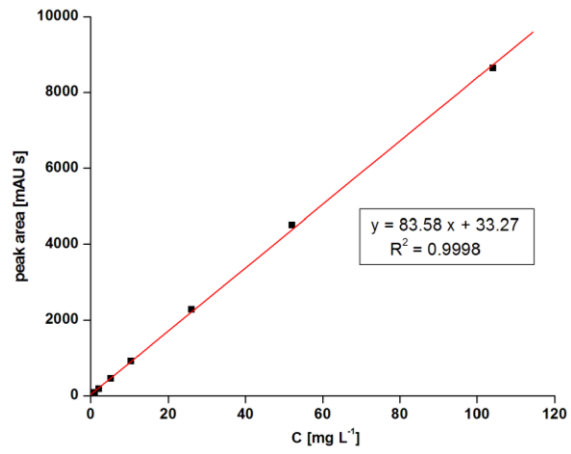
Figure 20: Calibration curve for TCP standard solution.
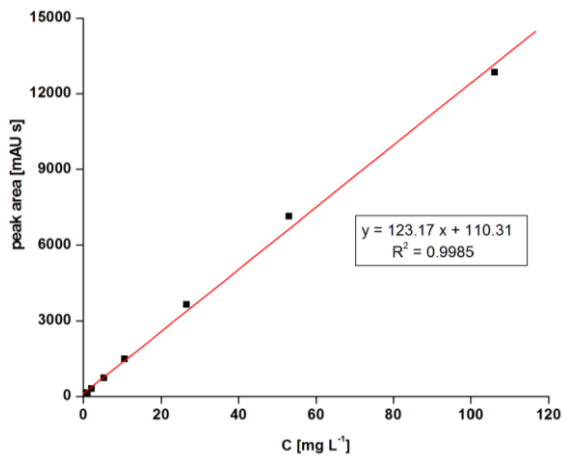
Figure 21: Calibration curve for 6CNA standard solution.

5.2 Stability studies under laboratory conditions

The results of stability tests for IMP, TCP and 6CNA in double deionised water performed at room temperature (22 °C) under exposure to sunlight and in the dark (in the refrigerator at 4 °C) are shown in Table 6.

Table 6: Disappearance rate (in %) of IMP, TCP and 6CNA within ageing in a refrigerator and under sunlight.

time [days]	refrigerator (T = 4°C) c/c_0[%]			sunlight (T = 22°C) c/c_0[%]		
	IMP	TCP	6CNA	IMP	TCP	6CNA
0	100.0	100.0	100.0	100.0	100.0	100.0
7	99.6	99.6	96.8	99.8	81.8	97.2
17	100.0	99.6	96.8	99.8	68.7	98.9
28	100.0	98.3	100.0	100.0	59.5	96.9
45	99.1	97.8	93.8	99.2	51.2	93.9
62	99.0	96.7	95.0	98.3	40.0	94.7
90	97.8	98.2	91.6	98.1	28.9	91.1

The experiments performed at 4 °C in the darkness clearly indicate that the degradation or transformation is very low in case of all three substances over the 90 days of experiment. Moreover, the concentration of IMP and 6CNA samples exposed to sunlight decreased for 2 % and 9 %, respectively, and can easily be compared with the samples kept in the refrigerator, where the observed decrease was very similar, i.e. 3 % and 8 %.

However, experiments with TCP performed at room temperature (22 °C) and exposed to sunlight led to an important transformation. Within 90 days of experimentation, 70 % conversion was observed, compared to the sample kept in the dark which resulted in only 2 % conversion. It should be noted, that this result clearly shows the transformation of TCP into another compound(s), which were not recorded and monitored at that time. It is worth mentioning that the TCP aqueous solution after a few days of exposure coloured slightly purple, indicating a possible formation of intermediate(s) with maximum absorbance in range of 320-400 nm.

The pH of the IMP solution during the period of 90 days on the laboratory desk did not change significantly, i.e. from starting 6.89 to 6.64 at the end of experiment. In the dark (refrigerator at 4 °C) the pH changed from starting at 6.89 to finally 5.93. This change cannot be connected with change in concentration, therefore I assume that an error occurred or contamination of an electrode occurred.

Meanwhile, the pH of the TCP aqueous solution on the laboratory desk changed significantly from 4.88 at the beginning to the 3.95 at the end, indicating the formation of possible acidic by-products, as described above. However, in dark conditions, the change in pH of the TCP was low from 4.88 to 5.09 at the end of experimentation.

On the other hand, the pH of the 6CNA aqueous solution on the laboratory desk did not change significantly during the period of 90 days i.e. from starting at 4.20 to 4.23. In the dark (refrigerator at 4 °C) the pH changed from starting at 4.20 to finally 4.24.

The stability of all samples was also tested within different pH (4, 7 and 10) and in the dark. It is worth noting, that no significant change in concentration was observed. However, in the literature, the molar absorption spectra of TCP as a function of pH have been proposed (Shemer *et al*., 2005). Nevertheless, the changes were very small and this may be the reason why I did not observe any changes in the TCP concentration when exposed to different pH.

Therefore, on the basis of gathered data, it can be assumed that at room temperature degradation or transformation of 6CNA and IMP is very slow and that 6CNA and IMP are not an easily degradable chemical when dissolved in double deionised water. On the contrary, TCP demonstrated to be a photosensitive chemical with fast transformation to another product. The pH value of media did not have an influence of IMP, TCP and 6CNA concentration changes.

5.3 Stability studies under simulated sunlight using SUNTEST apparatus

5.3.1 Stability study of IMP aqueous solution within simulated sunlight

Experimental data collected through HPLC-DAD and TOC measurements showed that the concentration of IMP within irradiation time of six hours decreased slightly within all three applied intensities, as shown in Table 7 and Table 8.

Table 7: Disappearance rate (in %) and mineralisation rate (in %) of IMP within stability studies under simulated sunlight (250 W m⁻²) for exposed samples and dark control.

IMP	250 W m^{-2}			
	dark control		*exposed samples*	
time [h]	C/C_0 [%]	TOC/TOC_0 [%]	C/C_0 [%]	TOC/TOC_0 [%]
0	100.0	100.0	100.0 ± 0.0	100.0 ± 0.0
1	99.3	96.2	99.6 ± 0.4	97.0 ± 0.7
2	99.3	97.2	99.7 ± 0.5	97.0 ± 0.5
3	99.3	95.6	99.1 ± 0.5	96.5 ± 0.2
4	98.9	95.6	99.5 ± 0.5	96.5 ± 0.3
5	99.1	97.2	99.1 ± 0.2	97.7 ± 0.7
6	99.1	98.3	99.3 ± 0.3	96.7 ± 0.1

In case of dark control, the concentration decreased by only 1 % and the TOC decreased by 2 %, therefore, I can easily conclude that no degradation took place. Since there was no thermal degradation observed in dark control, it was conducted just at single intensity.

Table 8: Disappearance rate (in %) and mineralisation rate (in %) of IMP within stability studies under simulated sunlight (500 W m⁻² and 750 W m⁻²) for exposed samples.

IMP	500 W m^{-2}		750 W m^{-2}	
time [h]	C/C_0 [%]	TOC/TOC_0 [%]	C/C_0 [%]	TOC/TOC_0 [%]
0	100.0 ± 0.0	100.0 ± 0.0	100.0 ± 0.0	100.0 ± 0.0
1	100.0 ± 0.0	100.0 ± 0.0	100.0 ± 0.0	99.0 ± 1.5
2	99.4 ± 0.4	99.7 ± 0.5	99.8 ± 0.3	99.0 ± 0.2
3	99.9 ± 0.2	99.8 ± 0.3	99.8 ± 0.2	99.2 ± 0.8
4	99.2 ± 0.8	98.1 ± 0.2	99.8 ± 0.0	99.3 ± 1.0
5	99.8 ± 0.3	99.7 ± 0.3	99.9 ± 0.0	100.3 ± 0.0
6	100.1 ± 0.0	97.9 ± 0.0	100.3 ± 0.0	99.1 ± 0.7

The disappearance of IMP after six hours expressed in percentage is very low at all intensities. The concentration did not decrease more than 1 % and it can be easily neglected or considered as normal error within the measurements. Moreover, the low levels of TOC decrease (in all cases less than 3 %) confirmed the fact that no mineralisation occurred within the employed conditions. It turned out, that the TOC/TOC_0 and C/C_0 ratio at certain measurements exceeded the value of 100 %. However, this does not indicate an increase in concentration during treatment, but only could be an uncertainty within the measurements.

This fact was also further confirmed by UV-Vis measurements, as shown in Figure 22, where no change in absorbance spectra, for all intensities within exposure time, was observed.
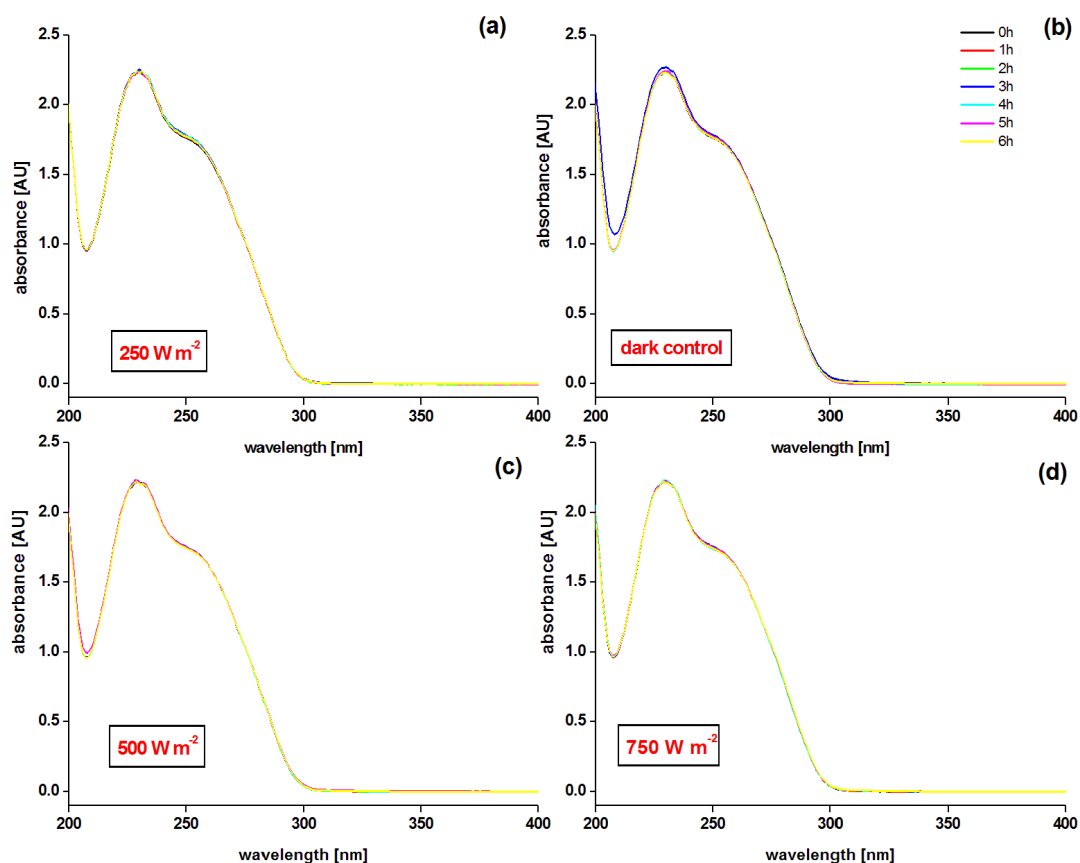
Figure 22: UV-Vis absorbance spectra of IMP aqueous solution during stability studies under simulated sunlight for 250 W m⁻² (a), for dark control (b), for 500 W m⁻² (c) and for 750 W m⁻² (d).

It can be easily observed, that the absorbance spectra remained the same for all six hours of exposure throughout all conditions, including the dark control, and therefore confirmed the HPLC and TOC results that no degradation occurred.

Additional attention was also paid to the toxicity testing, where even small changes can be reflected in higher toxicity of treated samples. The toxicity of selected samples was tested with the luminescent bacteria *V. fischeri*, for all conditions employed and were compared also with a dark control. The samples were taken at time intervals 0, 2, 4 and 6 hours. The results are presented in Figure 23.
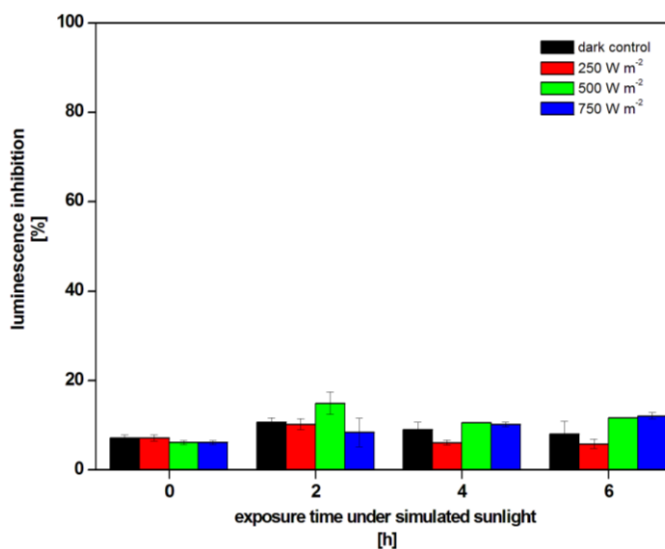
Figure 23: Luminescence inhibition for **V. fischeri** *of IMP aqueous solution during stability studies under simulated sunlight for dark control, for 250 W m⁻², for 500 W m⁻² and for 750 W m⁻².*

From Figure 23 it can be observed that the luminescence inhibition for all samples did not differentiate significantly. After two hours of exposure time at irradiance 500 W m⁻², there appeared to be a slight increase in toxicity inhibition. However, the increment is low, i.e. 4 %, and it can be attributed to the fact, that the toxicity testing includes live organisms, where the standard deviation could sometimes be quite significant. Therefore, the data clearly pointed out, that toxicity did not increase during exposure.

When taking into account all gathered data within six hours of experimentation under simulated sunlight conditions using Suntest apparatus, I can conclude that IMP when dissolved in double deionised water, would not degrade even at the high intensities applied. As a result, the toxicity of the luminescent bacteria *V. fischeri* did not increase.

5.3.2 Stability study of 6CNA aqueous solution within simulated sunlight

Very similar scenario, as with IMP stability, was observed also with the 6CNA aqueous solution when exposed to simulated sunlight conditions for six hours. The HPLC-DAD and TOC measurements (Table 9 and Table 10) revealed slight change in concentration for the dark control (3 % for TOC), proposing that no degradation occurred and therefore, the dark control was again conducted just at single intensity.

Table 9: Disappearance rate (in %) and mineralisation rate (in %) of 6CNA within stability studies under simulated sunlight (250 W m^{-2}) for exposed samples and dark control.

6CNA	250 W m^{-2}			
	dark control		*exposed samples*	
time [h]	C/C_0 [%]	TOC/TOC_0 [%]	C/C_0 [%]	TOC/TOC_0 [%]
0	100.0	100.0	100.0 ± 0.0	100.0 ±0.0
1	100.0	96.8	99.9 ± 0.0	97.7 ± 1.5
2	99.8	96.5	99.8 ± 0.3	97.2 ± 1.2
3	100.0	97.6	99.7 ± 0.1	96.9 ± 2.1
4	100.0	97.2	99.8 ± 0.0	97.6 ± 3.4
5	99.8	95.7	99.4 ± 0.2	96.3 ± 1.7
6	99.6	97.3	99.8 ± 0.2	97.0 ± 2.6

Table 10: Disappearance rate (in %) and mineralisation rate (in %) of 6CNA within stability studies under simulated sunlight (500 W m^{-2} and 750 W m^{-2}) for exposed samples.

6CNA	500 W m^{-2}		750 W m^{-2}	
time [h]	C/C_0 [%]	TOC/TOC_0 [%]	C/C_0 [%]	TOC/TOC_0 [%]
0	100.0 ± 0.0	100.0 ± 0.0	100.0 ± 0.0	100.0 ± 0.0
1	99.9 ± 0.1	99.3 ± 1.0	99.6 ± 0.3	99.8 ± 0.4
2	100.0 ± 0.0	99.7 ± 0.5	99.9 ± 0.2	99.4 ± 0.8
3	99.9 ± 0.2	98.0 ± 0.8	99.6 ± 0.4	99.8 ± 0.2
4	100.0 ± 0.0	98.5 ± 0.5	99.5 ± 0.1	98.1 ± 1.1
5	99.7 ± 0.4	98.1 ± 0.2	99.8 ± 0.2	99.5 ± 0.8
6	100.2 ±0.0	98.3 ± 0.4	99.1 ± 0.1	98.0 ± 0.0

Samples exposed to different intensities revealed almost no degradation of the parent compound. The concentration did not decrease more than 1 % and consequently low levels of TOC decrease during experimentation were noticed, in all cases less than 3 %. The C/C_0 ratio at certain measurements exceeded the value of 100 %. Again, this can be neglected and considered as a possible uncertainty within the measurements.

This fact was further confirmed also by UV-Vis measurements shown in Figure 24, where the absorbance spectra of the dark control, as well as of samples taken at different intensities, did not change at all during the six hours of experimentation.
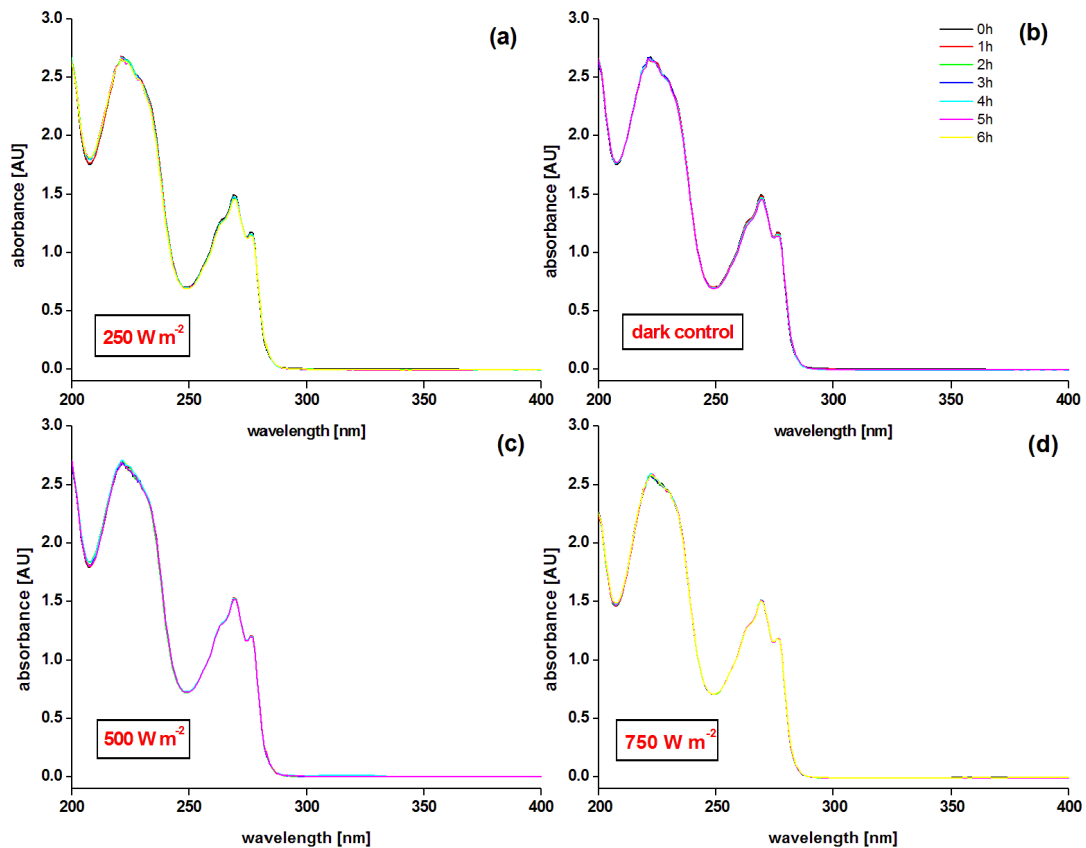
Figure 24: UV-Vis absorbance spectra of 6CNA aqueous solution during stability studies under simulated sunlight for 250 W m^{-2} (a), for dark control (b), for 500 W m^{-2} (c) and for 750 W m^{-2} (d).

The toxicity testing with *V. fischeri* was performed, in order to assess the possible increase in toxicity. The samples were taken at time intervals 0, 2, 4 and 6 hours. The results are presented in Figure 25, and they indicate an increase in luminescence inhibition for all samples from roughly 5 % to approximately 12 % for all samples at the end of experimentation. However, in my opinion, this increase cannot be due to the formation of new by-products. Since the luminescence inhibition increase was for all samples the same, including the dark control, there could be an uncertainty within the measurements, or an influence of different packaging of bacteria used during toxicity testing. Nevertheless, the luminescence inhibition is still very low and the samples cannot be considered as toxic to *V. fischeri* bacteria.
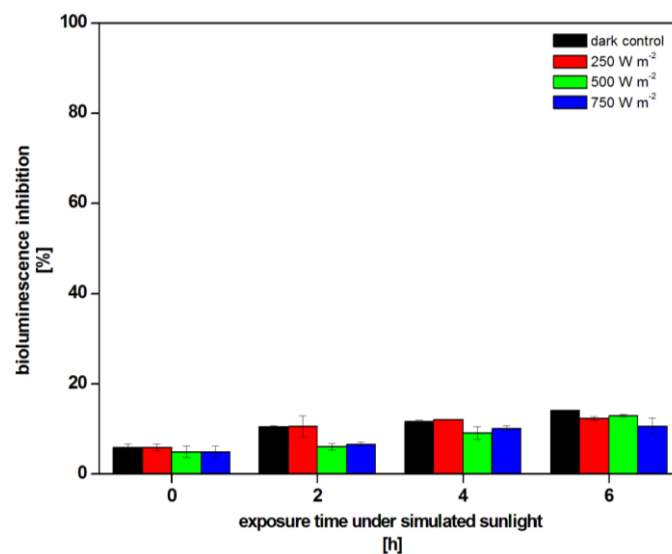
Figure 25: Luminescence inhibition for V. fischeri *of 6CNA aqueous solution within stability studies under simulated sunlight for dark control, for 250 W m^{-2}, for 500 W m^{-2} and for 750 W m^{-2}.*

The toxicity results correlate with HPLC-DAD, TOC and UV-Vis data collected within six hours of experimentation and therefore all raised data indicating that 6CNA also acts like persistent chemical under simulating sunlight conditions within all the experiment conditions applied.

5.3.3 Stability study of TCP aqueous solution within simulated sunlight

The stability testing of TCP under simulated sunlight conditions revealed a totally different scenario as in case of IMP and 6CNA. Plotting $\ln(C/C_0)$ versus irradiation time resulted in a linear relationship indicating pseudo first-order degradation kinetics for all intensities applied. Therefore, the slope gives the pseudo first-order degradation rate constant, as shown in Figure 26.
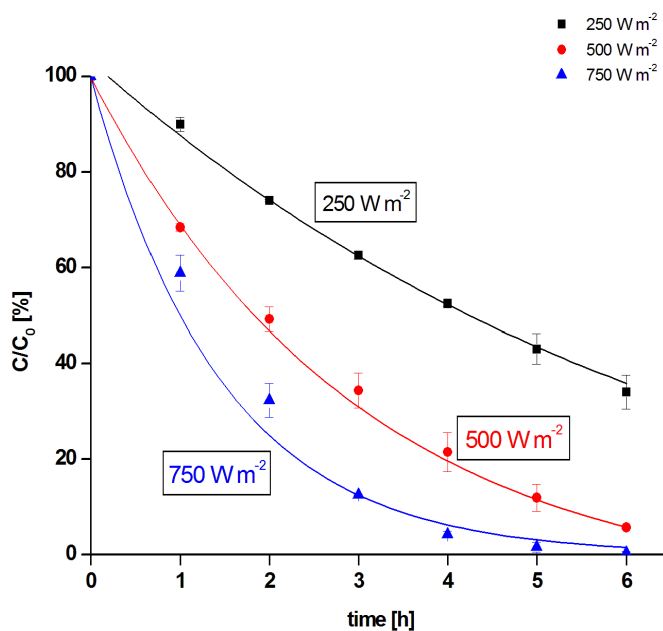
Figure 26: A first-order disappearance curve for TCP aqueous solution within stability studies under simulated sunlight for 250 W m^{-2} (■), for 500 W m^{-2} (●) and for 750 W m^{-2} (▲).

Experimental data showed that the concentration of TCP within six hours of irradiation at intensity 250 W m^{-2} decreased for 65.9 ± 3.5 % with an observed disappearance rate constant of k = 0.186 ± 0.008 h^{-1} and a half-life $t_{1/2}$ of 3.9 ± 0.1 h. At intensity 500 W m^{-2} the initial concentration of TCP decreased for 94.3 ± 0.4 %, with rate constant of k = 0.461 ± 0.001 h^{-1} and a half-life $t_{1/2}$ of 1.5 ± 0.0 h. When employing 750 W m^{-2} the concentration decreased for 99.5 ± 0.2 %, again with first-order decay kinetics with disappearance rate constant of k = 0.920 ± 0.006 h^{-1} and a half-life of $t_{1/2}$ of 0.8 ± 0.0 h.

No degradation was noticed during the dark experiment, suggesting that temperature did not rise so much, that thermal decomposition could be promoted.

Photodegradation of the TCP in an aqueous solution with a medium-pressure mercury lamp in the range 200-400 nm was already described in the literature, exhibiting also pseudo first-order degradation kinetics with a maximum photodegradation rate at pH 6 and above (Shemer *et al.*, 2005).

Absorbance spectra for TCP aqueous solution recorded during exposure to simulated sunlight conditions confirmed results collected by HPLC-DAD measurements and revealed a high decrease of absorbance in the range from 290-340 nm for all three employed intensities, as shown in Figure 27.
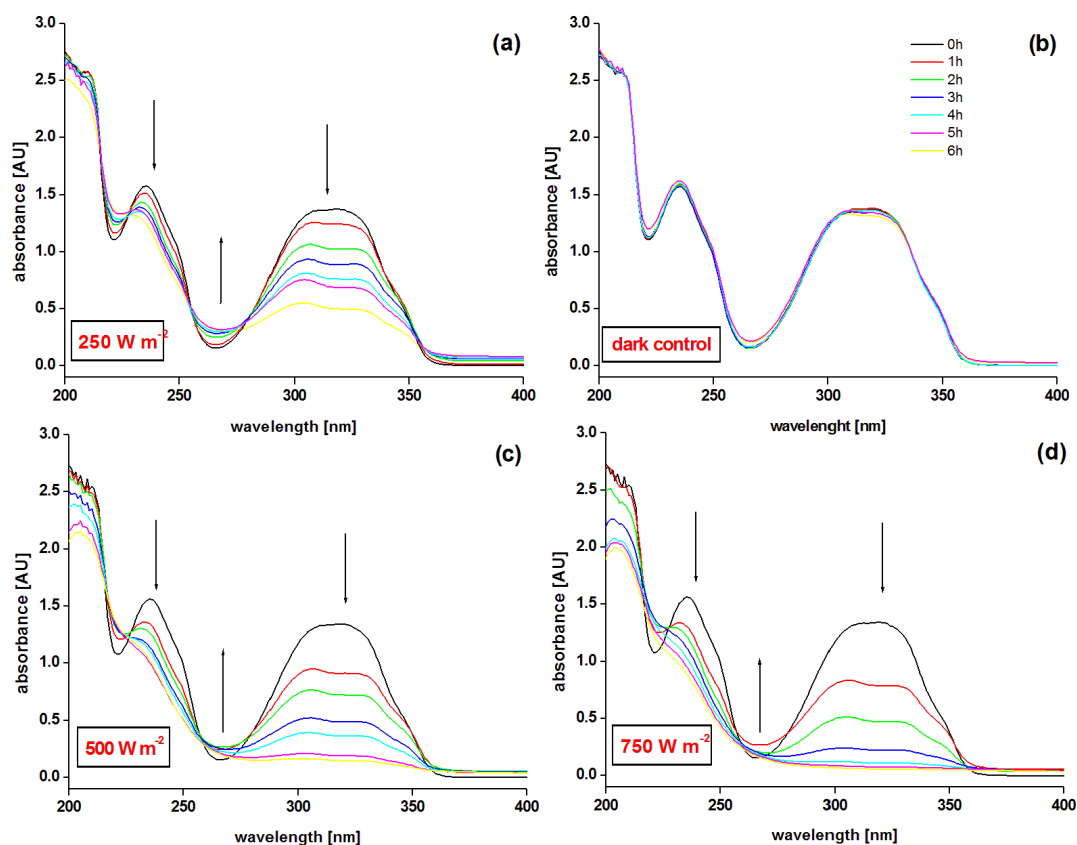
Figure 27: UV-Vis absorbance spectra of TCP aqueous solution during stability studies under simulated sunlight for 250 W m^{-2} (a), for dark control (b), for 500 W m^{-2} (c) and for 750 W m^{-2} (d).[1]

The presence of an isobestic points indicate that a photochemical reaction occurred. In contrast, the absorbance spectra of dark control did not change at all with time.

TOC measurements of samples (Table 11) showed negligible decrease in organic carbon in all the sets of experiments, as well in the dark control. At all intensities applied, the TOC values decreased less than 4 %. Therefore, the mineralization processes were not achieved and it can be assumed that TCP was, therefore, transformed to other compound(s). The TOC/TOC$_0$ ratio at certain measurements exceeded the value of 100 % and as mentioned in previous experiments, this small change could be due to an uncertainty within the measurements.

---

[1]The (↑) indicates increase of absorbance in and (↓) indicates decrease of absorbance within exposure.

Table 11: Mineralisation rate (in %) of TCP within stability studies under simulated sunlight (dark control, 250 W m⁻², 500 W m⁻² and 750 W m⁻²) for exposed samples.

TCP	dark control	250 W m⁻²	500 W m⁻²	750 W m⁻²
time [h]	TOC/TOC_0 [%]	TOC/TOC_0 [%]	TOC/TOC_0 [%]	TOC/TOC_0 [%]
0	100.0	100.0 ± 0.0	100.0 ± 0.0	100.0 ± 0.0
1	102.7	101.7 ± 0.0	98.1 ± 0.7	99.9 ± 0.1
2	102.0	101.0 ± 0.9	100.4 ± 0.1	98.1 ± 0.3
3	101.7	102.1 ± 0.2	99.5 ± 1.0	97.7 ± 0.9
4	102.0	101.7 ± 0.5	100.2 ± 0.2	95.1 ± 0.2
5	103.0	101.6 ± 0.7	98.3 ± 3.0	93.6 ± 0.0
6	100.1	99.7 ± 0.4	97.1 ± 1.9	95.5 ± 0.8

The degradation of TCP itself in aqueous solution under simulated sunlight conditions was assessed through HPLC-DAD and UV-Vis measurements. Additionally, the toxicity testing with *V. fischeri* was performed. The samples were taken every hour during experimentation thus compared along with the dark control where no degradation/transformation was observed. The Figure 28 clearly indicates the increase of luminescence inhibition with the time of exposure.
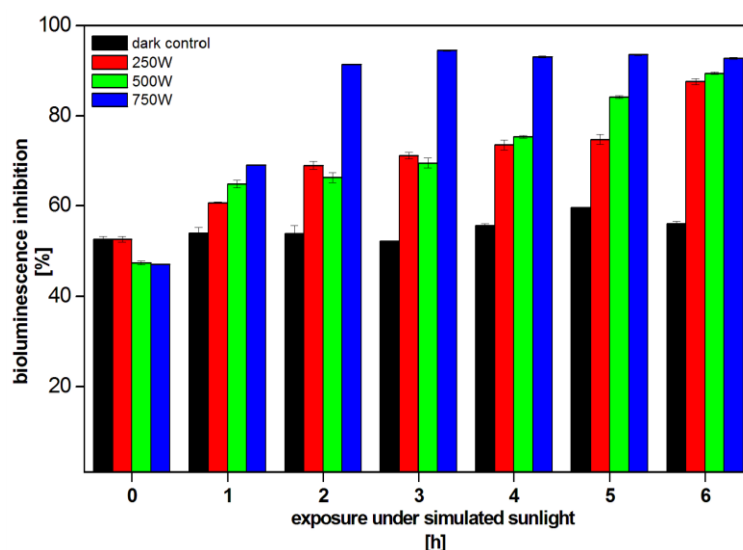
Figure 28: Luminescence inhibition for V. fischeri *of TCP aqueous solution during stability studies under simulated sunlight for dark control, for 250 W m⁻², for 500 W m⁻² and for 750 W m⁻².*

The lowest increase was observed when employing intensity 250 W m⁻² from 52.6 ± 0.7 % at the beginning to 87.6 ± 0.7 % at the end of experiment. When using the intensity of 500 W m⁻², the toxicity rose from 47.5 ± 0.5 % at the beginning to 89.5 ± 0.3 % at the end. The highest increase of toxicity was detected at intensity 750 W m⁻² where also the highest disappearance of TCP was noticed. The luminescence inhibition increased from 47.1 ± 0.0 % at the beginning to 92.8 ± 0.2 % at the end. It needs to be mentioned, that

the inhibition of luminescence for the highest intensity rose rapidly after starting the experiment and after two hours reached a plateau of approximately 90 %. Meanwhile, the luminescence inhibition for dark control did not change with time. These facts lead me to conclusion that more toxic product(s) than parent compound were formed.

In order to characterise the possible newly formed by-products, the first approach was to compare and evaluate the HPLC-DAD chromatograms collected within exposure time to detect any new peaks, as shown in Figure 29.
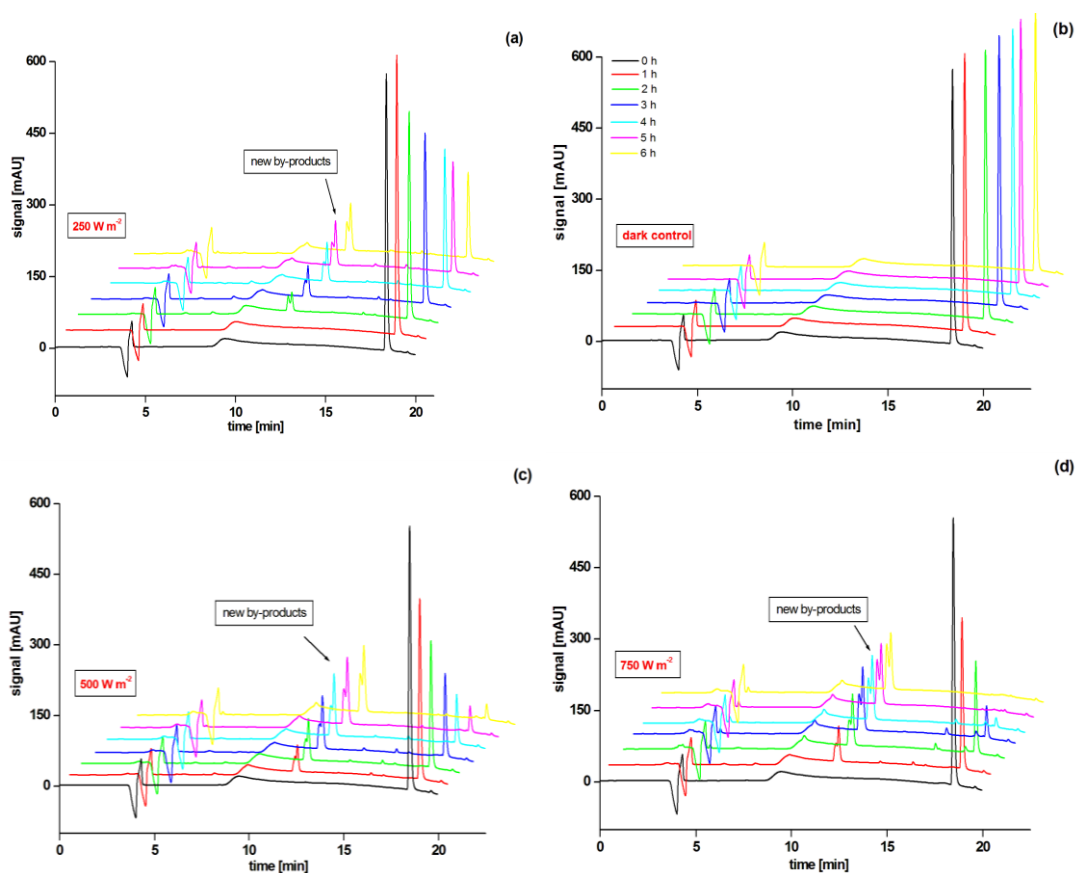
Figure 29: HPLC-DAD chromatograms of TCP aqueous solution during stability studies under simulated sunlight for 250 W m^{-2} (a), for dark control (b), for 500 W m^{-2} (c) and for 750 W m^{-2} (d).

From the chromatograms it is clearly seen, that formation of new and more polar by-products took place when irradiation under simulated sunlight conditions was performed. With all three intensities applied, the chromatographic peak at the retention time of approximately 11 min was detected, thus the intensities of the peaks were different when applying different conditions, according to the transformation of TCP. In case of the dark control, no disappearance of the parent compound was noticed and consequently no additional peaks were observed.

Furthermore, within all experiments, the pH of the solution was monitored and the results are presented in Table 12. The results of pH measurements clearly correlate with all data described above within the stability studies under simulated sunlight of TCP. During all experiments the pH drastically decreased, indicating a formation of acidic by-products. The decrease in pH is obviously associated with intensity applied – the higher in intensity, the more by-products are formed and as a result the pH of the solution lowers. On the contrary, the pH value of the dark control did not change significantly.

Table 12: The pH of TCP aqueous solution during stability studies under simulated sunlight for dark control, for 250 W m^{-2}, for 500 W m^{-2} and for 750 W m^{-2}.

time [h]	dark control	250 W m^{-2}	500 W m^{-2}	750 W m^{-2}
0	4.57	4.57	4.55	4.55
1	4.51	4.39	3.80	3.73
2	4.56	4.35	3.50	3.45
3	4.39	3.93	3.28	3.28
4	4.48	3.62	3.09	3.24
5	4.40	3.39	3.06	3.19
6	4.39	3.31	3.14	3.19

To have a better insight into the new by-products formed, additional analyses with LC-MS and GC-MS on CP-WAX 75 CB column as well as on CP-Sil 8 CB low bleed/MS column were performed. Unfortunately, as reported in the literature (Bavcon Kralj *et al.*, 2007b) the identification of TCP via GC-MS was unsuccessful, therefore, the LC-MS technique was further used. For the HPLC-DAD analyses, the Zorbax C_8 column was used, however for LC-MS analyses this column could not be utilised due to its bad signal/noise ratio. Therefore, a new monolith C_{18} column Purospher STAR from Merck was introduced and used for further separation processes. The gradient for mobile phases was carefully selected and optimised and is presented in Chapter 4.7.2 LC-ESI-MS/MS analyses.

The results of direct injection of TCP into the ESI-MS system indicated that the negative mode is the most suitable method regarding intensity and fragmentation. On the basis of the total ion chromatograms (TIC) for the TCP analytical standard and TCP exposed for 6 h to simulated sunlight, the new peaks were characterised.

Parent compound - TCP

The parent compound (TCP) eluted with the retention time 17.3 min and fragmentation resulted in major ESI$^-$ ions with *m/z* 196 [M–H–1], 198 [M–H+2] and 200 [M–H+4]

which can be attributed to the quasi-molecular ion of TCP (197 g mol^{-1}, taking the mass of chlorine 35 g mol^{-1}). Thus, taking into account that the molecule contains three chlorine atoms and therefore, the occurrence of the typical intensity signals pattern for molecules containing three chlorine atoms was also observed.

By-product(s) **A**

Additionally, the TIC of all samples after six hours of treatment revealed new peaks and this is completely in accordance with HPLC-DAD data described above. In all treated samples, a new peak at retention time <u>11.4 minutes</u> was observed with major ESI[-] ions with *m/z* 134, 136 and 138 (**A**), indicating a new compound with two chlorine atoms. The molecular mass of the new compound is 62 amu lower than that of the starting compound TCP, considering also loss of one chlorine atom, the difference would be 27 amu lower. It needs to be noted, that the tailing of the new chromatographic peak was obvious. Therefore, I assumed the formation of different isomers, which cannot be separated by the HPLC-DAD or LC-MS technique.

The photodegradation of TCP in an aqueous solution is not well described in the literature, in fact there is only one research (Feng *et al.*, 1998) conducting this experiment, thus with germicidal lamp and GC-MS technique with silylated derivatization. To my knowledge, there have not been, as yet, any attempts to describe the behaviour of TCP under sunlight and characterization of possible photodegradation products by the LC-MS technique.

Therefore, on the basis of published data (Feng *et al.*, 1998) and also on the basis of my results, I can propose possible structure(s) of product (**A**) as shown in Figure 30.
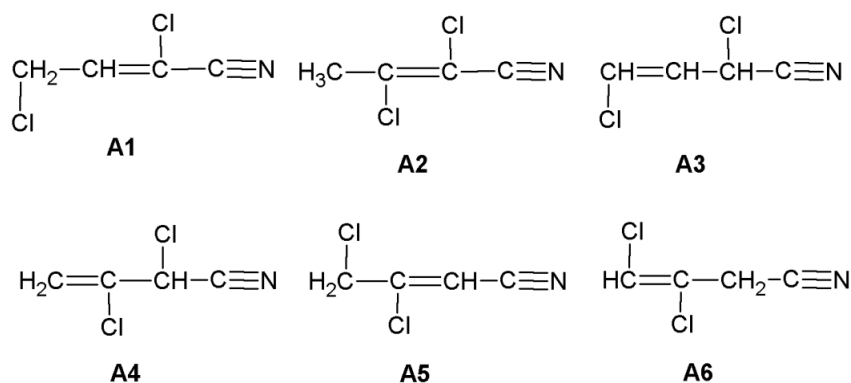
Figure 30: Proposed structures for TCP photodegradation products under simulated sunlight conditions; 2,4-dichloro-2-but-en-nitrile (A1), 2,3-dichloro-2-but-en-nitrile (A2), 2,-4-dichloro-3-but-en-nitrile (A3), 2,3-dichloro-3-but-en-nitrile (A4), 3,4-dichloro-2-but-en-nitrile (A5) and 3,4-dichloro-3-but-en-nitrile (A6).

These possible products could be a 2,4-dichloro-2-but-en-nitrile (**A1**), 2,3-dichloro-2-but-en-nitrile (**A2**), 2,-4-dichloro-3-but-en-nitrile (**A3**), 2,3-dichloro-3-but-en-nitrile (**A4**), 3,4-dichloro-2-but-en-nitrile (**A5**) and 3,4-dichloro-3-but-en-nitrile (**A6**). As can be seen from Figure 31, the cleavage of the pyridine ring took place within the photodegradation experiments and formation of a linear molecule has been proposed.

However, the pyridine ring consisted of five carbon atoms; while in products (**A1-A6**) the linear molecule consists of just four carbon atoms. When taking into consideration that the mineralization rate was negligible, possible formation of small molecules containing carbon was plausible, for example, HCOCl. However, the confirmation via LC-MS or GC-MS was not successful. Nevertheless, this small molecule was not detected using the LC-MS technique.

By-product(s) **B**

In addition, the LC-MS technique revealed a new peak at retention time 13.6 minutes, giving the major ESI$^-$ ion with *m/z* 178, 180 and 182 (**B**), indicating an occurrence of a molecule with two chlorine atoms. Again, the few positional isomers that could be formed, are suggested in Figure 31.

B1   **B2**   **B3**
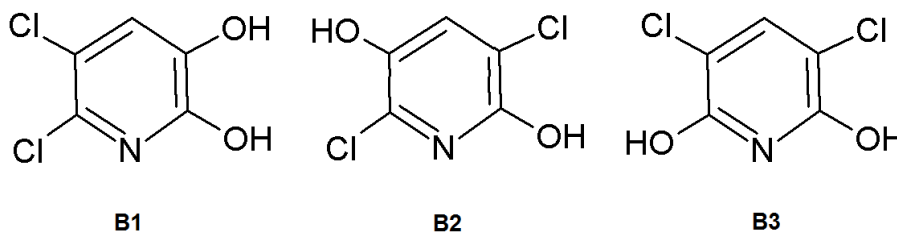
Figure 31: Suggested structures for TCP photodegradation products under simulated sunlight conditions; 5,6-dichloro-2,3-pyridin-diol (B1), 3,6-dichloro-2,5-pyridin-diol (B2) and 3,5-dichloro-2,6-pyridin-diol (B3).

These products could be 5,6-dichloro-2,3-pyridin-diol (**B1**), 3,6-dichloro-2,5-pyridin-diol (**B2**) and 3,5-dichloro-2,6-pyridin-diol (**B3**). Therefore, on the basis of the TCP structure, reaction conditions, LC-MS results and literature data (Feng *et al.*, 1998) I can propose the structures of all possible photodegradation product isomers as shown in Figure 31.

When taking into account all experimental data using Suntest apparatus, I can believe that TCP when dissolved in double deionised water acts like photosensitive chemical that would further transform into several other compounds, mostly isomers. However, from an environmental point of view, this transformation is not favourable due to a significant increase in luminescence inhibition for *V. fischeri* bacteria.

5.4 Photodegradation studies with a monochromatic low-pressure mercury lamp (245 nm)

The influence of the germicidal lamp emitting monochromatic light at 254 nm on the stability of IMP, TCP and 6CNA was assessed as possible changes in concentration within irradiation time were monitored. Experiments were performed in aerated as well as in deoxygenated aqueous solutions. Deoxygenated conditions were achieved by bubbling the solutions with argon for approximately 10 minutes. Under both experimental conditions, similar results were obtained for all three investigated solutions. In Table 13 the percentages of the initial concentrations still remained in the aerated solution for each sample after given irradiation times are presented.

Within 30 minutes of irradiation in an <u>aerated solution</u>, the highest disappearance rate was achieved for the TCP aqueous solution – it retained just 54 % of its initial concentration, but for the 6CNA and IMP the remaining concentrations in the solution were still relatively high, i.e. 90 % and 85 %, respectively, indicating that disappearance was not achieved.

Table 13: Disappearance rate (in %) of IMP, TCP and 6CNA within irradiation time with low-pressure mercury lamp (254 nm) in presence of oxygen, measured by HPLC-DAD.

time [min]	IMP		TCP		6CNA	
	C/C_0 [%]	C [mol L^{-1}]	C/C_0 [%]	C [mol L^{-1}]	C/C_0 [%]	C [mol L^{-1}]
0	100.0	1.18×10^{-4}	100.0	1.09×10^{-4}	100.0	1.35×10^{-4}
5	96.2	1.13×10^{-4}	83.9	9.15×10^{-5}	98.2	1.33×10^{-4}
10	93.7	1.11×10^{-4}	74.0	8.06×10^{-5}	96.6	1.30×10^{-4}
20	89.7	1.06×10^{-4}	61.7	6.73×10^{-5}	98.5	1.25×10^{-4}
30	84.6	9.98×10^{-5}	54.4	5.93×10^{-5}	89.8	1.21×10^{-4}

However, for <u>deoxygenated conditions</u>, within 20 minutes of irradiation, the highest disappearance rate was again achieved by the TCP aqueous solution – it retained just 62 % of its initial concentration, and again for the 6CNA and IMP the remaining concentrations in the solution were still relatively high, i.e. 85 % and 90 %, respectively. In Table 14 the percentages of initial concentrations still remained in the aerated solution for each sample after given irradiation times are presented.

Table 14: Disappearance rate (in %) of IMP, TCP and 6CNA within irradiation time with low-pressure mercury lamp (254 nm) in absence of oxygen measured by HPLC-DAD.

time [min]	IMP		TCP		6CNA	
	C/C_0 [%]	C [mol L^{-1}]	C/C_0 [%]	C [mol L^{-1}]	C/C_0 [%]	C [mol L^{-1}]
0	100.0	1.18×10^{-4}	100.0	1.09×10^{-4}	100.0	1.35×10^{-4}
5	97.1	1.15×10^{-4}	84.7	9.23×10^{-5}	95.2	1.28×10^{-4}
10	95.2	1.12×10^{-4}	73.5	8.01×10^{-5}	90.6	1.22×10^{-4}
20	90.2	1.06×10^{-4}	62.2	6.78×10^{-5}	84.5	1.14×10^{-4}

The disappearance of all three studied products in aqueous solutions was also monitored by UV-Vis spectroscopy within 200–400 nm or 200-600 nm. In Figures 32, 33 and 34 the absorption spectra of IMP, TCP and 6CNA in aerated and deoxygenated conditions are given as a function of irradiation time and compared.
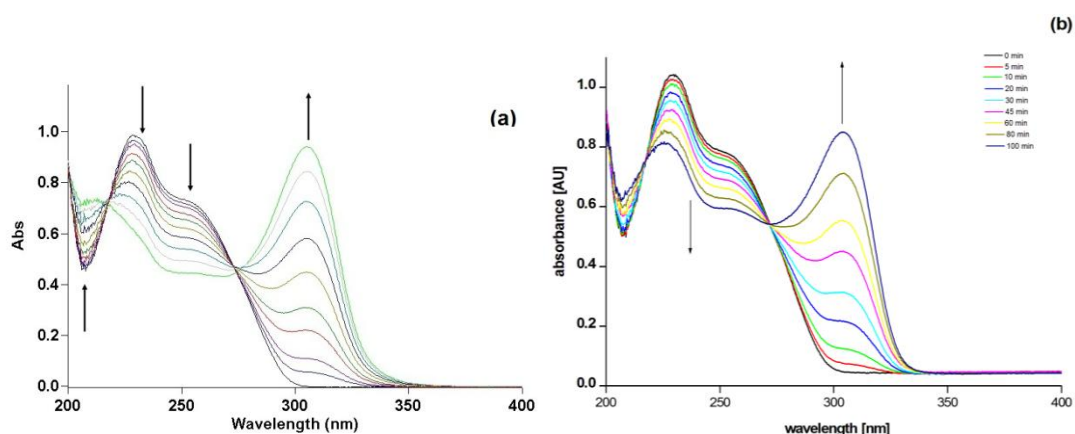
Figure 32: Absorption spectra for the aerated solution of IMP (a) and deoxygenated solution (b) upon excitation at 254 nm for 100 minutes. [2]

As shown in Figure 32a, the 254 nm irradiation of an aerated solution of IMP, led to important changes in the absorption spectrum. In the case of the aerated solution, the absorbance decreased within the wavelength range 225-275 nm which clearly reflects the photodegradation of IMP, whereas the absorbance significantly increased at wavelength range 275-340 owing to the formation of by-product(s). The presence of isobestic points were observed at 275 nm and 220 nm which lead to the conclusion that a clean photochemical reaction was occurring.

Meanwhile, the absorption spectra of deoxygenated solution of IMP, as shown in Figure 32b, also resulted in change of absorbance. The absorbance again decreased within the wavelength range 225-275 nm which clearly reflects the photodegradation of IMP, and a significant increase was observed at wavelength range 275-340 nm. It is worthy of

---

[2]The (↑) indicates increase of absorbance and (↓) indicates decrease of absorbance within exposure.

mention, that the higher increase in absorbance was noticed within aerated conditions, this is completely in accordance with HPLC-DAD data obtained in both conditions. Again, the presence of isobestic points was observed at 275 nm and 220 nm.

The same procedure was again recorded for the TCP aqueous solution upon excitation at 254 nm for 100 minutes. Detailed spectra of aerated and deoxygenated solutions are presented in Figure 33.
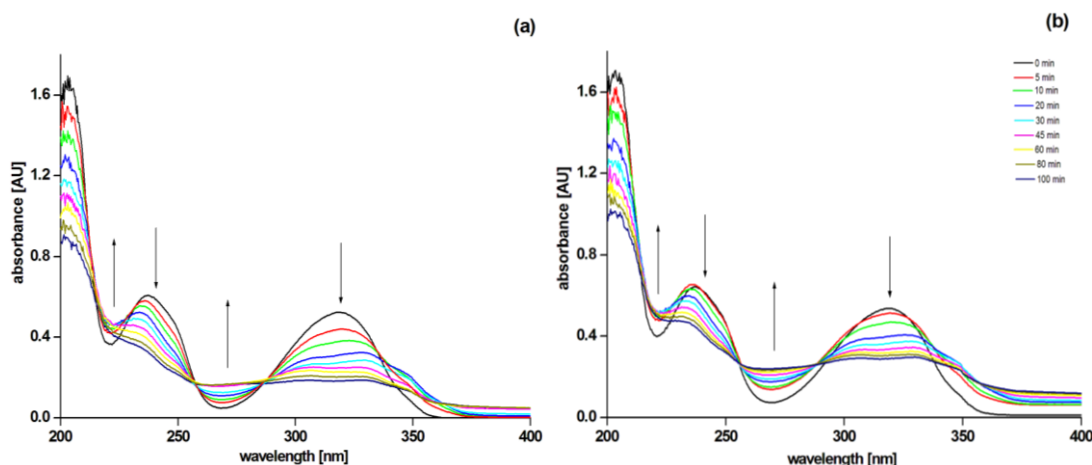
Figure 33: Absorption spectra for the aerated solution of TCP (a) and deoxygenated solution (b) upon excitation at 254 nm for 100 minutes.[3]

A similar trend has been observed in the case of TCP irradiation at 254 nm at aerated and deoxygenated conditions, Figure 33. In both cases, the absorbance decreased within the wavelength range 225-255 nm and 290-340 nm which demonstrates the transformation of TCP. However, in both cases the absorbance slightly increased within the wavelength range 255-290 nm and this was again attributed to the newly formed by-product. The HPLC-DAD measurements indicated, that the disappearance of TCP is slightly faster within aerated conditions, consequently the decrease in absorbance in the range 290-340 nm in Figure 33a is higher as in the case of deoxygenated conditions in Figure 34b.

Nevertheless, the photolytic degradation of TCP in an aqueous solution with a 30 W germicidal lamp was previously described in the literature showing a fast disappearance rate and a half-life time of approximately 25 minutes (Feng *et al.*, 1998). Further kinetic parameters were not described in detail.

---

[3]The (↑) indicates increase of absorbance and (↓) indicates decrease of absorbance within exposure.

Finally, the absorbance spectra for the 6CNA aqueous solution upon excitation at 254 nm for 100 minutes were compared and investigated and therefore, detailed spectra of aerated and deoxygenated solutions are presented in Figure 34.
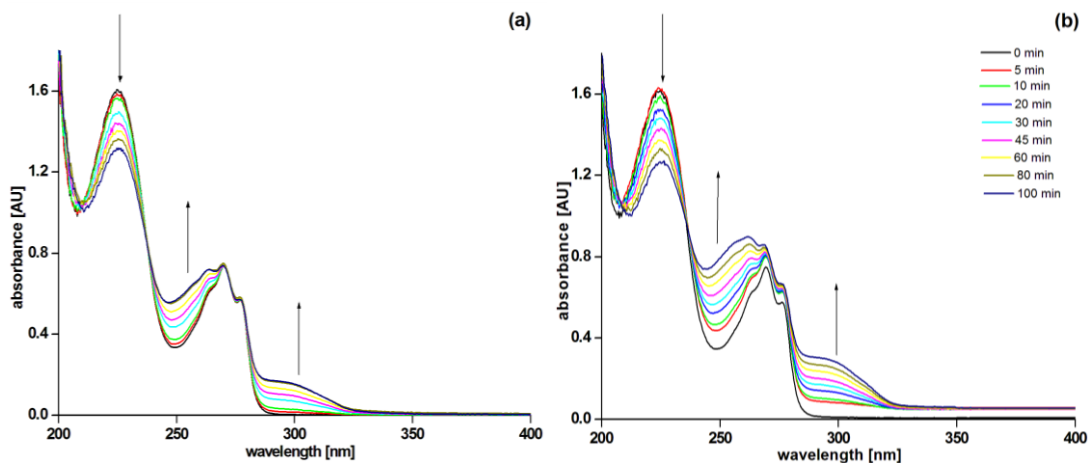
Figure 34: Absorption spectra for the aerated solution of 6CNA (a) upon excitation and for the deoxygenated solution of 6CNA (b) at 254 nm for 100 minutes.[4]

The smallest change in the evolution absorbance spectra for the aerated solution upon excitation at 254 nm was recorded in the case of the 6CNA aqueous solution, as shown in Figure 34a. There, a decrease in absorbance at wavelength range 210-235 nm was indicated and an increase at wavelength ranges 235-270 nm and 275-325 nm. The presence of at least three isobestic points is demonstrating a clean photochemical process.

In case of the 6CNA deoxygenated aqueous solution the picture did not remain the same. From the HPLC-DAD data, the influence of oxygen/argon was already observed in the case of 6CNA photodegradation, where the faster disappearance rate was recorded in the presence of argon. This fact was also further confirmed by UV-Vis measurements, since the absorbance decrease at wavelength range 210-235 nm is greater within deoxygenated conditions, as shown in Figure 34b. Moreover, the increase at wavelength ranges 235-270 nm and 275-325 nm is again greater within deoxygenated conditions, as shown in Figure 34b.

All the results are completely in compliance with HPLC-DAD data, where the highest photodegradation was recorded for the TCP aqueous solution within aerated conditions and the greatest change was noticed in the case of 6CNA aqueous solution – where the disappearance was significantly greater in case of deoxygenated conditions.

---

[4]The (↑) indicates increase of absorbance and (↓) indicates decrease of absorbance within exposure.

In order to better estimate the effect of aerated or deoxygenated conditions to TPs photodegradation, the quantum yields were calculated for each compound within specific conditions – for aerated conditions and for deoxygenated conditions. The calculated parameters, such as absorbances of all three TPs at lamp emitting wavelength, degradation rate constants and degradation quantum yields are presented in Table 15 for aerated conditions and in Table 16 for deoxygenated conditions.

Table 15: Parameters for photodegradation quantum yields for aerated samples of IMP, TCP and 6CNA with low-pressure mercury lamp (254 nm).

	IMP	TCP	6CNA
A [254 nm]	0.725	0.291	0.372
$-dC/dt$ [mol L^{-1} s^{-1}]	9.662×10^{-9}	2.620×10^{-8}	8.476×10^{-9}
Φ [molecules photons^{-1}]	0.015	0.069	0.019

All the parameters were calculated according to the procedure and detailed described in Chapter 4.4 Photodegradation studies with a monochromatic low-pressure mercury lamp (245 nm).

Table 16: Parameters for photodegradation quantum yields for deoxygenated samples of IMP, TCP and 6CNA with low-pressure mercury lamp (254 nm).

	IMP	TCP	6CNA
A [254 nm]	0.725	0.291	0.372
$-dC/dt$ [mol L^{-1} s^{-1}]	1.000×10^{-8}	3.330×10^{-8}	1.724×10^{-8}
Φ [molecules photons^{-1}]	0.016	0.088	0.039

In the case of the IMP aqueous solution, the quantum yields, as calculated from data obtained from both conditions, are very similar and low. However, the results are in compliance with degradation quantum yields for pesticides, calculated in similar research (Menager *et al.*, 2007). The quantum yield is the number of destroyed molecules divided by the number of photons absorbed by the system. This, therefore, means that only small portion of IMP molecules were actually degraded by absorbed photons. A slightly different situation appears with the quantum yields calculated from the experiment with the aqueous solution of TCP. Degradation quantum yield was

slightly higher in the case of deoxygenated conditions. Thus, it can be assumed that oxygen could have an inhibitory impact on the photo degradation of TCP. Obvious changes in degradation quantum yields for aerated and deoxygenated conditions were observed for the aqueous solution of 6CNA. When performing irradiation experiments in the presence of argon, the degradation quantum yield increased.

5.5 Photodegradation studies with polychromatic three low-pressure mercury lamps (355 nm)

5.5.1 Stability study of IMP aqueous solution within photolysis

Photolytic degradation of IMP within 120 min of the experiment could be described as first-order kinetics, as presented in Figure 35.
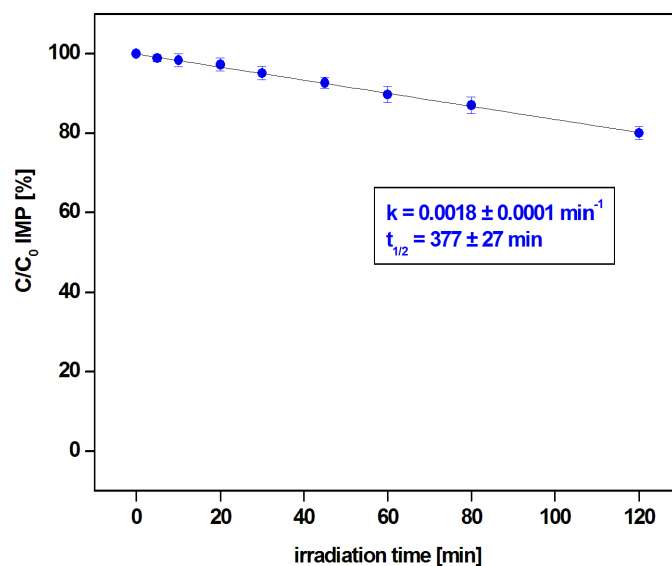
Figure 35: A disappearance curve for IMP aqueous solution during 120 min of photolytic degradation.

Plotting $\ln(C/C_0)$ versus irradiation time resulted in a linear relationship indicating pseudo first-order degradation kinetics. Therefore, the slope gives the pseudo first-order rate constant. The calculated disappearance rate constant was k = 0.0018 ± 0.0001 min^{-1} while the $t_{1/2}$ was 377 ± 27 min. It needs to be mentioned, that although three parallel experiments have been performed, for a better estimation of the disappearance rate and half-life time, the longer irradiation times should be applied.

Therefore, the concentration of IMP after 120 min of irradiation reached 80.0 ± 1.7 % of the initial concentration. This result is not in accordance with data collected during experiments with simulated sunlight conditions using Suntest apparatus (Chapter 5.3.3), where no disappearance of IMP aqueous solution was noticed. The possible explanation is this, that the Suntest apparatus was equipped with a xenon arc lamp and Special UV Glass filter restricting the transmission of wavelengths below 290 nm. Nevertheless, the instrument was also equipped with an internal radiometer and therefore provided the accurate and on-line measurements of emitted light. On the other hand, the tailor made photoreactor equipped with three polychromatic fluorescent lamps emitting in a range of 315–400 nm, did not have the ability to control

the emitting spectra. The producer provided the spectrum of the lamp, but it is not completely clear what the life-time is and how does the emitting spectrum change within usage of the lamps. The photolytic degradation of IMP aqueous solution under UV radiation was described by Lee *et al.* (2003) and small amount of IMP disappeared under the conditions employed. However, no details on lamp characteristics are given as well as no photon flux was reported.

Analyses of TOC and TN in samples during 120 min of photolysis showed negligible decrease, i.e. 2 %. The conductivity measurements revealed slight change from 3.3 ± 1.5 μS cm^{-1} to 11.3 ± 2.5 μS cm^{-1} at the end of experiment, indicating a possible formation of new by-products. All these results are presented in Table 17.

Table 17: Disappearance rate of total organic carbon, total nitrogen (in %) and conductivity measurements (in μS cm^{-1}) during photolytic degradation of IMP within 120 min.

time [min]	TOC/TOC_0 [%]	TN/TN_0 [%]	conductivity [μS cm^{-1}]
0	100.0 ± 0.0	100.0 ± 0.0	3.3 ± 1.5
5	99.2 ± 1.0	99.7 ± 1.5	3.7 ± 1.2
10	98.9 ± 0.4	99.9 ± 1.3	3.7 ± 1.2
20	98.8 ± 1.4	97.6 ± 0.6	4.3 ± 1.5
30	98.8 ± 1.0	97.6 ± 0.9	4.3 ± 1.5
45	98.8 ± 0.2	99.6 ± 1.1	4.7 ± 1.2
60	98.5 ± 0.5	98.1 ± 0.7	8.3 ± 5.1
80	98.5 ± 0.6	99.2 ± 1.5	7.3 ± 1.2
120	98.3 ± 1.2	99.6 ± 2.5	11.3 ± 2.5

To have better insight into degradation kinetics, the UV-Vis absorption spectra from 200 nm to 400 nm of IMP aqueous solution during degradation was recorded and the results are presented in Figure 36. It can be seen, that the absorbance slowly decreased in the wavelength range 220-290 nm and slightly increased at wavelengths below 220 nm. As mentioned, these observations are not in accordance with Suntest experiments, where no change in the absorbance spectra was observed. However, when a monochromatic 245 nm lamp for IMP degradation was applied, the absorbance spectra indicated a significantly increase at wavelength range 275-340 owing to the formation of by-product(s). This difference can be attributed to the fact, that different source of lights were used (monochromatic versus polychromatic), different wavelengths and consequently different energies were involved.
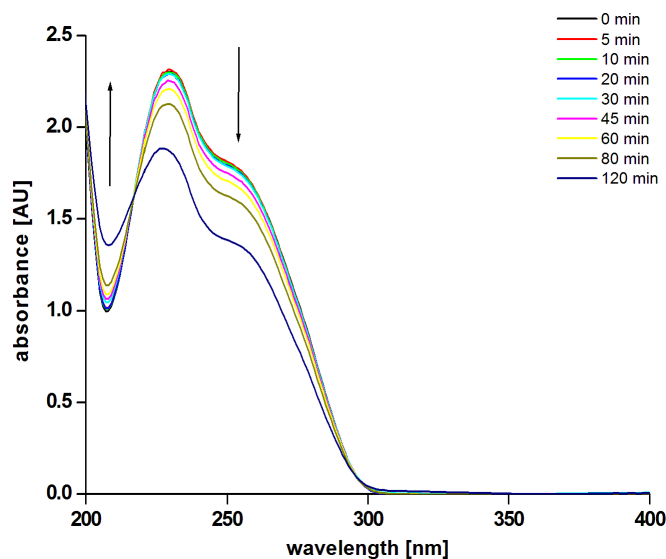
Figure 36: UV-Vis absorbance spectra of IMP aqueous solution during photolytic degradation of 120 min.[5]

The evaluation of toxicity was performed with luminescent bacteria *V. fischeri* and during the photolysis of IMP, the inhibition of luminescence decreased roughly by 2 %, from 11.8 ± 0.8 % at the beginning (time 0) to the 8.9 ± 1.2 % at the end of photolysis (120 min). The observed difference in luminescence inhibition is negligible; therefore in this case, all tested samples demonstrated very low toxicity.

Moreover, the HPLC-DAD chromatograms of the IMP aqueous solution during photolytic degradation were recorded and compared, as shown in Figure 37. The slow disappearance of the parent compound can be seen, but no additional peaks were observed.
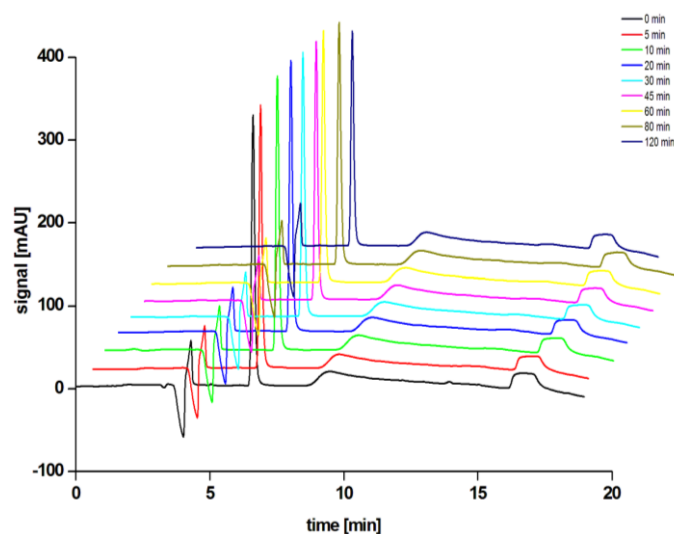
Figure 37: HPLC-DAD chromatograms of IMP aqueous solution during photolytic degradation for 120 min.

---

[5]The (↑) indicates increase of absorbance and (↓) indicates decrease of absorbance within exposure.

Furthermore, the LC-MS and GC-MS measurements of irradiated samples were performed, in order to evaluate the samples. The results of direct injection of IMP into the ESI-LC-MS system indicated that the negative mode was the most suitable method regarding the intensity and fragmentation. The parent compound (IMP) eluted with the retention time 7.2 min and fragmentation resulted in major ESI$^-$ ion with m/z 151 [M–H–1] which can be attributed to the quasi-molecular ion of IMP (152 g mol^{-1}). The total ion chromatogram of treated samples revealed no additional peaks beside the parent compound.

Furthermore, the aqueous samples were analysed by a GC-MS technique on a CP-WAX 75 CB column and the IMP eluted with retention time 27.0 min and fragments m/z 153 [M$^+$] and 137. Analyses of samples after photolytic degradation again revealed no additional peaks beside the parent compound.

To sum up, IMP does slightly degrade under polychromatic UV-A light and would further transform into other compound(s), which unfortunately were not detected. Nevertheless, this process does not cause higher toxicity to *V. fischeri* bacteria.

5.5.2 Stability study of TCP aqueous solution within photolysis

Photolytic degradation of TCP within 120 min of the experiment could be also described as first-order kinetics, as presented in Figure 38.
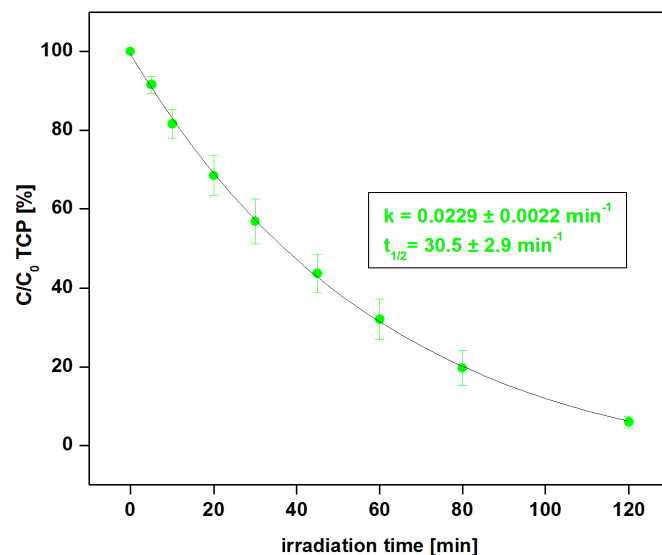
Figure 38: A first-order disappearance curve for TCP aqueous solution during 120 min of photolytic degradation.

Plotting $\ln(C/C_0)$ versus irradiation time resulted in a linear relationship indicating pseudo first-order degradation kinetics. The calculated disappearance rate constant was k = 0.0229 ± 0.0022 min^{-1} while the $t_½$ was 30.5 ± 2.9 min. Therefore, the concentration of TCP after 120 min of irradiation reached 5.9 ± 1.5 % of the initial concentration. For example, during the 6 h of photolytic degradation using Suntest at intensity 500 W m^{-2}, the initial concentration of TCP decreased by 94.3 ± 0.4 %, with rate constant of k = 0.0077 ± 0.0000 min^{-1} and a half-life $t_½$ = 90.0 ± 0.0 min. When employing 750 W m^{-2} the concentration decreased for 99.5 ± 0.2 %, with disappearance rate constant of k = 0.0153 ± 0.0001 min^{-1} and a half-life of $t_½$ of 48.0 ± 0.0 min.

Additionally, the measurements of TOC, TN and conductivity were conducted (Table 18) and showed no decrease in organic carbon, indicating that the mineralization process did not take place during photolytic degradation. This is in accordance with degradation under simulated sunlight conditions with the Suntest apparatus. On the other hand, a decrease of TN by roughly 15 % was observed and consequently it pointed out the possible formation of volatile nitrogen compounds.

Moreover, the conductivity drastically increased during the treatment and again suggested the possible degradation of TCP and transformation into other compound(s). Also, in this case, the TOC/TOC_0 ratio at certain measurements exceeded the value of 100 % and as mentioned in previous experiments, this could be an uncertainty within the measurements.

Table 18: Disappearance rate of total organic carbon, total nitrogen (in %) and conductivity measurements (in µS cm⁻¹) during photolytic degradation of TCP within 120 min.

time [min]	TOC/TOC_0 [%]	TN/TN_0 [%]	conductivity [µS cm⁻¹]
0	100.0 ± 0.0	100.0 ± 0.0	15.7 ± 0.6
5	100.7 ± 1.2	99.7 ± 0.5	24.3 ± 1.5
10	100.2 ± 0.5	98.5 ± 1.9	40.0 ± 5.6
20	101.8 ± 3.4	95.7 ± 2.7	60.3 ± 5.5
30	99.4 ± 1.4	93.9 ± 3.7	81.0 ± 6.6
45	99.4 ± 1.5	89.9 ± 2.6	104.3 ± 6.0
60	101.9 ± 3.5	89.1 ± 1.9	127.0 ± 4.4
80	99.3 ± 1.0	85.0 ± 2.0	149.7 ± 9.8
120	99.4 ± 0.3	83.1 ± 0.9	176.7 ± 9.9

Since the conductivity during photolytic treatment rose significantly, the next logical step was also to perform the ion chromatography measurements. It turned out, that the chloride concentration after 120 min of photolytic degradation reached approximately 19.4 mg L⁻¹ (quantitative transformation of chlorine into chloride would yield 26.7 mg L⁻¹) as shown in Figure 39. Unfortunately, the NO_3^- and NO_2^- could not be measured at that time.
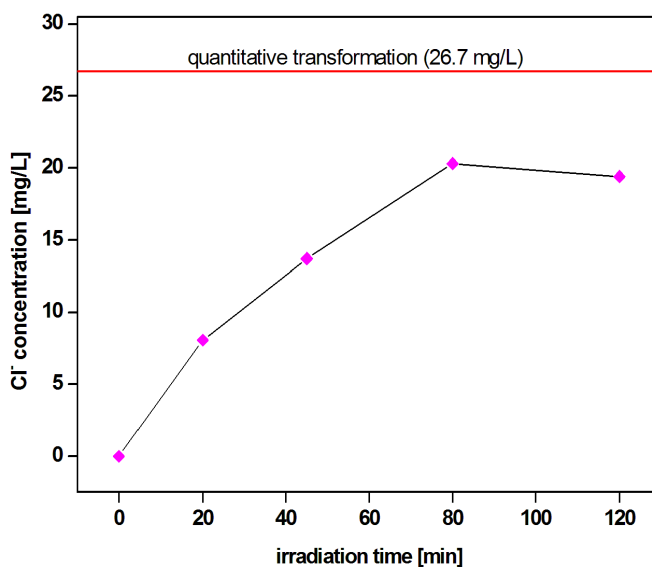
Figure 39: Chloride concentration for TCP aqueous solution during photolytic degradation of 120 min.

Finally, the absorbance spectra for the TCP aqueous solution upon photolytic degradation for 120 minutes were compared and investigated and are presented in Figure 40.
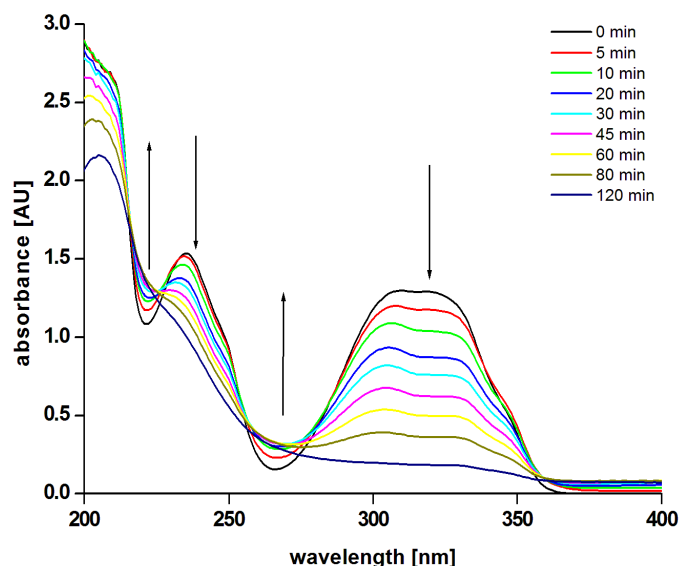
Figure 40: UV-Vis absorbance spectra of TCP aqueous solution during photolytic degradation of 120 min.[6]

A decrease of absorbance in the range 225-255 nm and 290-340 nm can be clearly seen, which demonstrates the transformation of TCP. Nevertheless, the increase in absorbance was noticed in the wavelength range 255-290 nm and this was again attributed to a newly formed by-product occurring. This is completely in accordance with the results obtained during the exposure to simulated sunlight conditions using the Suntest apparatus.

Due to the high disappearance of TCP during photolytic degradation, toxicity testing with the luminescent bacteria *V. fischeri* was carried out. Samples were taken at 0, 30, 60 and 120 minutes of experimentation and the results are demonstrated in Figure 41. At the beginning of the experiment, the luminescence inhibition exhibited to be 53 ± 1.1 % within 30 min of treatment increased to 82.4 ± 1.6 % and then decreased to 73.0 ± 3.0 % at the end of experimentation. The experiment under simulated sunlight conditions also resulted in a high increase in luminescence inhibition over a period of six hours. It needs to be mention that apparently, the disappearance rate in case of photolysis with 355 nm lamps is much higher (as demonstrated above) and probably the removal or disappearance of by-products, also took place. Thus, this could be the

---

[6]The (↑) indicates increase of absorbance and (↓) indicates decrease of absorbance within exposure.

reason why the luminescence inhibition after 60 min of photolysis decreases and it is much lower than the luminescence inhibition during Suntest experiments.
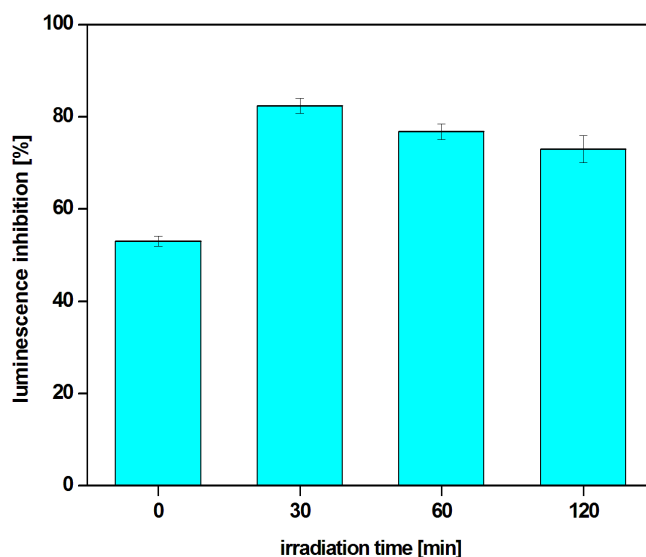
Figure 41: Luminescence inhibition for **V. fischeri** *of TCP aqueous solution during photolytic degradation for 120 min.*

In order to characterise the possible newly formed by-products the HPLC-DAD chromatograms collected within photolytic degradation were compared and evaluate in order to detect any new peaks, as shown in Figure 42. It can be clearly seen that the formation of new by-products occurred, furthermore, on the basis of HPLC-DAD data, it seems that the same by-products, as in the case with Suntest experiments, have been formed.
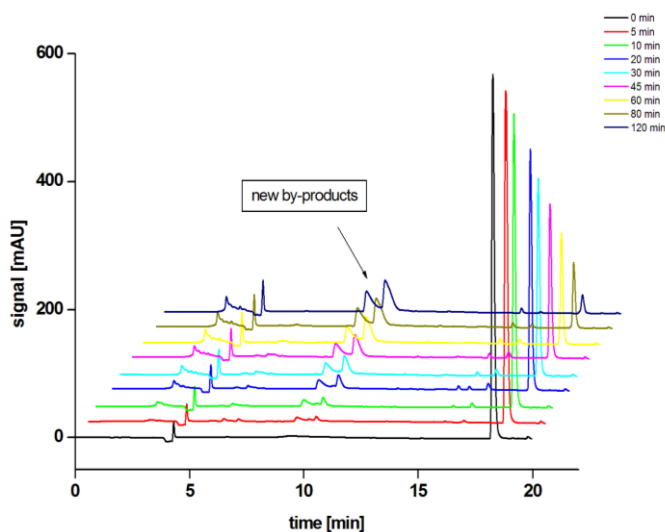
Figure 42: HPLC-DAD chromatograms of TCP aqueous solution during photolytic degradation for 120 min.

Additionally, the LC-MS and GC-MS analyses of exposed samples were performed. As already described, the GC-MS determination of the TCP and treated samples was unsuccessful. On the other hand, the LC-MS analyses point out the new by-product with retention time of 10 minutes with major ESI⁻ ions with *m/z* 134, 136 and 138 (**A**), indicating a new compound with two chlorine atoms. It needs to be mentioned, that the LC-MS analyses were performed on a different system and different column as HPLC-DAD. As described already in Chapter 4.7.1 and 4.7.2, the HPLC-DAD measurements were performed on a Zorbax C_8 column, while LC-MS measurements were performed on a Purospher star C_{18} column and, therefore, some differences were observed. On the basis of LC-MS data obtained from the Suntest experiments, published data (Feng *et al.*, 1998) and also on the basis of my results, I can propose possible structure(s) of product (**A**) as already shown in Figure 30 in Chapter 5.3.3 Stability study of TCP aqueous solution within simulated sunlight.

Also of great interest is the fact, that no detection of the chromatographic peak at 13.6 min, before giving the major ESI⁻ ion with *m/z* 178, 180 and 182, as in case of Suntest experiments was observed. This can be attributed to the fact, that the disappearance or transformation of TCP was faster in case of photolysis with 355 nm lamps and probably also the conversion from product **B** (pyridine ring) to linear products (**A**) was faster. And this was perhaps an explanation, as to why the product **B** was not detected during photolytic degradation with three 355 nm lamps.

Therefore, as was already confirmed before, TCP acts like photosensitive chemical, which rapidly transforms into several other compounds, depending on the light source used. With LC-MS technique some linear products have been detected. However, additional attention needs to be paid also to toxicity evaluation during the process due to higher toxicity at the end of the treatment.

5.5.3 Stability study of 6CNA aqueous solution within photolysis

Photolytic degradation of 6CNA within 120 min of the experiment was negligible and consequently the half-life time could not be calculated, as presented in Figure 43.
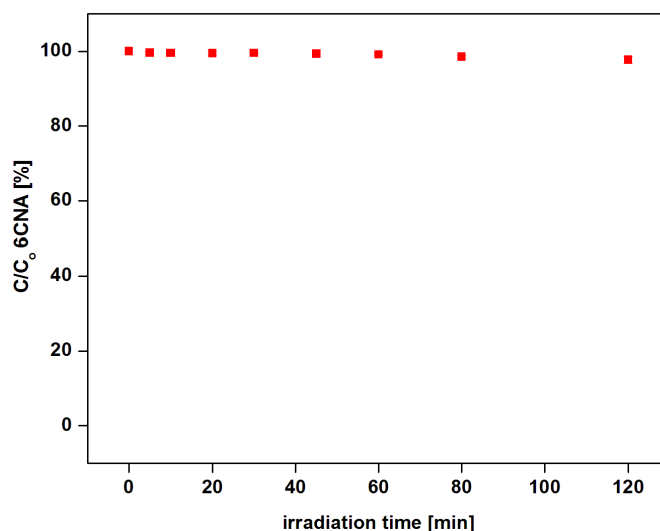
Figure 43: A disappearance trend for 6CNA aqueous solution during 120 min of photolytic degradation.

This result is completely in accordance with data collected during experiments with simulated sunlight conditions using Suntest apparatus (Chapter 5.3.2), where no disappearance of 6CNA aqueous solution was noticed.

Further, the conductivity measurements revealed no change as well. All these results are detailed presented in Table 19.

Table 19: Disappearance rate of total organic carbon, total nitrogen (in %) and conductivity measurements (in μS cm^{-1}) during photolytic degradation of 6CNA within 120 min.

time [min]	TOC/TOC_0 [%]	TN/TN_0 [%]	conductivity [μS cm^{-1}]
0	100.0 ± 0.0	100.0 ± 0.0	78.7 ± 2.1
5	99.0 ± 0.3	96.1 ± 1.9	78.7 ± 1.2
10	98.2 ± 1.3	95.0 ± 1.0	80.7 ± 2.1
20	97.8 ± 0.4	94.5 ± 0.7	80.3 ± 1.2
30	98.9 ± 1.5	95.0 ± 0.2	79.3 ± 0.6
45	98.0 ± 1.2	95.0 ± 0.6	78.7 ± 0.6
60	97.3 ± 2.3	95.6 ± 0.5	78.7 ± 1.2
80	98.5 ± 2.9	93.9 ± 1.9	79.6 ± 1.5
120	99.1 ± 2.2	99.9 ± 0.3	79.3 ± 1.5

Analyses of TOC and TN in samples during photolysis for 120 min showed no decrease at all and it needs to be noted that also no chloride was detected through ion chromatography measurements.

Moreover, the UV-Vis absorption spectra from 200 nm to 400 nm of 6CNA aqueous solution within photolytic degradation was recorded, but no changes were noted, as detailed presented in Figure 44.
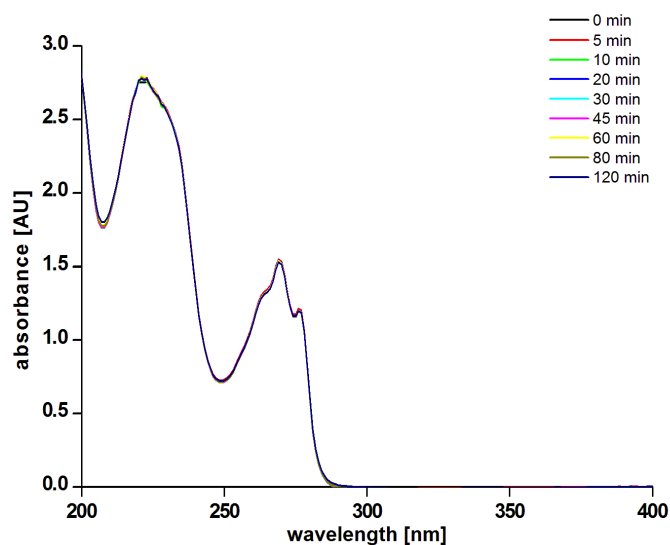
Figure 44: UV-Vis absorbance spectra of 6CNA aqueous solution during photolytic degradation of 120 min.

Within the photolytic degradation, the absorption spectrum of an investigated compound plays an important role. The lamp used within photolytic experiments was UV-A lamp with a range of 315–400 nm but the absorption of 6CNA is very little in this specific range and, therefore, the disappearance of 6CNA could not be observed. Nevertheless, the energy of the UV-A light (approx. 350 kJ mol^{-1}) used in the photolytic degradation processes is simply too low to cause heterolytic or homolytic breakages in the molecule of 6CNA.

The next step in the photolytic treatment of 6CNA aqueous solution was the evaluation of toxicity again with the luminescent bacteria *V. fischeri.* At the beginning, the luminescence inhibition was 7.5 % ± 1.5 % and increased roughly for 3 % to 10.6 % ± 0.2 % after 120 minutes of treatment. Therefore, the difference in luminescence inhibition before and after photolysis is probably only due to the uncertainties in the measurements and, in this case, the toxicity could be accounted only by the parent compound.

Collected results indicated that 6CNA cannot degrade easily in double deionised water when exposed to photolytic treatment with polychromatic low-pressure mercury lamp and as a result no change in toxicity with luminescent bacteria was observed as well as mineralisation rate and conductivity.

5.6 Photocatalytic studies with polychromatic low-pressure mercury lamps (355 nm) and immobilised TiO_2

5.6.1 Photocatalytic degradation of IMP in aqueous solution

The kinetic results of IMP aqueous solution within photocatalytic degradation with immobilised TiO_2 resulted in first-order degradation reaction, as shown in Figure 45. The observed rate constant was $k = 0.012 \pm 0.001$ min^{-1} and a half-life time $t_{1/2} = 56.6 \pm 5.9$ min^{-1}. Therefore, the concentration of IMP after 120 min of irradiation with presence of the TiO_2 catalyst reached 22.3 ± 4.0 % of the initial concentration.
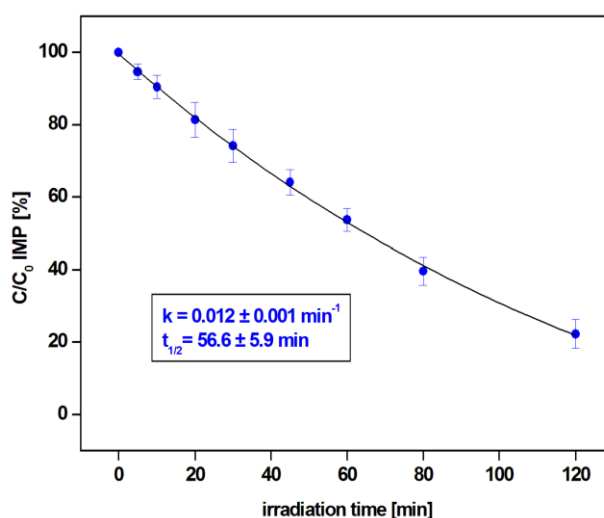
Figure 45: A first-order disappearance curve for IMP aqueous solution during photocatalysis with TiO_2.

TOC analysis of IMP samples during photocatalytic degradation for 120 min revealed not so high mineralisation as expected, only i.e. 14.5 ± 5.3 %, as shown in Figure 46.
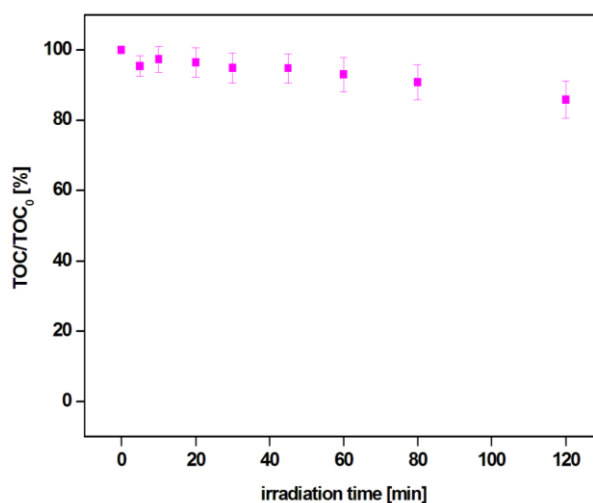
Figure 46: The mineralisation trend for IMP aqueous solution during photocatalytic degradation with TiO_2.

This fact was additionally confirmed by TN and conductivity measurements, where just 3 % of total nitrogen decrease was observed and a slight increase of conductivity after 120 min of photocatalysis, as presented in Table 20.

Table 20: Disappearance rate of total nitrogen (in %) and conductivity measurements (in µS cm⁻¹) during photocatalytic degradation of IMP within 120 min.

time [min]	TN/TN_0 [%]	conductivity [µS cm^{-1}]
0	100.0 ± 0.0	2.3 ± 0.6
5	100.0 ± 0.7	6.3 ± 1.5
10	100.5 ± 0.3	6.3 ± 1.5
20	100.5 ± 0.8	6.7 ± 1.5
30	99.2 ± 0.8	7.7 ± 2.1
45	100.4 ± 0.7	9.7 ± 1.5
60	99.5 ± 0.4	10.7 ± 2.1
80	99.0 ± 0.9	13.3 ± 1.5
120	97.3 ± 2.4	18.7 ± 4.0

Also in this case, the TN/TN_0 ratio at certain measurements exceeded the value of 100 % and as mentioned in previous experiments, this could be an uncertainty within the measurements.

The UV-Vis absorbance spectra during photocatalytic degradation showed an interesting evolution of spectra. Substantial difference was noticed between IMP evolution spectra during photolysis (showed in Figure 36) and photocatalysis with immobilised TiO_2, as presented in Figure 47. The main differences are exhibited within the absorbance after 120 minutes of treatment, where in case of photolysis, the decrease of absorbance was not high and the absorbance peak around 230 nm is still present. On the other hand, after 120 minutes of photocatalytic treatment, this specific peak disappeared and the absorbance decreased significantly.

Figure 47 demonstrates that IMP has two absorption peaks, which result from a pyrimidine ring (Manson, 1962). The first peak around 230 nm is from $\pi \rightarrow \pi^*$ transition and the second peak around 260 nm is from $n \rightarrow \pi^*$ transition. These peaks were recognised (in lower absorbance, obviously) during photolytic degradation with 355 nm lamps. On contrary, after photocatalytic degradation with TiO_2 the peak at 230 nm disappeared, suggesting that a pyrimidine ring opening might have taken place, as already described by Lee *et al.* (2003).
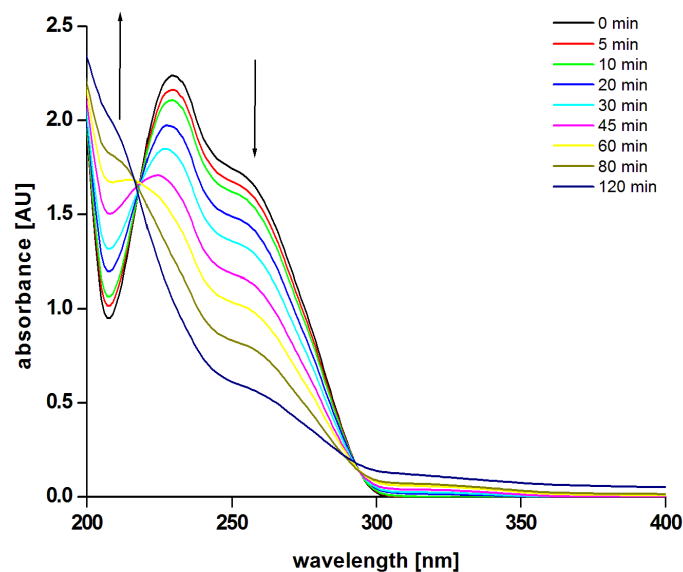
Figure 47: UV-Vis absorbance spectra of IMP aqueous solution during photocatalysis with TiO$_2$.[7]

Even though a sufficient removal of IMP was observed via HPLC-DAD measurements, the toxicity testing through *V. fischeri* bacteria indicated an increase in luminescence inhibition from 10.6 ± 1.1 % at the beginning to 14.4 ± 1.6 % at the end of the treatment.

To compare, within photolytic degradation of IMP, the observed rate constant was significantly lower, k = 0.0018 ± 0.0001 min^{-1} while the half-life $t_{½}$ was 377 ± 27 min and the mineralisation was not achieved at all. Additionally, the luminescence inhibition was lower within photolysis, reaching the value of 8.9 ± 1.2 % at the end of experiment.

For possible by-products investigation, the HPLC-DAD chromatograms of IMP samples during photocatalysis were compared. As it can be observed from the Figure 48, no additional peaks were noticed, however further LC-MS analyses were conducted.

---

[7]The (↑) indicates increase of absorbance and (↓) indicates decrease of absorbance within exposure.
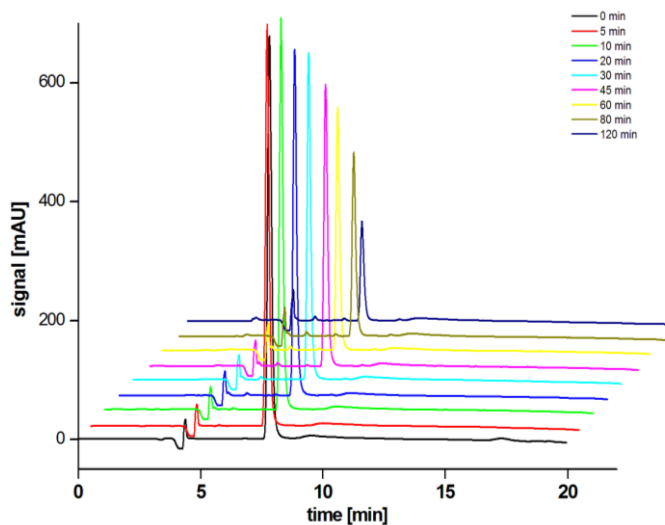
Figure 48: HPLC-DAD chromatograms of IMP aqueous solution during photocatalytic degradation for 120 min.

The results of direct injection of IMP into the ESI-MS system showed that the negative mode is the most suitable method The parent compound (IMP) eluted with the retention time 7.2 min and fragmentation resulted in major ESI$^-$ ion with *m/z* 151 [M–H–1] which can be attributed to the quasi-molecular ion of IMP (152 g mol^{-1}). The total ion chromatogram of treated samples revealed a new peak at retention time 4.2 min. Furthermore, the mass scan of peak 4.2 min was extracted in order to characterise the ESI$^-$ ions and gave major ESI$^-$ ions with *m/z*, 167 and 137 and 109. The new compound is, therefore, 16 amu higher than the parent one, and thus it might correspond to a new compound with an additional oxygen atom (**C1** or **C2**), i.e. hydroxy-IMP. Several possible positional isomers could be formed, as presented in Figure 49 and the positions of OH group are circled in red.
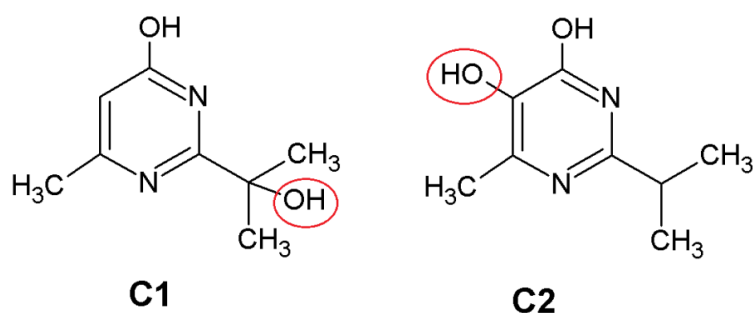
Figure 49: Suggested structures for IMP photocatalytic products (C1 and C2) on the basis of LC-MS data.

Muñoz *et al.,* (2011) studied the atmospheric degradation of diazinon under simulation chamber in a large outdoor photoreactor and, interestingly, besides the well known diazinon photoproduct, i.e. IMP, they suggested the formation of hydroxy-IMP. In their

case, they accepted the structure of compound **C1** but without additional NMR analysis. However, when taking into consideration the possible positional isomers, in my opinion, the compound **C2** is more plausible due to its less sterical barriers around hydroxyl group than in case of compound **C1**.

On the basis of the UV-Vis data, the pyrimidine ring opening might have taken place during the photocatalysis. However, no linear products were detected during the analyses. The reason for this could be the fact that newly formed linear molecules were very polar and they eluted with the mobile phase in the LC system and probably they do not absorb at wavelengths applied for HPLC measurements. To solve this problem, I introduced a new hydrophilic interaction liquid chromatography (HILIC) but no success was attained as well.

In addition, the aqueous samples were analysed by the GC-MS technique on a CP-WAX 75 CB column and the IMP eluted with retention time 27.0 min and fragments *m/z* 153 [M+] and 137. The analyses of the samples after photocatalysis revealed a new peak with retention time of 14.7 min and fragments *m/z* 88, 72 and 44 which, on the basis of the GC-MS library, corresponds to the compound **D** (isobutyramide), as shown in Figure 50.
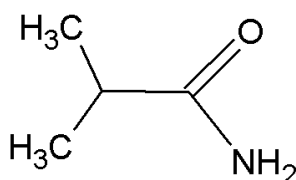
D

Figure 50: Suggested structure for IMP photocatalytic product (D) on the basis of GC-MS data.

This fact can consequently clearly indicate, that the IMP pyrimidine ring-opening took place during photocatalytic treatment.

Photocatalytic degradation of the IMP aqueous solution was investigated by Lee *et al.* (2003) and my results correlate with published data. The reaction rate constant depended on the pH of the solution; however, for the pH of 6.3 (close to pH of IMP aqueous solution ∼ 50 mg L-1) the reaction rate constant was 0.0223. This rate constant is twice higher than calculated in my experiments. However, it needs to be taken into account, that Lee *et al.* (2003) used powder catalyst with concentration 200 mg L-1 while in my experiments, the immobilized catalyst was used and, therefore, a direct comparison cannot be made. The change in UV-Vis spectra (Lee *et al.*, 2003) during the

irradiation time correlates with my observations, but a greater mineralisation rate was reported. The by-products were monitored via GC-MS and acetamide was detected as possible product. Nevertheless, the detailed data is not provided – no retentions times and no fragments of the parent compound as well as of by-products.

5.6.2 Photocatalytic degradation of TCP in aqueous solution

The photocatalytic degradation of the TCP aqueous solution with immobilised TiO_2 resulted in first-order degradation reaction, as shown in Figure 51. The observed rate constant was $k = 0.024 \pm 0.001$ min^{-1} and a half-life time $t_{\frac{1}{2}} = 28.5 \pm 1.3$ min^{-1} and the concentration of TCP after 120 min of irradiation with presence of the TiO_2 catalyst, reached 4.5 ± 0.6 % of the initial concentration.
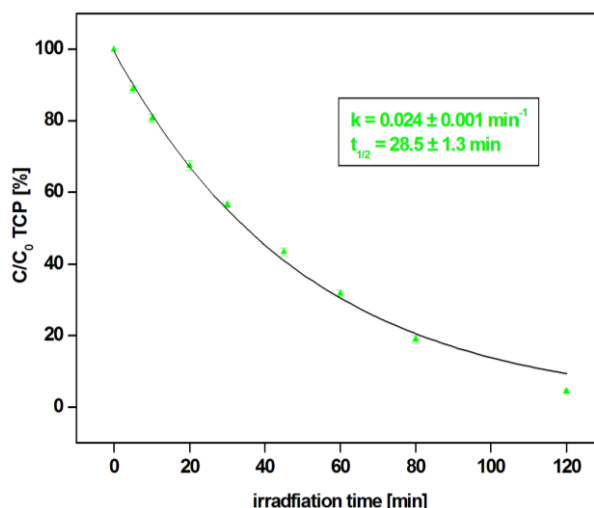
Figure 51: A first-order disappearance curve for TCP aqueous solution during photocatalysis with TiO_2.

Additionally, the TOC measurements were conducted within all samples, in order to investigate the possible mineralization since high disappearance rate of the parent compound was achieved. The analyses revealed a surprisingly high mineralization rate after 120 minutes of photocatalysis, i.e. 53.6 ± 1.9 % at the end of the experiment, Figure 52.
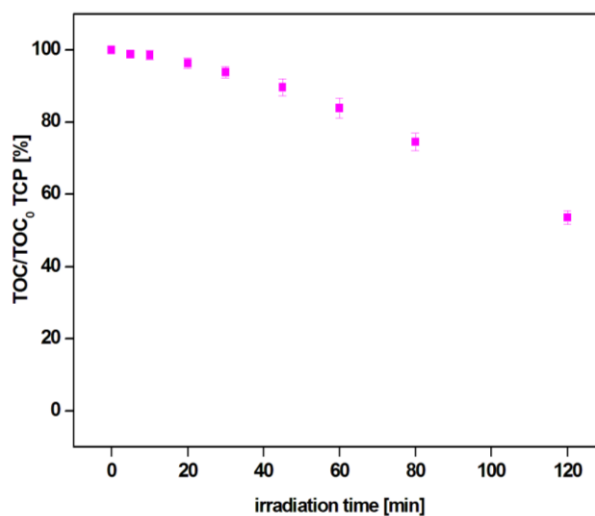
Figure 52: The mineralisation trend for TCP aqueous solution during photocatalytic degradation with TiO_2.

What is more, the TN and conductivity values confirmed the high AOP efficiency with almost 30 % of total nitrogen removal. Moreover, the conductivity values significantly increased during treatment, indicating a possible release of ions. Detailed values are presented in Table 21.

Table 21: Disappearance rate of total nitrogen (in %) and conductivity measurements (in µS cm^{-1}) during photocatalytic degradation of TCP within 120 min.

time [min]	TN/TN_0 [%]	conductivity [µS cm^{-1}]
0	100.0 ± 0.0	17.0 ± 1.7
5	97.4 ± 0.7	30.3 ± 2.9
10	95.5 ± 1.8	42.7 ± 4.0
20	91.5 ± 1.9	69.0 ± 5.3
30	89.4 ± 1.7	89.7 ± 8.5
45	86.1 ± 2.2	119.3 ± 9.9
60	82.3 ± 2.5	146.3 ± 9.0
80	78.1 ± 2.1	173.3 ± 11.6
120	71.7 ± 1.1	202.0 ± 15.1

The ion chromatography measurements confirmed the conductivity measurements and revealed almost quantitative transformation of chlorine into chloride, the concentration of chloride after 120 minutes of photocatalytic degradation reached 26.6 mg L^{-1}, as shown in Figure 53.
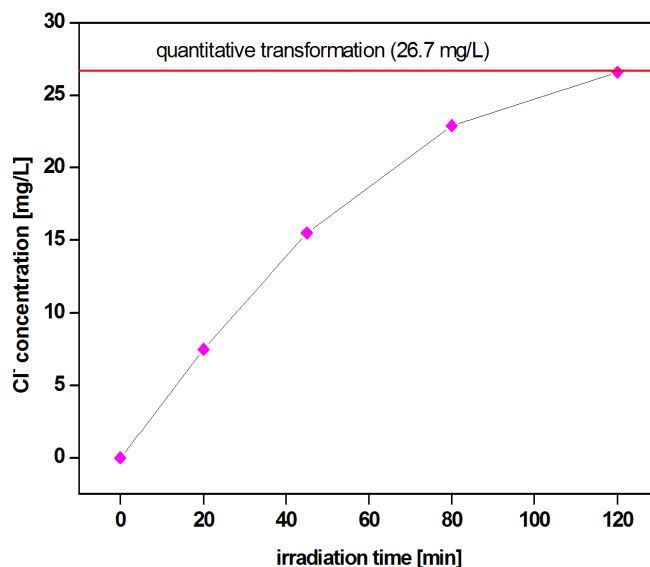
Figure 53: Chloride concentration for TCP aqueous solution treated during photocatalysis with TiO$_2$ for 120 min.

As a matter of course, the UV-Vis spectra of the TCP aqueous solution during photocatalysis were recorded and compared. From Figure 54, a decrease of absorbance in the whole recorded range can be clearly seen, indicating a transformation of TCP into

other compounds and also a mineralisation of these compounds into CO_2 and H_2O. When compared to the photolytic spectra of TCP, no increase of absorbance in the wavelength range 255-290 nm was observed.
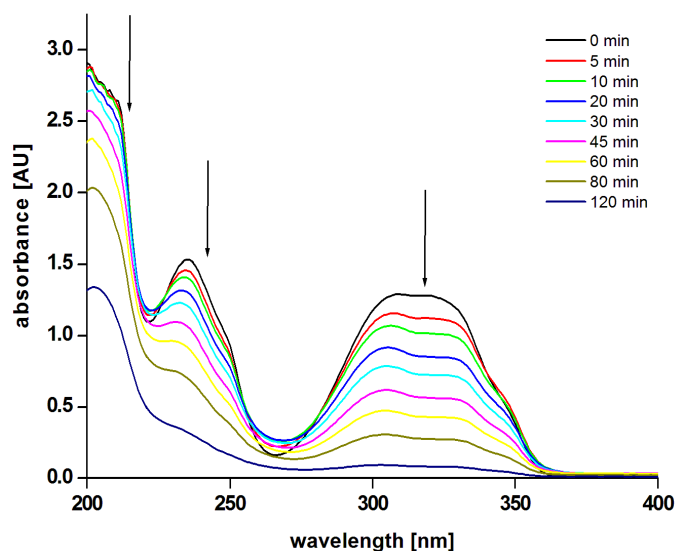
Figure 54: UV-Vis absorbance spectra of TCP aqueous solution treated during photocatalysis with TiO₂.[8]

Moreover, the evaluation of AOPs efficiency was the toxicity testing with the luminescent bacteria *V. fischeri.* It can be emphasised, that the TCP samples, after applying photocatalysis showed increased luminescence inhibition in comparison to the parent compound as shown in Figure 55. Inhibition of luminescence after 120 min of photocatalytic degradation increased from starting at 57.1 ± 0.2 % to 87 ± 1.0 %, regardless, a high mineralisation rate was achieved.
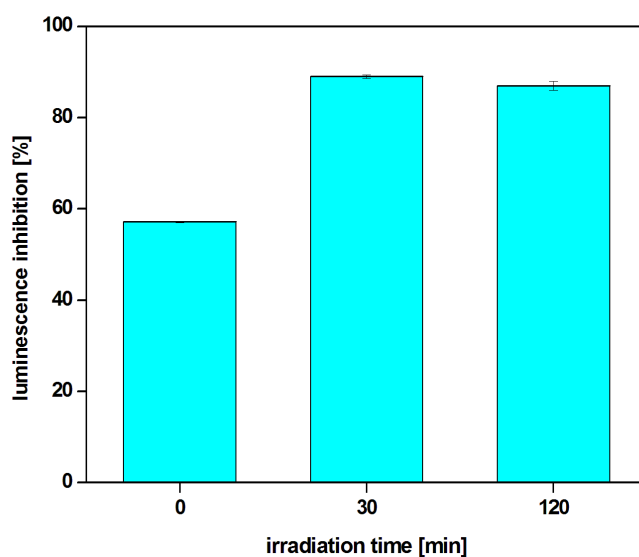
Figure 55: Luminescence inhibition for **V.** fischeri *of TCP aqueous solution during photocatalytic degradation with immobilised TiO₂.*

---

[8]The (↑) indicates increase of absorbance and (↓) indicates decrease of absorbance within exposure.

This phenomenon could arise due to the formation of possible toxic by-products or intermediates and consequently causing higher toxicity of the treated solution. It is worth mentioning, that also the synergistic effects of newly formed by-products cannot be excluded.

To compare, within photolytic degradation of TCP, the observed rate constant was slightly lower, i.e. $k = 0.0229 \pm 0.0022$ min^{-1} while the half-life time was $t_{\frac{1}{2}}$ 30.5 $\pm$ 2.9 min, the mineralisation was not achieved at all and the chloride concentration after 120 minutes of photolysis reached 19.4 mg L^{-1}. Additionally, the luminescence inhibition appeared to be lower as within photocatalysis, reaching the value of 73.0 $\pm$ 3.0 % at the end of experiment.

Additionally, the HPLC-DAD chromatograms within photocatalytic degradation were compared to extract the potential new peaks which would indicate formation of new by-products, presented in Figure 56. In comparison to stability of TCP under simulated sunlight and in comparison to TCP under photolytic conditions, within photocatalytic treatment, different chromatographic peaks were observed, resulting in possible different observed by-products.
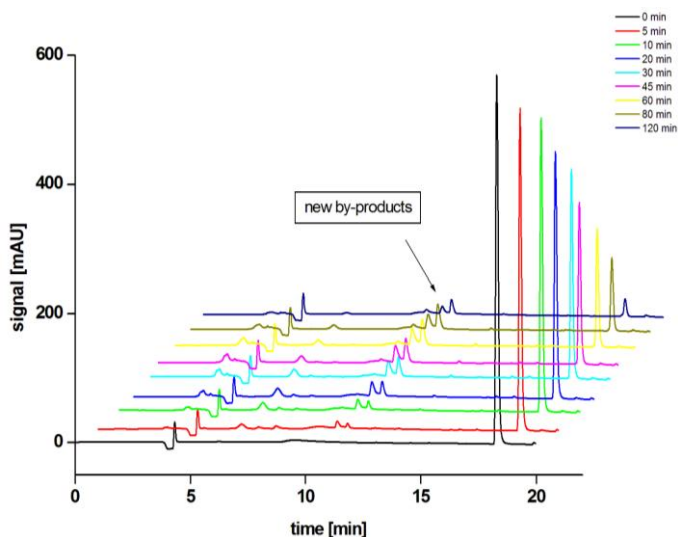
Figure 56: HPLC-DAD chromatograms of TCP aqueous solution during photocatalytic degradation for 120 min.

Seeing that, the mineralisation rate was significantly high (approx. 50 %), the identification of possible new products was tough task. In Figure 56, new peaks were observed at the retention time of 10 minutes and therefore, the logical steps in the identification process were the analyses with LC-MS and GC-MS.

As mentioned before, the GC-MS analyses were not successful for the identification of TCP, since it is not volatile compound and unfortunately also the new by-product(s) could not be identified via GC-MS.

On the other hand, the LC-MS investigation revealed interesting results. The parent compound (TCP) eluted with the retention time 17.3 min and fragmentation resulted in major ESI- ions with m/z 196 [M–H–1], 198 [M–H+2] and 200 [M–H+4] which can be attributed to the quasi-molecular ion of TCP (197 g mol^{-1}, taking the mass of chlorine 35 g mol^{-1}). Thus, taking into account that the molecule contains three chlorine atoms and therefore the occurrence of the typical intensity signals pattern for molecules containing three chlorine atoms was also observed.

TIC of samples after photocatalytic treatment revealed many new peaks, as described in detail in Table 22.

Table 22: Observed peaks in TIC of TCP after photocatalysis.

retention time [min]	major ESI- ions [m/z]	assignation
17.9	196, 198, 200	parent compound
13.0	178, 180;182	**B1, B2, B3**
8.8	134, 136, 138	**A1, A2, A3, A4, A5, A6**
3.8	161, 163, 165	**E1, E2, E3**
	112, 97	

The structures **A** and **B** were already described in previous chapters within TCP photolysis, Chapter 5.3.3 Stability study of TCP aqueous solution with simulated sunlight. However, a new additional by-product was detected (**E**), apparently with two chlorine atoms - the fragmentation pattern was clearly indicated. Since the mass of the new product seems to be 35 amu lower, a dechlorination of the TCP was observed, and the tentative structures are proposed in Figure 57.
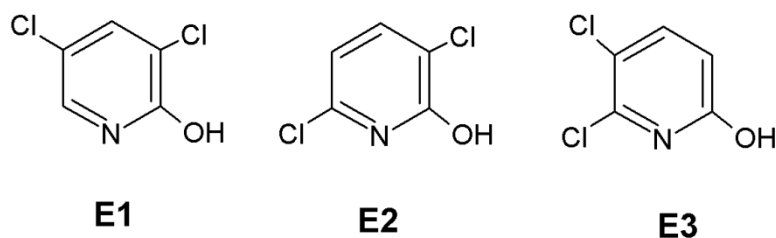
Figure 57: Tentative structures for TCP photocatalytic products (E1, E2 and E3) on the basis of LC-MS data.

5.6.3 Photocatalytic degradation of 6CNA in aqueous solution

The data obtained from irradiated samples of 6CNA in the presence of the TiO_2 catalyst indicate the relatively high disappearance constant and short half-live, as shown in Figure 58.
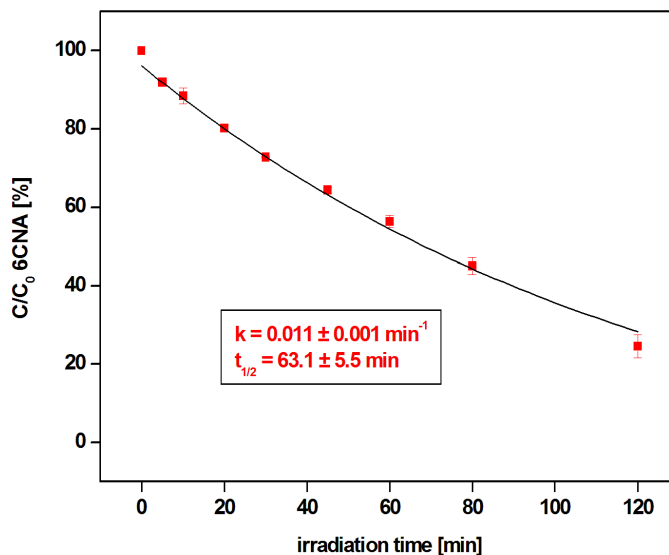
Figure 58: A first-order disappearance curve for 6CNA aqueous solution during photocatalysis with TiO₂.

Plotting $\ln(C/C_0)$ versus irradiation time resulted in a linear relationship indicating pseudo first-order degradation kinetics. Therefore, the slope gives the pseudo first-order rate constant. The calculated disappearance rate constant was $k = 0.011 \pm 0.001$ min^{-1} while the $t_{1/2}$ was 63.1 ± 5.5 min. Therefore, the concentration of 6CNA after 120 min of irradiation with presence of the TiO_2 catalyst reached $24.6 \pm 2.9\%$ of the initial concentration.

The pH of the solution within photocatalytic degradation decreased from 4.23 ± 0.01 at the beginning to 4.05 ± 0.01 at the end of experimentation, which indicates the formation of slightly acidic by-products.

TOC analysis of samples treated via photocatalysis for 120 min revealed 45.5 ± 7.1 % mineralisation. The complete mineralisation of 6CNA in an aqueous solution was, however, reached after 360 min of photocatalytic degradation. Detailed results are presented in Figure 59.
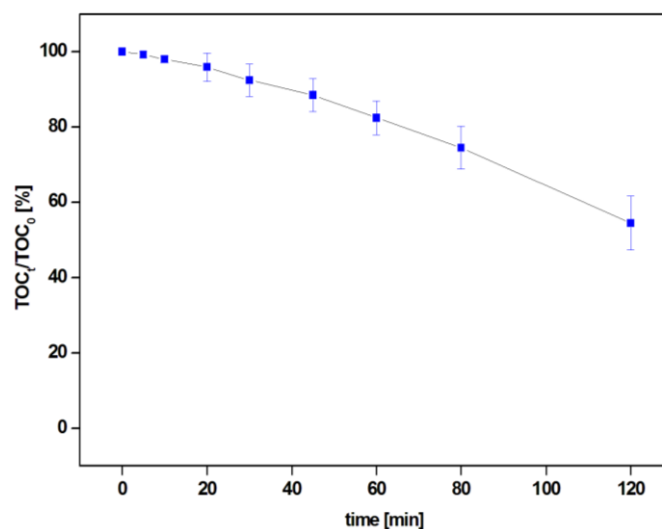
Figure 59: The mineralisation trend for 6CNA aqueous solution during photocatalytic degradation with TiO$_2$.

In the photocatalytic experiments with TiO$_2$ the chloride concentration after 120 min reached approximately 9.4 mg L^{-1} (quantitative transformation of chlorine into chloride would yield 11.3 mg L^{-1}). Moreover, the concentration of NO$_3^-$ rose significantly within 120 min of the experiment from 0 to 17.1 mg L^{-1} (quantitative transformation of nitrogen into NO$_3^-$ would yield 20.3 mg L^{-1}) The NO$_2^-$ was not detected in any experiment. This can be attributed to the fact that within photocatalytic experiments NO$_2^-$ could be rapidly oxidised to NO$_3^-$. The detailed results are presented in Figure. 60.
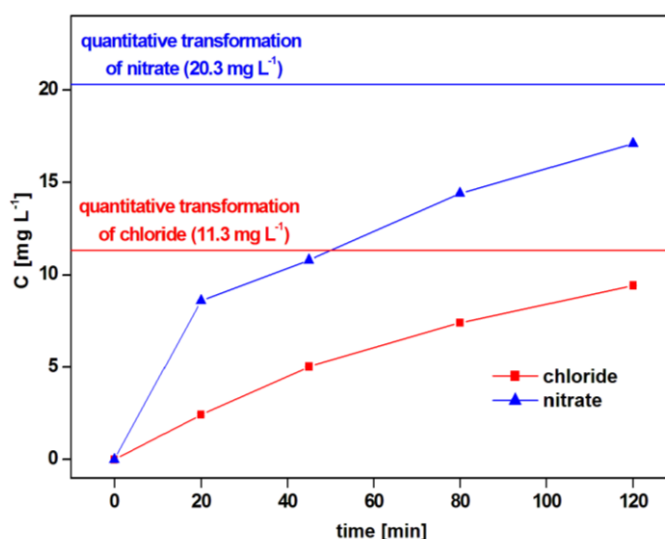
Figure 60: Chloride concentration (red ■) and nitrate (blue ▲) for 6CNA aqueous solution during photocatalysis with TiO$_2$.

The ion chromatographic data are completely in accordance with other published data on imidacloprid photocatalysis with TiO$_2$ (Kitsiou *et al.*, 2009), where almost

104

quantitative transformation of both chloride anion and nitrate anion was detected. Nevertheless, the conductivity of the 6CNA aqueous solution during photocatalytic treatment with immobilised TiO_2 increased from initial 75.3 ± 5.0 µS cm^{-1} to the 99.0 ± 6.2 µS cm^{-1} at the end of experiment and therefore correlates with the ion chromatographic results. Furthermore, the total nitrogen measurements were conducted and they revealed little mineralisation, i.e. 9 %. All these results are detailed presented in Table 23.

Table 23: Disappearance rate of total nitrogen (in %) and conductivity measurements (in µS cm^{-1}) during photocatalytic degradation of 6CNA within 120 min.

time [min]	TN/TN_0 [%]	conductivity [µS cm^{-1}]
0	100.0 ± 0.0	73.7 ± 4.5
5	100.1 ± 1.1	79.3 ± 4.6
10	99.8 ± 2.1	80.7 ± 4.2
20	99.6 ± 3.3	84.3 ± 3.8
30	98.7 ± 3.6	87.0 ± 4.4
45	98.5 ± 3.0	89.7 ± 5.5
60	94.8 ± 2.8	91.0 ± 7.0
80	94.8 ± 3.7	95.3 ± 6.5
120	91.8 ± 1.7	99.0 ± 6.2

Spectra recorded during the photocatalytic experiments showed a high decrease of absorbance in the range from 200 nm to 280 nm within 120 min which indicates degradation of the initial compound, as shown in Figure 61.
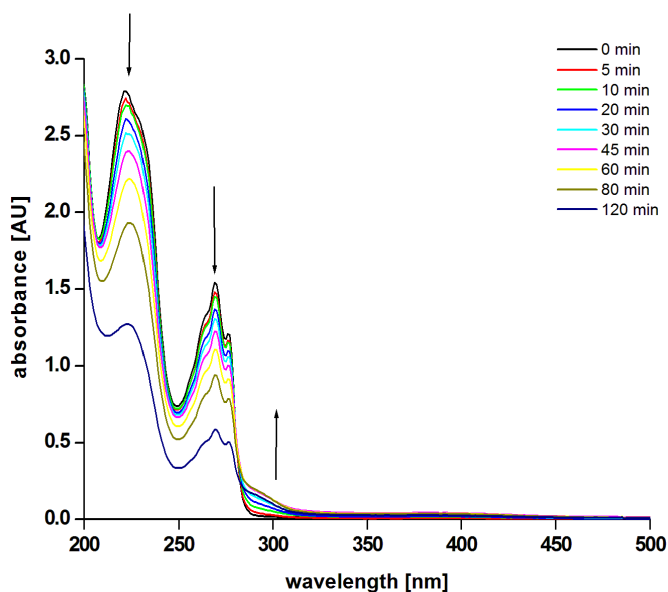
Figure 61: UV-Vis absorbance spectra of 6CNA aqueous solution during photocatalysis with TiO_2.[9]

---

[9]The (↑) indicates increase of absorbance and (↓) indicates decrease of absorbance within exposure.

From all collated results, it could be proposed, that the formation of new by-products took place within the photocatalytic degradation of 6CNA. Therefore, the HPLC-DAD signals through photocatalysis were collected and compared. As it can be seen from Figure 62, an additional peak at approximately 10 minutes appeared.
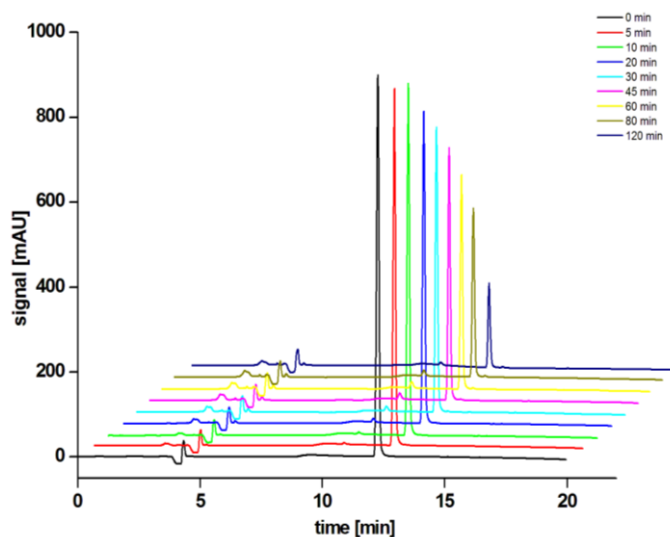
Figure 62: HPLC-DAD chromatograms of 6CNA aqueous solution within photocatalytic degradation for 120 min.

Moreover, to characterise this new peak, the additional analyses by LC-MS were performed. The results of direct injection of 6CNA into the ESI-MS system showed that the positive mode is the most suitable method regarding the intensity and fragmentation. On the basis of the obtained results, a comparison of total ion chromatograms (TIC) for the 6CNA analytical standard and 6CNA irradiated with presence of TiO_2 catalyst is presented in Figure 63. The TIC of the parent compound (6CNA) is presented in Figure 63a with the retention time 11.16 min and it is in accordance with the HPLC–DAD data. In Figure 63c, it is shown that fragmentation of 6CNA results in major ESI+ ions with *m/z* 158 [M+H] and *m/z* 160 [M+H+2] which can be attributed to the quasi-molecular ion of 6CNA (157 g mol^{-1}), thus taking into account that the occurrence of the ion with mass *m/z* 160 is correlated with the chlorine isotope with mass 37 g mol^{-1}. ESI+ fragment with *m/z* 122 corresponds to the quasi-molecular ion of 6CNA with loss of a chlorine atom. Since the concentrations of generated products within the photocatalytic degradation were very low, the samples for LC–MS and GC–MS analyses were preconcentrated 100 times as described in Chapters 2.4.4 and 2.4.5.
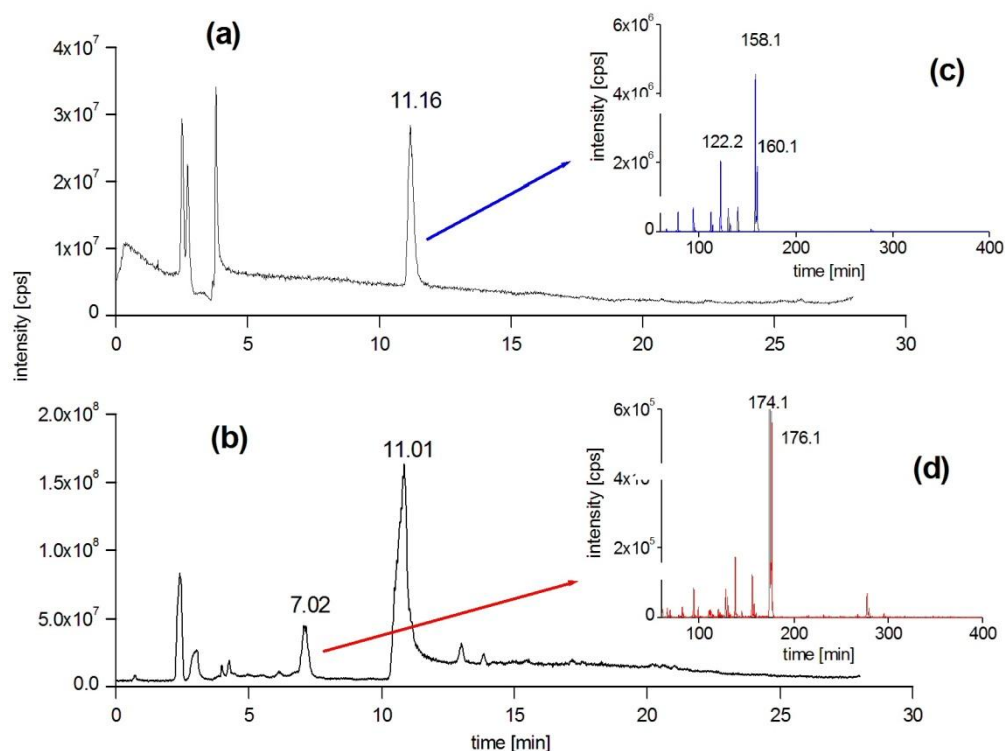
Figure 63: Total ion chromatogram of 6CNA standard (a), total ion chromatogram of 6CNA treated with TiO$_2$ (b) with extracted ions for peaks at 11.16 min (c) and 7.02 min (d).

In the samples treated with photocatalytic degradation, an additional peak at 7.02 min was observed as shown in Figure 63b. Furthermore, the mass scans of peak 7.02 min and 11.01 min were extracted in order to characterise the ESI+ ions. The additional new peak eluting at 7.02 min gave major ESI+ ions with *m/z*, 174 and 176, as presented in Figure 63d. To confirm that these two ESI+ ions, eluting at 7.02 min, correspond only to a newly formed compound within photocatalytic degradation, extraction of these specific ions was performed. These two ions could not be observed neither in the blank sample nor in the untreated sample of 6CNA. Further identification was then confirmed by the tandem mass spectrometry fragmentation profile of the [M+H+16] ion. This technique revealed that the ESI+ ion with *m/z* 174 eluting at time 7.02 min gave major MS^2 fragments with *m/z*, 128, 94 and 69. The molecular mass of the new compound was 16 amu higher than that of the starting compound 6CNA and it seems plausible that its molecule contains an additional oxygen atom.

An additional confirmation analysis of samples after photocatalytic degradation was also performed with the GC–MS technique. The peak of the parent compound 6CNA is eluting at time 10.58 min giving the major ions with *m/z* 157, 140, 112 and 76 and it is completely in accordance with previously published GC–MS analyses data on 6CNA (Agüera *et al.*, 1998; Dell'Arciprete *et al.*, 2009). The most abundant fragment with

mass *m/z* 157 corresponds to the quasimolecular ion of 6CNA [M - H]⁻. At the time 6.32 min an additional peak was observed within GC analyses and the MS technique extracted major ions with *m/z* 171, 140, 112, 76. Fragments with *m/z* 140, 112 and 76 are the same for parent compound (6CNA) and for the newly detected degradation product, so I can assume that the common reaction, addition to an aromatic ring (Burrows *et al.*, 2002), took place within the photocatalytic degradation. The most abundant ion with mass *m/z* 171 [M-2] could correspond to the same compound as previously detected with the LC–MS technique. As mentioned above, the difference in mass of 16 amu could represent several different compounds as presented in Figure 64. The first possibility is the formation of the N-oxide, (compound **F**) and the second possibility is the formation of hydroxyl derivate of 6CNA, however, the hydroxyl group could form three positional isomers (compounds **G**, **H**, **I**).
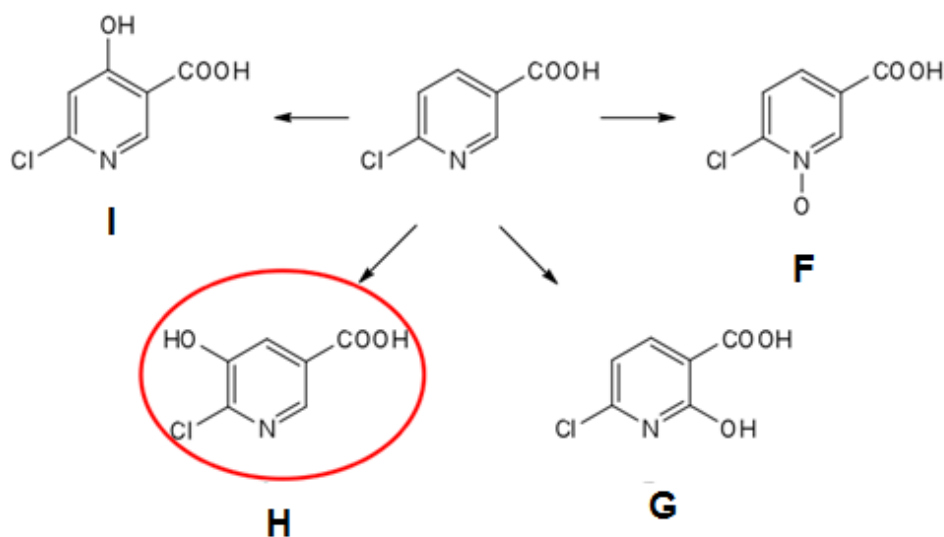
Figure 64: Proposed possible photodegradation products (F, G, H and I) of 6CNA in the presence of TiO₂ photocatalyst.[10]

Therefore, extra analyses with ¹H NMR were performed in order to obtain a complete insight into the structure of the new degradation product. Compound **F**, the N oxide, was ruled out by ¹H NMR as well as by HPLC with the comparison of spectra and chromatogram of an independently prepared standard (Liotta and Hoff, 1980). Of the three positional isomers (**G**, **H**, **I**), the isomer **H** (6-chloro-5-hydroxynicotinic acid) is the most plausible one on the basis of the ¹H NMR analyses. In the ¹H NMR spectrum for the reaction mixture after photocatalysis, besides the peaks of the starting 6CNA and some minor by products, a pair of doublets with coupling constant of 1.9 Hz was discernible. Such value of the coupling constant is characteristic for two protons at the

---

[10]The confirmed photodegradation product on the basis of LC-MS/MS and ¹H NMR data is marked with red colour.

positions 2 and 4 on the pyridine ring. The ^{1}H NMR spectrum of the reaction mixture exhibited two sets of peaks, one belonging to the starting 6CNA and one to the intermediate, formed during photolysis. Methanol d4, δ/ppm, 6-CNA: 7.57 (d, J = 8.3 Hz, 1H); 8.34 (dd, J = 8.3; 2.4 Hz, 2H); 8.92 (d, J = 1.9 Hz, 1H). Newly formed product: 7.80 (d, J = 1.9 Hz, 1H); 8.42 (d, J = 1.9 Hz, 1H) is marked with red colour in Figure 64.

Final step in the evaluation of the AOPs efficiency was the toxicity testing with the luminescent bacteria *V. fischeri.* It can be emphasised that the samples, after applying photocatalytic degradation with TiO$_2$, showed increased luminescence inhibition in comparison to the parent compound as shown in Figure 65. Inhibition of luminescence after 30 min of photocatalytic degradation increased from starting at 8.9 ± 1.8 % to 25.7 ± 1.6 %, Moreover, after 120 min the luminescence inhibition reached 31.9 ± 2.8 % despite the fact, that a good mineralisation rate was achieved. This fact, however, can be attributed to the formation of possible toxic by-products or intermediates and consequently causing higher toxicity of the water solution. It is worth mentioning, that also synergistic effects of newly formed by-products cannot be excluded.
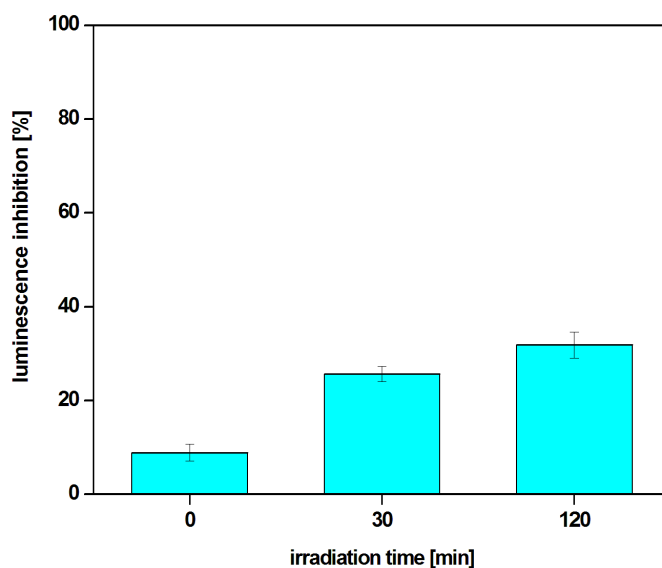
Figure 65: Luminescence inhibition for **V.** fischeri *of 6CNA aqueous solution during photocatalytic degradation with immobilised TiO$_2$.*

In general, toxicity studies of the 6CNA solution with photocatalytic treatment with TiO$_2$ are in agreement with the other published data including toxicity monitoring of pesticides within photocatalytic degradation (Sakkas *et al.*, 2004; Dell'Arciprete *et al.*, 2009, 2010).

Since the photocatalytic degradation was performed with immobilised TiO_2, the possible effect of titanium particles leaching from the glass slides into the solution was investigated. The completely dry glass slides with immobilised TiO_2 were weighted before and after photocatalytic degradation, but no difference in mass was detected. Nevertheless, the possible toxic effect of dissolved TiO_2 in the 6CNA aqueous solution within treatment was also assessed. The photocatalytic experiment of pure double deionised water was additionally performed and the water samples were afterwards exposed to the luminescent bacteria *V. fischeri* in the same intervals as in case of the 6CNA photocatalytic degradation experiments. No increase in toxicity was noticed, so I can easily claim, that the increased toxicity after photocatalytic degradation of 6CNA aqueous solution was only due to new by-products formed within the reaction and not due to TiO_2 used as catalyst.

To compare, within photolytic degradation of the 6CNA aqueous solution, no degradation was observed and no mineralization as well. The UV-Vis spectra did not change during irradiation and the toxicity of selected samples presented no change in luminescence inhibition during treatment.

5.7 Toxicity experiments

5.7.1 Toxicity testing with *Vibrio fischeri*

Toxicity testing of aqueous solutions for all three substances was performed and the results revealed the highest toxicity in case of TCP, while for IMP and 6CNA solutions at any concentration did not cause significant inhibition in the luminescence of *V. fischeri* bacteria. The results are presented in Table 24.

Table 24: Inhibition of luminescence in V. fischeri *bacteria for IMP, 6CNA and TCP aqueous solution.*

concentration [mg L^{-1}]			inhibition of the luminescence [%]		
IMP	6CNA	TCP	IMP	6CNA	TCP
54.0	55.0	52.0	7.6 ± 0.7	21.4 ± 1.1	80.1 ± 0.1
27.0	27.5	26.0	6.6 ± 0.0	14.8 ± 1.3	65.6 ± 0.4
13.5	13.8	13.0	7.3 ± 0.1	8.3 ± 0.9	45.3 ± 1.1
6.8	6.9	6.5	3.6 ± 2.2	8.7 ± 2.7	25.1 ± 1.9
3.4	3.4	3.3	3.2 ± 0.5	5.0 ± 1.6	10.0 ± 0.2

On the basis of results listed above, the dose response curve for TCP was derived and the 30 min EC$_{50}$ value was 15.1 mg L^{-1} and the 30 min EC$_{20}$ was 4.7 mg L^{-1} Dose response curve for the TCP aqueous solution is presented in Figure 66.
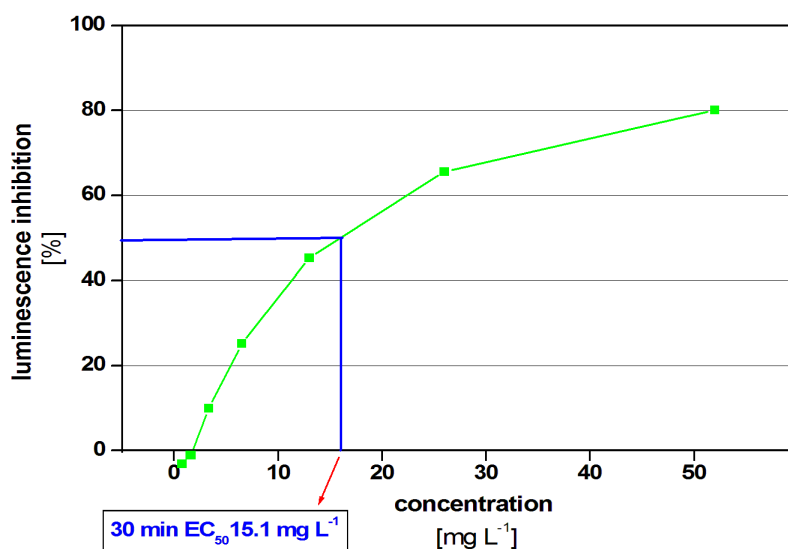
Figure 66: Dose response curve for aqueous solution of TCP for V. fischeri *luminescent bacteria within 30 minutes of exposure.*

For IMP and 6CNA, the inhibition of luminescence with applied concentrations was too low to calculate 30 min EC$_{50}$. The 30 min EC$_{20}$ for 6CNA also cannot be precisely calculated.

Following the EU legislation, the toxicity categories based on the EC_{50} values were established (European Commission Directive 93/67/EEC). The terms "*very toxic to aquatic organisms*" ($EC_{50} \leq 1$ mg L^{-1}), "*toxic*" (EC_{50} in the range of 1–10 mg L^{-1}), and "*harmful*" (EC_{50} in the range of 10–100 mg L^{-1}) were introduced. However, according to Hernando *et al.* (2007) an additional category for $EC_{50} > 100$ mg L^{-1} has been included and classified as *"not harmful to aquatic organisms"*. These facts were furthermore applied in this research in order to classify the investigated compounds into proper categories.

Based on the collected results I can classify TCP (30 min EC_{50} = 15.1 mg L^{-1}) as "*harmful to aquatic organisms*". Alternatively 30 min EC_{50} for 6CNA and IMP could not be calculated due to the very low inhibition of luminescence for given dilution levels. Nevertheless, the used concentrations were still very high from the environmental point of view.

5.7.2 Toxicity testing with *Porcellio scaber*

5.7.2.1 Effects of IMP on Porcellio scaber

The effect of IMP on the survival of *P. scaber* is presented in Figure 67.
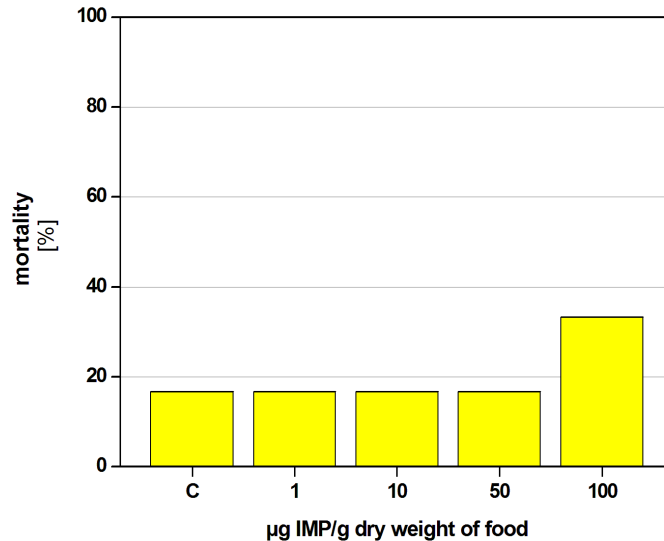
Figure 67: Mortality of adult P. scaber *during two weeks of exposure to uncontaminated food (C) and leaves contaminated with 1, 10, 50 and 100 µg IMP/g dry food (N = 12 for each group).*

Mortality was observed in all groups, in control and in exposed groups. Within the two weeks of exposure, mortality in the control group was 16.7 % of the animals, which in detail means two animals from twelve. In the following groups (1, 10 and 50 µg IMP/g dry food) the mortality was the same, i.e. two animals out of twelve died. On the other hand, at the highest exposure concentration, 100 µg IMP/g dry food, the highest mortality was observed. Here 33.3 % of animals died, meaning that four out of twelve animals died. The results suggest that IMP, in higher concentrations, could negatively effect the survival of the *P. scaber* within two weeks of exposure. It needs to be noted, that no clear causes of death were observed (i.e. fungus).

Furthermore, the effect of IMP on body weight change of *P. scaber* was studied and the results are presented in Figure 68.
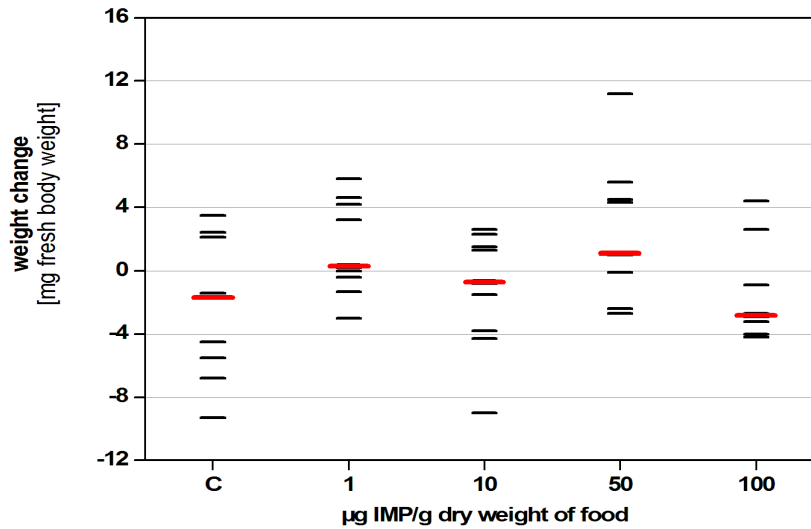
Figure 68: Body weight change (in mg fresh weight) of adult P. scaber *after two weeks of exposure to uncontaminated food (C) and leaves contaminated with 1, 10, 50 and 100 µg IMP/g dry food (N = 10 for C; N = 10 for 1 µg/g; N = 10 for 10 µg/g; N = 10 for 50 µg/g; N = 8 for 100 µg/g). Red longer lines indicate median values.*

As it can be observed from Figure 68, in the control (unexposed) group the median value indicates a decrease in weight change. This, however, was expected due to the induced stress since the animals were captured in a terrarium during the experiment, weighted and finally transferred to Petri dishes. Decrease in body weight for the control group was also noticed by Stanek *et al.* (2006). It is well known, the captivity or transfer from the natural environment and also spraying and monitoring of the animals does affect them. But, no significant weight change in comparison to the control group was observed in any exposed group, meaning that the food containing IMP does not affect significantly weight change of adult *P. scaber* within two weeks of exposure.

Another studied indicator was defecation of animals during exposure. From Figure 69, the faecal pellets production within two weeks for all groups is presented and compared. Within the non exposed group, the daily defecation was not as scattered as in case of all exposed groups. Nevertheless, the median values for all groups do not differ much and consequently, the Mann-Whitney statistics did not show any significant difference in faecal pellet production between the unexposed group and exposed groups.

114
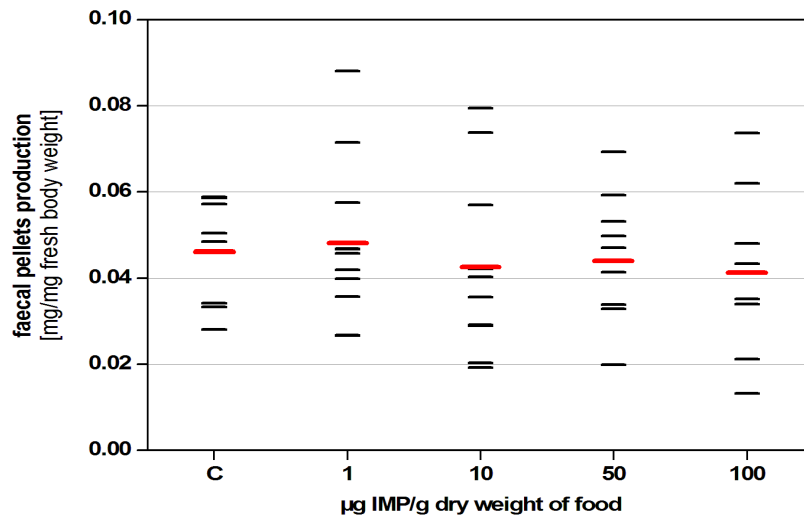
*Figure 69: Faecal pellets production (in mg dry weight/mg fresh body weight/day) of adult **P. scaber** after two weeks of exposure to uncontaminated food (C) and leaves contaminated with 1, 10, 50 and 100 µg IMP/g dry food (N = 10 for C; N = 10 for 1 µg/g; N = 10 for 10 µg/g; N = 10 for 50 µg/g; N = 8 for 100 µg/g). Red longer lines indicate median values.*

The effect of IMP on the food consumption within two weeks of exposure is presented in Figure 70. A very similar picture, as with defecation, can be observed with consumption rate. The values for the unexposed group are scattered as well as values for exposed groups. The median values of exposed groups do not differ from the control group, indicating no influence of IMP on consumption rate for *P. scaber* within two weeks of experimentation. This fact was also further confirmed by Mann-Whitney non parametric test, where no significant difference between the control group and exposed groups was observed.
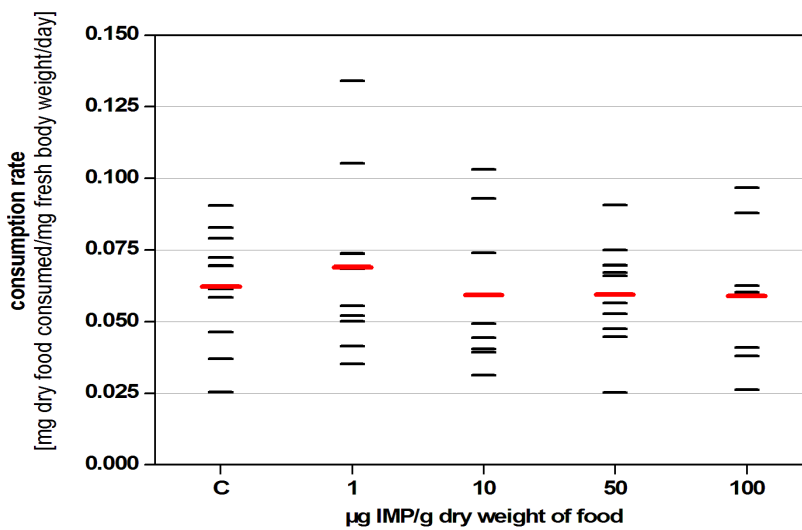
*Figure 70: Consumption rate (in mg food consumed/mg fresh body weight/day) of adult **P. scaber** after two weeks of exposure to uncontaminated food (C) and leaves contaminated with 1, 10, 50 and 100 µg IMP/g dry food (N = 10 for C; N = 10 for 1 µg/g; N = 10 for 10 µg/g; N = 10 for 50 µg/g; N = 8 for 100 µg/g). Red longer lines indicate median values.*

Assimilation efficiency, as shown in Figure 71, again revealed no significant difference between the control group and exposed groups. However, a high scattering of values is noticed at concentration 1 µg IMP/g dry food, but nevertheless, the median values for all exposed groups do not differentiate significantly from the control group.
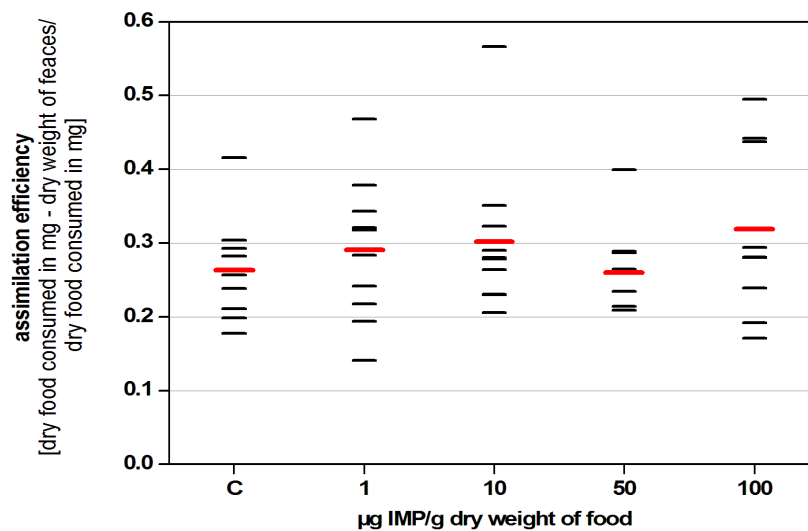
Figure 71: Assimilation efficiency of adult P. scaber *after two weeks of exposure to uncontaminated food (C) and leaves contaminated with 1, 10, 50 and 100 µg IMP/g dry food (N = 10 for C; N = 10 for 1 µg/g; N = 10 for 10 µg/g; N = 10 for 50 µg/g; N = 8 for 100 µg/g). Red longer lines indicate median values.*

What caught my attention is the fact that the ecotoxicological exposure of *P. scaber* to IMP showed no statistical difference between control and exposed groups for all calculated physiological parameters. In the literature, the effect of diazinon (the parent compound of IMP) was already studied by several authors. Widianarko and Van Straalen (1996) studied the mortality of *P. scaber* when exposed for different period of time to different concentrations of diazinon in soil. The results clearly indicated high mortality for concentrations 8.00 µg/g and 11.31 µg/g soil and the LC_{50} value was 4.4 µg of diazinon/g dry weigh soil.

On the other hand, Stanek *et al.,* (2006) studied the linkage along levels of biological complexity in juvenile and adult fed *P. scaber.* They assessed the effects of diazinon on AChE activity, lipid, protein and glycogen content, weight change, feeding activity and mortality of juvenile and adult terrestrial isopods. The non-observed effect concentration (NOEC) for AChE activity after exposure within two weeks was below 5 µg/g diazinon. Glycogen and lipid content, feeding activity and weight change were not affected in two weeks exposure up to 100 µg/g diazinon.

Since, on the physiological level, no influence of IMP to *P. scaber* was observed, the levels of lipid peroxidation in hepatopancreatic digestive glands were assessed. The hepatopancreas plays an important role in xenobiotic metabolism in *P. scaber* and therefore, the oxidative stress as a consequence could be promoted. As previously described in the theoretical section, the lipid peroxidation can be asses via MDA measurements. As it is presented in Figure 72, there is no significant difference in lipid peroxidation levels between control the group and exposed groups.
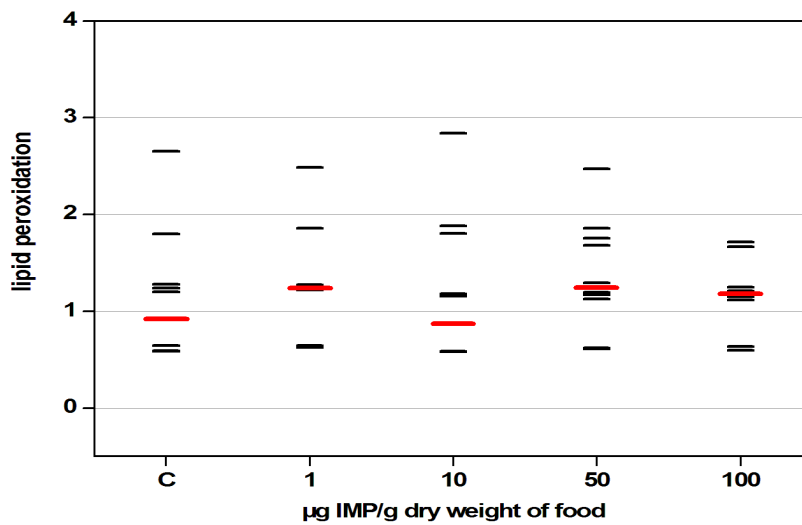
Figure 72: Lipid peroxidation in hepatopancreas of adult **P. scaber** *after two weeks of exposure to uncontaminated food (C) and leaves contaminated with 1, 10, 50 and 100 µg IMP/g dry food (N = 10 for C; N = 10 for 1 µg/g; N = 10 for 10 µg/g; N = 10 for 50 µg/g; N = 8 for 100 µg/g). Red longer lines indicate median values.*

The values of lipid peroxidation for all groups are normalized, meaning that the mean value for the control group is one. As it can be seen from Figure 72, no difference between the control group and exposed groups can be observed.

Therefore, it can be assumed, on the basis of gathered data, IMP does not have an acute affect on *P. scaber* through food exposure for two weeks. For better risk assessment of IMP to terrestrial organisms, additional tests should be performed. Of great interest would also be testing the effect of IMP on *P. scaber* when applied topically, since the *P. scaber* can be in contact with contaminated soil, leaves and water.

5.7.2.2 Effects of TCP on Porcellio scaber

The effect of TCP on survival of *P. scaber* is presented in Figure 73.
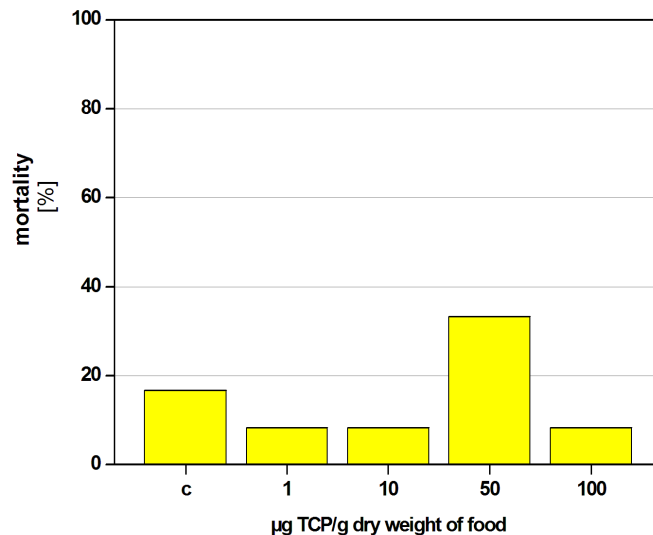
Figure 73: Mortality of adult P. scaber during two weeks of exposure to uncontaminated food (C) and leaves contaminated with 1, 10, 50 and 100 µg TCP/g dry food (N = 12 for each group).

As can be noted, mortality was observed in all groups, in the control and in exposed groups. Within the two weeks of exposure, 16.7 % of animals in the control group died, which in detail means two animals from twelve. In following groups (1, 10 and 100 µg TCP/g dry food) the mortality rate was lower, 8.3 %, meaning that one animal out of twelve died. However, the highest mortality rate was observed at an exposure concentration 50 µg TCP/g dry food. Here 33.3 % of animals died, meaning that four out of twelve animals died. It needs to be mentioned, that in the control group, mortality was probably due to the fungus that was observed in Petri dishes of both dead animals. Interestingly, the highest mortality was not observed at highest concentration and my proposal is that this happened due to the effect of the hormesis.

The body weight change of *P. scaber* exposed to TCP was assessed and the results in detail are presented in Figure 74. Similar to previous experiments, the median value of the unexposed group again indicates a decrease in weight change. For exposed groups, the trend is different. At concentrations 1 µg/g and 10 µg/g dry food, the scattering of results is high, some animals, as a matter of fact, increased in body weight. On the other hand, for concentrations 50 µg/g and 100 µg/g dry food the values are similar to the unexposed group.
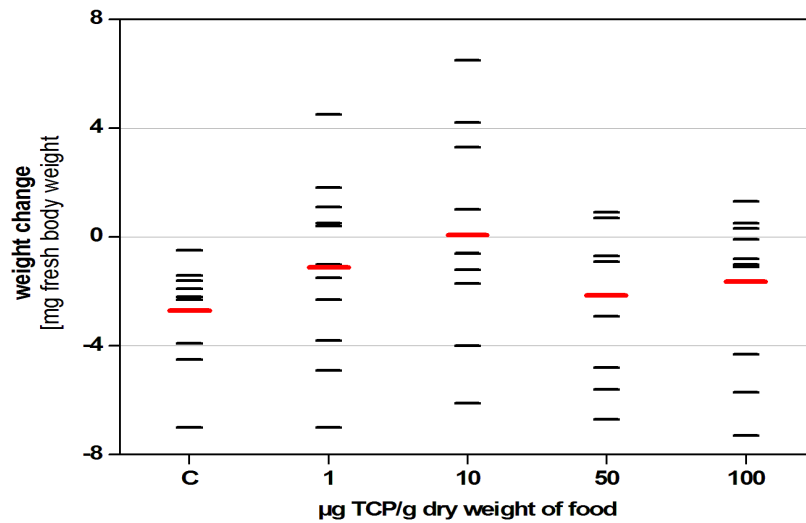
Figure 74: Body weight change (in mg fresh weight) of adult P. scaber after two weeks of exposure to uncontaminated food (C) and leaves contaminated with 1, 10, 50 and 100 µg TCP/g dry food (N = 10 for C; N = 11 for 1 µg/g; N = 11 for 10 µg/g; N = 8 for 50 µg/g; N = 11 for 100 µg/g). Red longer lines indicate median values.

Moreover, this increase of body weight during two weeks of exposure could indicate a higher metabolism rate due to the presence of a xenobiotic, i.e. TCP. The defecation assessment further highlighted this phenomenon and the detailed results are presented in Figure 75.
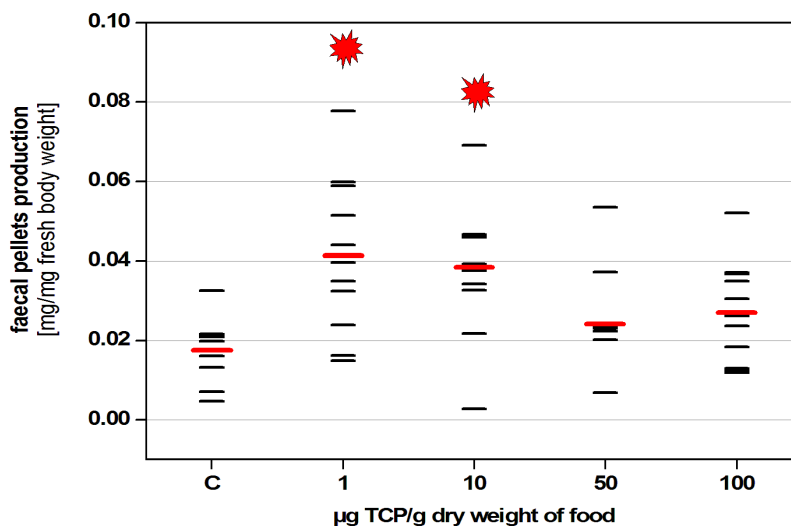
Figure 75: Faecal pellets production (in mg dry weight/mg fresh body weight/day) of adult P. scaber after two weeks of exposure to uncontaminated food (C) and leaves contaminated with 1, 10, 50 and 100 µg TCP/g dry food (N = 10 for C; N = 11 for 1 µg/g; N = 11 for 10 µg/g; N = 8 for 50 µg/g; N = 11 for 100 µg/g). Red longer lines indicate median values and the asterisk indicates significant difference in relation to control according to Mann-Whitney statistics.

My hypothesis of higher metabolism at lower TCP concentrations seems to be plausible. The daily faecal pellet production is very low in the case of the control group (i.e. median value of approximately 0.018 mg/mg/day) and a statistically significant difference was in comparison to the control group was observed for TCP concentrations of 1 μg/g and 10 μg/g dry food. In both cases, the defecation was higher, but also more scattered. No significant difference was observed for higher concentrations of TCP.

The results for consumption rate, as presented in Figure 76, did not follow the trend described above. No statistically significant difference in the consumption rate between the control group and exposed groups was noticed. However, it needs to be mentioned, that the median values of concentrations 1 μg/g and 10 μg/g dry food are much higher from median values of the control group. In future, more experiments, or experiments with higher numbers of animals, should be performed to clarify these indications.
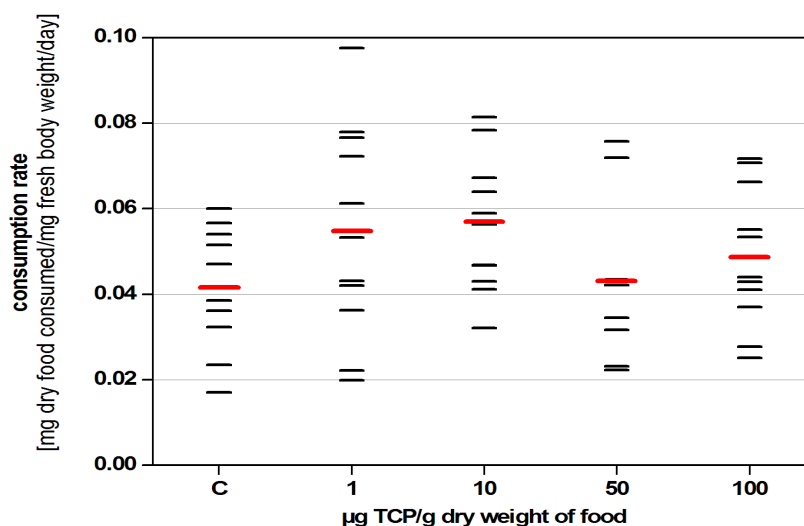
Figure 76: Consumption rate (in mg food consumed/mg fresh body weight/day) of adult **P. scaber** *after two weeks of exposure to uncontaminated food (C) and leaves contaminated with 1, 10, 50 and 100 μg TCP/g dry food (N = 10 for C; N = 11 for 1 μg/g; N = 11 for 10 μg/g; N = 8 for 50 μg/g; N = 11 for 100 μg/g). Red longer lines indicate median values.*

Assimilation efficiency within two weeks of exposure again indicated higher metabolism at lower TCP concentrations. As presented in Figure 77, the median value for assimilation efficiency for the control group was 0.59, while for exposed groups with low TCP concentrations (1 μg/g and 10 μg/g dry food) the median values were 0.25 and 0.34, respectively. Further analysis with Mann-Whitney non-parametric test showed significant statistical difference between the control group and groups with concentration 1 μg/g and 10 μg/g. For concentrations 50 μg/g and 100 μg/g dry food,

the median values for assimilation efficiency were 0.47 and 0.46, respectively and consequently no significant statistical difference was observed.
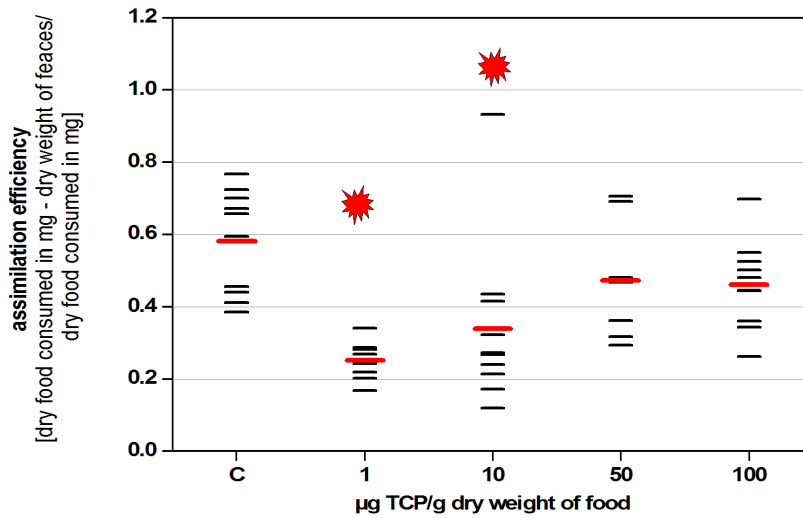
Figure 77: Assimilation efficiency of adult P. scaber *after two weeks of exposure to uncontaminated food (C) and leaves contaminated with 1, 10, 50 and 100 µg TCP/g dry food (N = 10 for C; N = 11 for 1 µg/g; N = 11 for 10 µg/g; N = 8 for 50 µg/g; N = 11 for 100 µg/g). Red longer lines indicate median values and the asterisk indicates significant difference in relation to control according to Mann-Whitney statistics.*

The hepatopancreatic lipid peroxidation values for adult *P. scaber* are presented in Figure 78. The median value for the control group is set at one and for exposed groups all median values are higher.
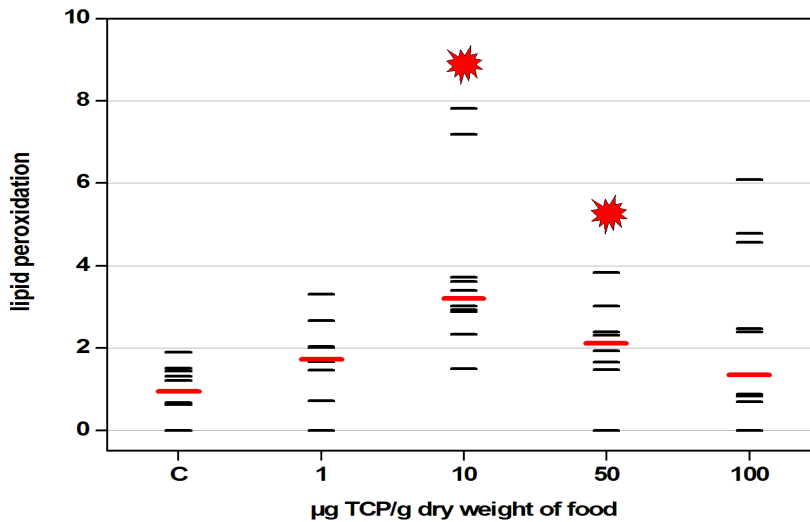
Figure 78: Lipid peroxidation in hepatopancreas of adult P. scaber *after two weeks of exposure to uncontaminated food (C) and leaves contaminated with 1, 10, 50 and 100 µg TCP/g dry food (N = 10 for C; N = 11 for 1 µg/g; N = 10 for 10 µg/g; N = 8 for 50 µg/g; N = 11 for 100 µg/g). Red longer lines indicate median values and the asterisk indicates significant difference in relation to control according to Mann-Whitney statistics.*

On the basis of results calculated previously, I assumed that the lipid peroxidation would increase for the low concentrations of TCP. To the contrary, for 1 µg/g dry food, no statistical difference was observed when compared to the control group. While at 10 µg/g and 50 µg/g dry food, a high increase for lipid peroxidation median values were observed, i.e. 3.2 and 2.1, respectively. The Mann-Whitney statistic, therefore, showed a significant statistical difference when compared to the control group. On the other hand, no significant difference (increase) was observed for the highest concentration 100 µg/g dry food.

All collated results indicate, that TCP could have a negative effect on terrestrial isopod *P. scaber* exposed through food. The daily defecation increased significantly in comparison to the control group for groups of 1 µg/g and 10 µg/g dry food and the assimilation efficiency showed high decrease for the same exposed groups. The consumption rate increased for these two already mentioned exposed groups, but statistics did not show significant difference. Finally, hepatopancreatic lipid peroxidation clearly pointed to the presence of significantly higher oxidative stress for exposed groups of 10 µg/g and 50 µg/g dry food. Of great concern is the fact that TCP in absence of sunlight acts like very persistent chemical and thus can be found in the soil and on the leaves in the upper level of the soil.

A study performed by Achuthan Nair *et al.,* (2002) reports the effects of chlorpyrifos as a parent compound of TCP, to *P. scaber*. Adult animals were exposed for different periods of time to a known quantity of the dry lemon leaves, soaked with known concentration of chlorpyrifos. Unfortunately, the detailed procedure is not clearly explained. The growth, feeding rate, assimilation rate and assimilation efficiency were calculated after 14 days of experimentation. Chlorpyrifos was found to be highly toxic to *P. scaber* and the 24 h LD_{50} was observed to be 27.5 ppm. Significant difference in feeding rate, assimilation rate and assimilation efficiency was observed for all applied concentrations.

5.7.2.3 Effects of 6CNA on Porcellio scaber

The survival of *P. scaber* exposed to 6CNA for two weeks is presented in Figure 79.
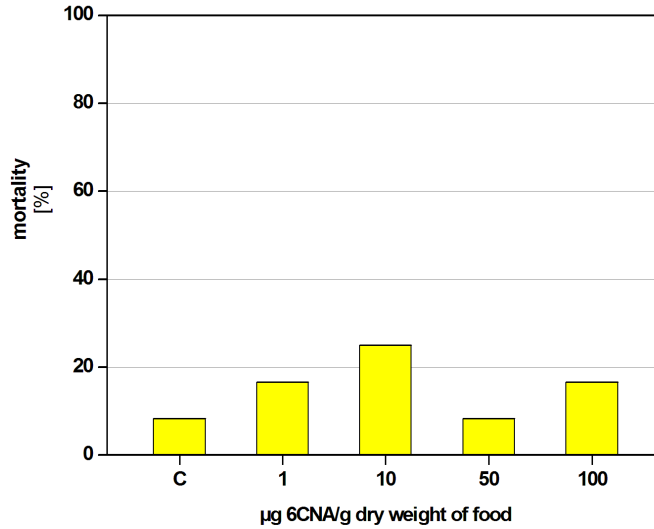
Figure 79: Mortality of adult P. scaber *during two weeks of exposure to uncontaminated food (C) and leaves contaminated with 1, 10, 50 and 100 μg 6CNA/g dry food (N = 12 for each group).*

The mortality of *P. scaber* after two weeks of exposure to 6CNA revealed interesting results, as it is shown in Figure 79. The highest mortality, i.e. 25 % was observed at concentration 10 μg/g dry food, meaning that three out of twelve animals died. On the other hand, the lowest mortality i.e. 8.3 % was observed within control group and concentration 50 μg/g dry food, meaning that one out of twelve animals died.

Additional results for body weight change during exposure are presented in Figure 80 and it is clearly seen that the control group showed low dissipation and the median value indicates the decrease of fresh body weight after exposure. In the case of exposed groups, a very similar scenario is observed for concentrations 1 μg/g and 100 μg/g dry food. When applied the concentration 10 μg/g dry food, the median value indicated the slight increase in body weight when compared to the control group. In contrary, at concentration 50 μg/g dry food, the median value of weight change showed the decrease when compared to control group. It needs to be mentioned, that at this particular concentration, the values were very scattered, some of them showed increase while other showed high decrease of body weight. Nevertheless, the Mann-Whitney test showed no significant statistical difference between control group and exposed groups.
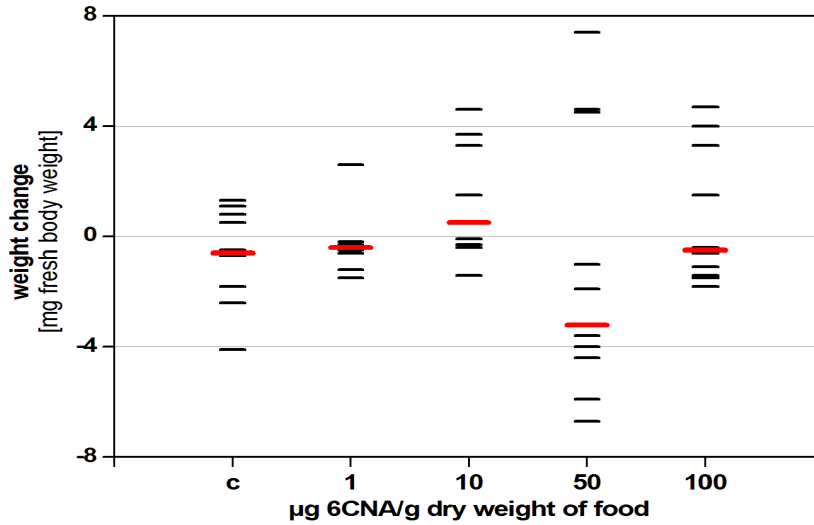
Figure 80: Body weight change (in mg fresh weight) of adult P. scaber *after two weeks of exposure to uncontaminated food (C) and leaves contaminated with 1, 10, 50 and 100 µg 6CNA/g dry food (N = 11 for C; N = 10 for 1 µg/g; N = 9 for 10 µg/g; N = 11 for 50 µg/g; N = 10 for 100 µg/g). Red longer lines indicate median values.*

The daily defecation, as presented in Figure 81, showed no significant change between the control group and exposed groups. However, a trend of increase is observed, since the median values for all groups are increasing with the increasing 6CNA concentration in the food. In the control group, the faecal pellets production reached the median value of 0.029 and other groups were increased as follows; 0.032 for 1 µg/g, 0.033 for 10 µg/g, 0.034 for 50 µg/g and 0.040 for 100 µg/g dry food. Finally, the Mann-Whitney test showed no significant statistical difference between the control group and exposed groups.
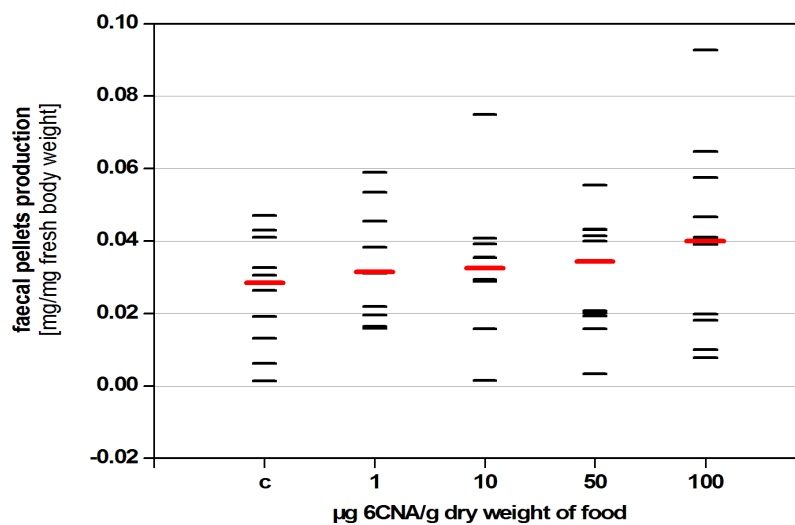
Figure 81: Faecal pellets production (in mg dry weight/mg fresh body weight/day) of adult P. scaber *after two weeks of exposure to uncontaminated food (C) and leaves contaminated with 1, 10, 50 and 100 µg 6CNA/g dry food (N = 11 for C; N = 10 for 1 µg/g; N = 9 for 10 µg/g; N = 11 for 50 µg/g; N = 10 for 100 µg/g). Red longer lines indicate median values.*

Moreover, the consumption rate, as presented in Figure 82, followed the same trend as described above.
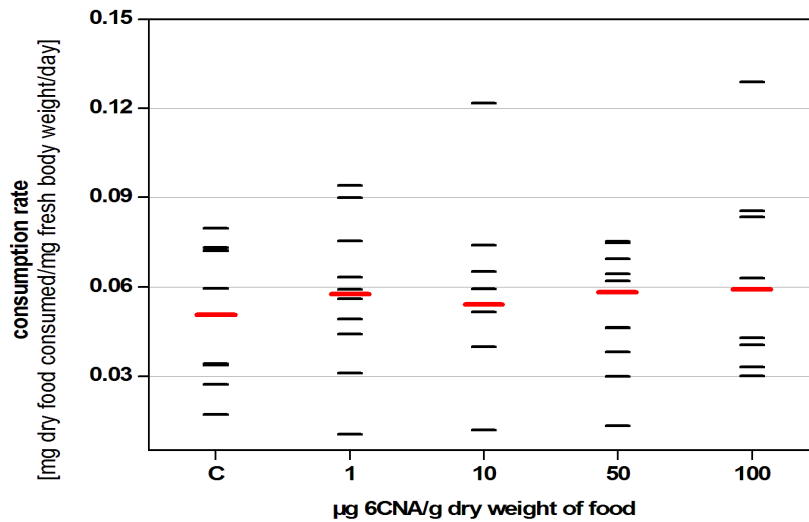
Figure 82: Consumption rate (in mg food consumed/mg fresh body weight/day) of adult **P. scaber** *after two weeks of exposure to uncontaminated food (C) and leaves contaminated with 1, 10, 50 and 100 µg 6CNA/g dry food (N = 11 for C; N = 10 for 1 µg/g; N = 9 for 10 µg/g; N = 11 for 50 µg/g; N = 10 for 100 µg/g). Red longer lines indicate median values.*

Assimilation efficiency assessment again showed similar results as obtained previously – there is a trend of median values decreasing. As it can be seen from Figure 83, the assimilation efficiency for group of adult animal*s* exposed to non contaminated food resulted in median value of 0.048, while for 1 µg/g the median value was 0.044, for 10 µg/g 0.49, for 50 µg/g 0.45 and for the last group of 100 µg/g the median value was 0.44.
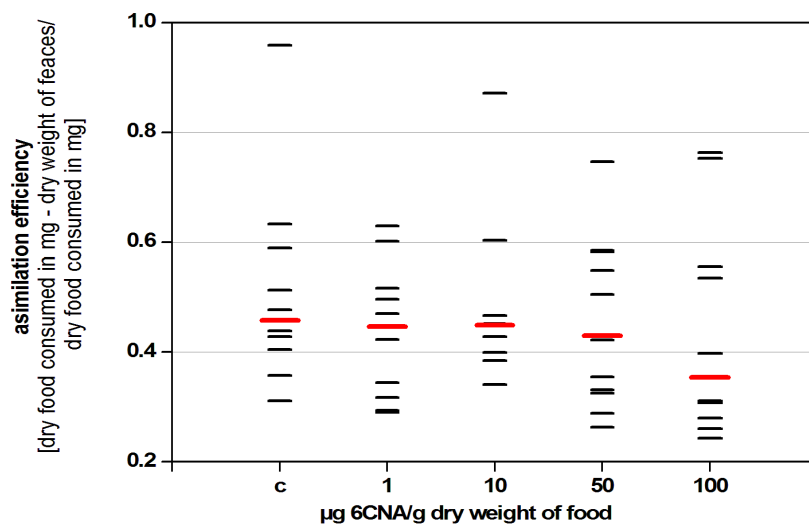
Figure 83: Assimilation efficiency of adult **P. scaber** *after two weeks of exposure to uncontaminated food (C) and leaves contaminated with 1, 10, 50 and 100 µg 6CNA/g dry food (N = 11 for C; N = 10 for 1 µg/g; N = 9 for 10 µg/g; N = 11 for 50 µg/g; N = 10 for 100 µg/g). Red longer lines indicate median values.*

Nevertheless, a high scattering of results within the last exposed groups was observed and finally, the Mann-Whitney test showed no statistical significant difference compared to the control group.

Additionally, the lipid peroxidation level in the digestive glands of the hepatopancreas was assessed for all groups. The values for the control group were, as previously, normalized to number one. As it can be observed from Figure 84, the values for control group are not scattered and not many outlayers can be observed. On the other hand, for the exposed groups, again high scattering of the values is observed. The median values for all groups did not significantly distinguish, i.e. from 0.90 for the control group to 1.65 for the exposed group with concentration of 100 μg/g dry food. The Mann-Whitney test, however, did not show any significantly statistical difference between the control group and all exposed groups.
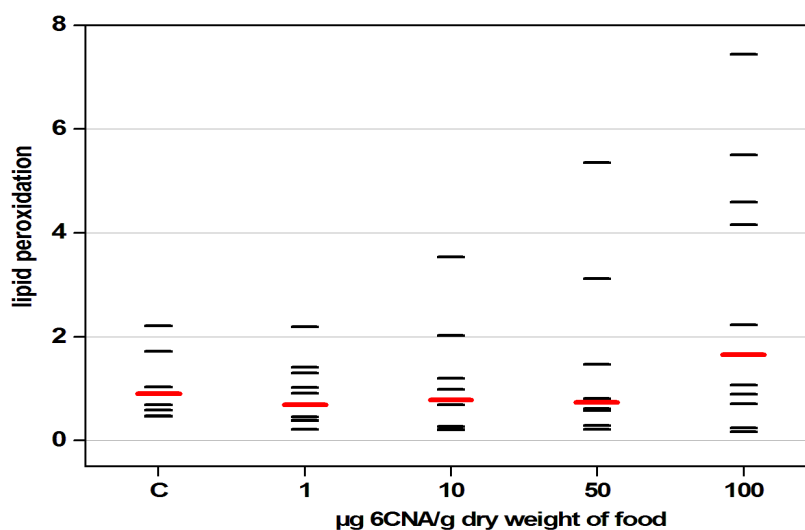
Figure 84: Lipid peroxidation in hepatopancreas of adult P. scaber *after two weeks of exposure to uncontaminated food (C) and leaves contaminated with 1, 10, 50 and 100 μg 6CNA/g dry food (N = 10 for C; N = 10 for 1 μg/g; N = 9 for 10 μg/g; N = 11 for 50 μg/g; N = 10 for 100 μg/g). Red longer lines indicate median values.*

On the basis of all gathered data, I can propose, that 6CNA does not have a negative effect on *P. scaber* isopods via food. It needs to be noted, that the apparent increase of the parameters was observed when animals were exposed to higher concentrations. On the other hand, the Mann-Whitney test showed no significant difference and, therefore, no significant negative effect to the animals.

To completely ensure that 6CNA can act like non-toxic chemical, additional tests with a higher number of animals and some extra tests with sublethal endpoints should be performed.

In addition, the effect of imidacloprid, the parent compound of 6CNA, on terrestrial isopods *P. scaber* was thoroughly studied by Drobne *et al.,* (2008). The authors suggested, that weight gain, feeding rate, total protein contents, GST and digestive gland epithelial thickness in juveniles and adults were most affected. Moreover, an estimate of actual intake rates suggests that imidacloprid affects isopods at similar exposure concentrations as insects. On the other hand, effect of acetamiprid, a second parent compound of 6CNA, on terrestrial isopods was not studied at all and to my knowledge no data is available in scientific databases.

6   CONCLUSIONS

The main goal of my research was to investigate the possible persistence, degradation and toxicity of three transformation products; 2-isopropyl-6-methyl-4-pyrimidinol, the TP of diazinon; 3,5,6-trichloro-2-pyridinol, the TP of chlorpyrifos and 6-chloronicotinic acid, the common TP of acetamiprid and imidacloprid.

The stability study under laboratory conditions revealed high stability of 6CNA and IMP in aqueous solution when exposed to sunlight or darkness. However, alternatively, TCP showed to be a photolabile compound, which in the presence of sunlight undergoes fast transformation into other compound(s).

Furthermore, the stability testing of aqueous solution of all three TPs when exposed to simulated sunlight conditions using the Suntest apparatus, confirmed the laboratory study results. IMP and 6CNA were very stable at all applied intensities of irradiation, while on the other hand, TCP again showed disappearance within few hours when exposed to simulated sunlight. In all cases, the TOC measurements revealed no mineralization. What is of greatest concern is the fact that the luminescence inhibition for *Vibrio fischeri* bacteria increased significantly during irradiation of TCP, leading me to the conclusion that more toxic compound(s) are forming within photolysis.

Following the legislation, for food safety, in vegetables and fruits, only parent insecticides are monitored but, the most important and the most critical fact is that little attention, and consequently almost no control, is paid to the presence of metabolites which can be formed after the application. Since the UV-C germicidal lamp is widely used as a tool for food preservation, the stability of IMP, TCP and 6CNA under a monochromatic low-pressure mercury lamp (254 nm) in oxygenated and deaerated conditions were investigated. Results clearly indicated the fact that a clean photochemical reaction is occurring along with new by-products formation.

Furthermore, the photolytic and photocatalytic degradation with immobilised TiO_2 of IMP, TCP and 6CNA were performed. Results indicated that IMP and 6CNA cannot degrade easily in double deionised water under photolytic conditions. The work, however, suggests that photocatalytic degradation with immobilised TiO_2 is a fast process with pseudo first-order kinetics for all three investigated compounds. Mineralisation rates, estimated through TOC measurements, revealed absolutely no carbon removal in the case of photolytic degradation. However, through photocatalytic degradation with TiO_2, substantial mineralisation was achieved. Moreover, analyses of

inorganic ions indicated almost quantitative transformation of chlorine and nitrogen into chloride and nitrate but, on the other hand, without the presence of nitrite ions. Toxicity testing with *V. fischeri* luminescent bacteria revealed higher toxicity of samples from photocatalytic experiments, when compared to samples treated in photolytic experiments, although via photocatalytic degradation a higher removal of the initial compound, as well as higher mineralisation, were achieved. This fact can be attributed to the fact, that during photocatalysis more toxic by-products were formed.

In addition, the mass spectrometry techniques such as LC–ESI–MS and GC–MS were performed in almost all experiments and they revealed the formation of possibly new by-products after performing the degradation experiments. Some of the compounds, due to their different isomer positions, were further analysed and successfully confirmed with ^{1}H NMR techniques.

At the end, the toxicity testing of IMP, TCP and 6CNA was performed on luminescent bacteria *V. fischeri,* indicating very low luminescence inhibition after 30 min of exposure for IMP and 6CNA. TCP, however, showed to have negative effect on *V. fischeri* luminescence and therefore the 30 min EC_{50} was 15.1 mg L^{-1}. Moreover, the influence of three TPs on non-target terrestrial isopod *Porcellio scaber* was investigated. The animals were exposed for two weeks to contaminated food and the results show no significant difference compared to the control group for IMP and 6CNA, however, for TCP, the daily defecation, assimilation efficiency and lipid peroxidation ratio show significant difference for low concentrations in comparison to the control group.

Throughout the experiment the importance of pesticides' TP monitoring was demonstrated due to their persistence under environmental and simulated conditions and their possible transformations into more toxic by-product(s). The results of my study have also confirmed that application of AOPs cannot be evaluated only in terms of initial compound degradation and mineralisation rates, but also toxicity testing plays an important role. An extensive set of various analytical and biological methodologies should be implemented into degradation processes in order to successfully perform the efficiency evaluation. Furthermore, toxicity testing revealed negative effect of the TCP on non target organisms *P. scaber* and therefore highlights the necessity to implement several different organisms into toxicity testing. In conclusion, this research highlights the high importance of toxicity testing and the identification of the by-products.

7 ACKNOWLEDGEMENTS

8 REFERENCES

Abu-Qare A.W., Abou-Donia M.B. 2001a. High performance liquid chromatographic determination of diazinon, permethrin, DEET (N,N-diethyl-m-toluamide), and their metabolites in rat plasma and urine. Fresenius J Anal Chem. 370, 403-407.

Abu-Qare A.W., Abou-Donia M.B. 2001b. Quantification of nicotine, chlorpyrifos and their metabolites in rat plasma and urine using high-performance liquid chromatography. J. Chrom. B. 757, 295-300.

Acetamiprid Material Safety Data Sheet Sigma-Aldrich (http://www.sigmaaldrich.com/catalog/DisplayMSDSContent.do).

Achuthan Nair G., Mohamed A.I., Haeba M.H. 2002. Laboratory studies on LD_{50} of the woodlouse *Porcellio scaber* Latreille (Isopoda, Oniscidea) exposed to Chlorpyrifos (Dursban®). Afr. J. Ecol. 40, 393-395.

Agüera, A., Almansa E., Malato S., Maldonado M.I., Fernandez-Alba A.R. 1998. Evaluation of photocatalytic degradation of imidacloprid in industrial water by GC–MS and LC–MS. Analusis 26 (7), 245–251.

Allende A., Artés F. 2003. UV-C radiation as a novel technique for keeping quality of fresh processed »Lollo Rosso« lettuce. Food. Res. Int. 36, 739-746.

Anwar S., Liaquat F., Khan Q.M., Khalid Z.M., Iqbal S. 2009. Biodegradation of chlorpyrifos and its hydrolysis product 3,5,6-trichloro-2-pyridinol by *Bacillus pumilus* strain C2A1. J. Haz. Mat. 168, 400–405.

Arbeli Z., Fuentes C.L. 2007. Accelerated biodegradation of pesticides: An overview of the phenomenon, its basis and possible solutions; and a discussion on the tropical dimension. Crop Prot. Vol. 26, 12, 1733-1746.

Badawy M.I., Ghaly M.Y., Gad-Allah T.A., 2006. Advanced oxidation processes for the removal of organophosphorus pesticides from wastewater. Desalination. 194, 166–175.

Ballesteros Martin M.M., Sanches Perez J.A., Casas Lopez J.L., Oller I., Malato Rodriguez S., 2009. Degradation of a four-pesticide mixture by combined photo-Fenton and biological oxidation. Water Res. 43, 653–660.

Barceló D., Durand G., Bertrand N.D. 1993. Photodegradation of the organophosphorus pesticides chlorpyrifos, fenamiphos and vamidothion in water, Toxicol. Environ. Chem. 38, 183–199.

Barr D.B., Allen R., Olsson A.O., Bravo R., Caltabiano L.M., Montesano A., Nguyen J., Udunka S., Walden N., Walken R.D., Weerasekra G., Whitehead R.D., Schober S.E., Needham L.L. 2005. Concentrations of selective metabolites of organophosphorus pesticides in the United States population. Environmental Research 99, 314-326.

Bavcon M., Trebše P., Zupančič-Kralj L. 2003. Investigations of the determination and transformations of diazinon and malathion under environmental conditions using gas chromatography coupled with a flame ionisation detector. Chemosphere 50, 595-601.

Bavcon Kralj, M., Černigoj, U., Franko, M., Trebše, P., 2007a. Comparison of photocatalysis and photolysis of malathion, isomalathion, malaoxon, and commercial malathion-Products and toxicity studies. Water Res. 41, 4504–4514.

Bavcon Kralj, M., Franko, M., Trebše, P., 2007b. Photodegradation of organophosphorus insecticides – Investigations of products and their toxicity using gas chromatography–mass spectrometry and AChE-thermal lens spectrometric bioassay. Chemosphere 67, 99–107.

Belfroid A.C., van Drunen M., Beek M.A., Scharp S.M., van Gestel C.A.M., van Hattun B. 1998. Relative risks of transformation products of pesticides for aquatic ecosystems. Sci. Total. Environ. 222, 167-183.

Bicker W., Lämmerhofer M., Lindner W. 2005. Determination of chlorpyrifos metabolites in human urine by reversed-phase/weak anion exchange liquid chromatography-electrospray ionisation-tandem mass spectrometry. J.Chrom. B. 822, 160-169.

Budd R., O'geen A., Goh K.S., Bondarenko S., Gan J. 2011. Removal mechanisms and fate of insecticides in constructed wetlands. Chemosphere, Vol.83, 11, 1581-1587.

Burrows H.D., Canle M.L., Santaballa J.A., Steenken S. 2002. Reaction pathways and mechanisms of photodegradation of pesticides. J. Photochem. Photobio. B 67, 71–108.

Cáceres T., He W., Naidu R., Megharaj M. 2007. Toxicity of chlorpyrifos and TCP alone and in combination to *Daphnia carinata*: The influence of microbial degradation in natural water. Wat. Res. 41, 4497-4503.

Chambers, J.E., Levi P.E. (Eds.), Organophosphates, Chemistry, Fate, and Effects. Academic Press, San Diego, 1992, pp. 10, 15, 39, 47-73, 61,

Chiron S., Fernandez-Alba A., Rodriguez A. 1997. Pesticide chemical oxidation processes: an analytical approach. TrAC Trends Anal. Chem. 16 (9), 518-527.

Chiron S., Fernandez-Alba A., Rodriguez A., Garcia-Calvo E. 2000. Pesticide chemical oxidation:State-of-the-are. Water Research 34, 366-377.

Chlorpyrifos Material Safety Data Sheet, Sigma-Aldrich (http://www.sigmaaldrich.com/catalog/DisplayMSDSContent.do).

Chowdhury P., Viraraghavan T. 2009. Sonochemical degradation of chlorinated organic compounds, phenolic compounds and organic dyes – A reviw. Sci. Total. Environ. 407. 2474–2492.

Černigoj U., Lavrenčič Štangar U., Trebše P., Opara Krašovec U., Gross, S., 2006. Photocatalytically active TiO_2 thin films produced by surfactant-assisted sol–gel processing. Thin Solid Films 495 (1–2), 327–332.

Černigoj U., Lavrenčič Štangar U., Trebše P., 2007a. Degradation of neonicotinoid insecticides by different advanced oxidation processes and studying the effect of ozone on TiO_2 photocatalysis. Appl. Catal., B 75, 229–238.

Černigoj U., Lavrenčič Štangar U., Trebše P. 2007b. Evaluation of a novel carberry type photoreactor for the degradation of organic pollutants in water. J. Photochem. Photobiol. A. Chem., 188: 169–176.

Čolović M, Krstić D., Petrović S., Leskovac A., Joksić G., Savić J., Franko M., Trebše P., Vasić V. 2010. Toxic effects of diazinon and its photodegradation products. Toxicol. Lett. 193, 9-18.

Čolović M., Krstić D.Z., Ušćumlić G.S., Vasić V.M. 2011. Single and simultaneous exposure of acetylcholinesterase to diazinon, chlorpyrifos and their photodegradation products. Pestic. Biochem. Phys. 100, 16–22.

Daraghmeh A., Shraim A., Abulhaj S., Sansour R., Ng J.C., 2007. Imidacloprid residues in fruits, vegetables and water samples from Palestine. Environ. Geochem. Health 29, 45–50.

de Erenchun R. N., de Balugera Z .G., Goicolea M.A., Barrio R.J. 1997. Determination of imidacloprid and its major metabolite in soils by liquid chromatography with pulsed reductive amperometric detection. Anal. Chim. Acta. 349, 199-206.

del Mar Gómez-Ramos M., Pérez-Parada A., García-Reyes J.F., Fernández-Alba A.R., Agüera A. 2011. Use of an accurate-mass database for the systematic identification of transformation products of organic contaminants in wastewater effluents. J. Chromatogr. A, Vol. 1218, 44, 8002-8012.

Dell'Arciprete M.L., Santos-Juanes L., Sanz A.A., Vincente R., Amat A.M., Furlong J.P., Martire D.O., Gonzalez M.C., 2009. Reactivity of hydroxyl radicals with neonicotinoid insecticides: mechanism and changes in toxicity. Photochem. Photobiol. Sci. 8, 1016–1023.

Dell'Arciprete M.L., Santos-Juanes L., Arques A., Vercher R.F., Amat A.M., Furlong J.P., Martire D.O., Gonzalez M.C., 2010. Reactivity of neonicotinoid pesticides with singlet oxygen. Catal. Today 151, 137–142.

Díaz-Cruz M.S., Barceló D. 2006. Highly selective sample preparation and gas chromatographic-mass spectrometric analysis of chlorpyrifos, diazinon and their major metabolites in sludge and sludge-fertilized agricultural soils. J. Chrom. A. 1132, 21-27.

Diazinon Material Safety Data Sheet, Sigma-Aldrich (http://www.sigmaaldrich.com/catalog/DisplayMSDSContent.do).

Doong R.-A., Chang W.-H. 1997. Photoassisted titanium dioxide mediated degradation of organophosphorous pesticides by hydrogen peroxide, J. Photochem. Photobiol. A 107, 239–244.

Dr. Dennis Kunkel Microscopy, Inc./Visuals Unlimited, Inc. (http://visualsunlimited.photoshelter.com/image/I0000EnVts1cNFa0).

Drobne D., 1997. Terrestrial isopods – a good choice for toxicity testing of pollutants in the terrestrial environment. Environ. Tox. Chem. 16, 1159-1164.

Drobne D., Blažič M., C.A.M. Van Gestel, Lešar V., Zidar P., Jemec A., Trebše P. 2008. Toxicity of imidacloprid to the terrestrial isopod *Porcellio scaber* (Isopoda, Crustacea). Chemosphere 71, 1326-1334.

Duirk S.E., Tarr J.C., Collette T.W. 2008. Chlorpyrifos Transformation by Aqueous Chlorine in Presence of Bromide and Natural Organic Matter. J. Agric. Food. Chem. 56, 1328-1335.

El Hassani, A.K., Dacher, M., Gary, V., Lambin, M., Gauthier, M., Armengaud, C., 2008. Effects of sublethal doses of Acetamiprid and Thiamethoxam on the behavior of the honeybee (*Apis mellifera*). Arch. Environ. Contan. Toxicol. 54, 653–661.

European Union Council Directive 91/414/EEC of 15 July 1991 concerning the placing of plant protection.

European Union Council Directive 79/117/EEC of 21 December 1978 prohibiting the placing on the market and use of plant protection products containing certain active substances.

European Comission Regulation (EU) No 540/2011 of 25 May 2011 implementing Regulation (EC) No 1107/2009 of the European Parliament and of the Council as regards the list of approved active substances European Comission Regulation (EC) No 850/2004 of 29 April 2004 on persistent organic pollutantsand amending Directive 79/117/EEC.

European Comission Technical guidance documents in support of Directive 93/67/EEC on risk assessment of new notified substances and Regulation (EC) No. 1488/94 on risk assessment of existing substances (Parts I, II, III and IV).

European Commission Directive EC 1107/2009 of 21 October 2009 concerning the placing of plant protection products on the market and repealing Council Directives 79/117/EEC and 91/414/EEC .

European Commission Directive 93/67/EEC of 20 July 1993 laying down the principles for assessment of risks to man and the environment of subtances notified in accordance with Council Directive 67/548/EEC.

European Commission Regulation (EC) No 850/2004 of 29 April 2004 on persistent organic pollutantsand amending Directive 79/117/EEC.

Feng Y., Minard R.D., Bollag, J.-M., 1998. Photolytic and microbial degradation of 3,5,6-trichloro-2-pyridinol. Environ. Toxicol. Chem. 17 (5), 814-819.

Fernandez-Alba, A.R., Hernando, D., Agüera, A., Caceres, J., Malato, S., 2002. Toxicity assays: a way for evaluating AOPs efficiency. Water Res. 36, 4255–4262.

Garrido Frenich A., Egea Gonzalez F.J., Martinez Vidal J.L., Parrilla Vazquez P., Mateu Sanchez M., 2000. Determination of imidacloprid and its metabolite 6-chloronicotinic acid in greenhouse air by high-performance liquid chromatography with diode-array detection. J. Chromatogr. A 869, 497–504.

Geveke D.J. 2008. UV Inactivation of E. coli in Liquid Egg White. Food. Bioprocess. Technol. 1, 201-206.

Ghezzar M.R., Abdelmalek F., Belhadj M., Benderdouche N., Addou A. 2007. Gliding arc plasma assisted photocatalytic degradation of anthraquinonic acid green 25 in solution with TiO_2. Appl. Catal. B 72, 304–313.

Gil García M.D., Martínez Galera M., Santiago Valverde R., Galanti A., Girotti S. 2007. Column switching liquid chromatography and post-column photochemically fluorescence detection to determine imidacloprid and 6-chloronicotinic acid in honeybees. J. Chrom A., 1147, 17–23.

Guizzetti M., Pathak S., Giordano G., Costa L.G. 2005. Effect of organophosphorus insecticides and their metabolites on astroglial cell proliferation. Toxicology 215, 182-190.

Guohong X., Guoguang L., Dezhi S., Liqing Z., 2009. Kinetics of acetamiprid photolysis in solution. Bull. Environ. Contam. Toxicol. 82, 129–132.

Guzsvány V., Banic N., Papp Z., Gaal F., Abramović B., 2010. Comparison of different iron-based catalysts for photocatalytic removal of imidacloprid. React. Kinet. Mech. Catal. 99 (1), 225–233.

Guzsvány V. J., Csanádi J.J., Lazić S.D., Gaál F. F. 2009. Photocatalytic Degradation of the Insecticide Acetamiprid on TiO_2 Catalyst. J. Braz. Chem. Soc. Vol. 20, 1, 152-159.

Hanley T.R.. Carney E. W., Marshall Johnson E.M. 2000. Developmental Toxicity Studies in Rats and Rabbits with 3,5,6-Trichloro-2-pyridinol, the Major Metabolite of Chlorpyrifos. Toxicol. Sci. 53, 100–108.

Hernández F., Marín J.M., Pozo Ó.J., Sancho J.V., López F.J., Morell I. 2008a. Pesticide residues and transformation products in groundwater from a Spanish agricultural region on the Mediterranean Coast. Inter. J. Environ. Anal. Chem. 88, 409-424.

Hernández F., Sancho J.V., Ibañez. M., Grimalt S. 2008b. Investigation of pesticide metabolites in food and water by LC-TOF-MS. TrAc – Trend. Anal. Chem. Vol.27, 10.

Hernando M.D., De Vettori S., Martínez Bueno M.J., Fernández-Alba A.R. 2007. Toxicity evaluation with *Vibrio fischeri* test of organic chemicals used in aquaculture Chemosphere. 68 (4), 724-730.

Imidacloprid Material Safety Data Sheet, Sigma-Aldrich (http://www.sigmaaldrich.com/catalog/DisplayMSDSContent.do).

IMP Material Safety Data Sheet, Sigma-Aldrich (http://www.sigmaaldrich.com/catalog/DisplayMSDSContent.do).

ISO 11348-2. Water quality – Determination of the inhibitory effect of water samples on the light emission of *Vibrio fischeri* (Luminescent bacteria test) – Part 2: Method using liquid-dried bacteria. ISO Standard No. 11348-2. ISO, Geneve, 2007.

Iwasa T., Motoyama N., Ambrose J.T., Roe M.R. 2004. Mechanism for the differential toxicity of neonicotinoid insecticides in the honey bee, *Apis mellifera*. Crop Prot. 23, 371-378.

Jemec A., Drobne D., Tišler T., Trebše P., Roš M., Sepčić K. 2007a. The applicability of acetylcholinesterase and glutathione S-transferase in *Daphnia magna* toxicity test. Comp. Biochem. Phys. C. 144 (4), 303-309.

Jemec A., Lešer V., Drobne D., 2011. The link between antioxidant enzymes catalase and glutathione S-transferase and physiological condition of a control population of terrestrial isopod (*Porcellio scaber*). Ecotox. Environ. Safe., 1-6. doi:10.1016/j.ecoenv.2011.11.040.

Jemec A., Tišler T., Drobne D., Sepčič K., Fourniner D., Trebše P. 2007b. Comparative toxicity of imidacloprid, of its commercial liquid formulation and of diazinon to a non-target arthropod, the microcrustacean *Daphnia magna*. Chemosphere 68, 1408-1418.

Jeschke P., Moriya K., Lantzsch R., Seifert H., Lindner W., Jelich K., Göhrt A.,. Beck M. E, Etzel W. 2001**.** *Pflanzenschutz-Nachrichten Bayer*, 54, 147–160.

Kale S.P., Carvalho F.P., Raghu K., Sherkhane P.D., Pandit G.G., Mohan Rao A., Mukherjee P.K., Murthy N.B.K. 1999. Studies on degradation of ^{14}C-chlorpyrifos in the marine environment. Chemosphere 39, 969-976.

Kamel A. 2010. Refined Methodology for the Determination of Neonicotinoid Pesticides and Their Metabolites in Honey Bees and Bee Products by Liquid Chromatography – Liquid Chromatography – Tandemm Mass Spectrometry (LC-MS/MS). J. Agric. Food. Chem. 58, 5926-5931.

Kamiya M., Kameyama K. 1998. Photochemical effects of humic substances on the degradation of organophosphorus pesticides. Chemosphere 36, 2337–2344.

Khan A., Haque M.M., Mir N.A., Muneer M., Boxall C., 2010. Heterogeneous photocatalysed degradation of an insecticide derivative acetamiprid in aqueous suspensions of semiconductor. Desalination 261, 169–174.

Kim J.-R., Ahn Y.J. 2009. Identification and characterization of chlorpyrifos-methyl and 3,5,6-trichloro-2-pyridinol degrading Burkholderia sp. strain KR100. Biodegradation 20, 487–497.

Kitsiou V., Filippidis N., Mantzavinos D., Poulios I. 2009. Heterogeneous and homogeneous photocatalytic degradation of the insecticide imidacloprid in aqueous solutions. Appl. Catal., B 86, 27–35.

Kolpin D.W., Battaglin W.A., Conn K.E., Furlong E.T., Glassmeyer S.T., Kalkhoff S.J., Meyer M.T., Schnoebelen D.J. 2009. Handbook of Environmental Chemistry, Volume 2P, Transformation Products of Synthetic Chemicals in the Environment, p. 83-100.

Konstantinou I.K., Albanis T.A., 2003. Photocatalytic transformation of pesticides in aqueous titanium dioxide suspensions using artificial and solar light: intermediates and degradation pathways. Appl. Catal., B 42, 319–335.

Kousba A.A., Sultatos L.G., Poet T.S. Timchalk C. 2004. Comparison of chlorpyrifos-oxon and paraoxon Acetylcholinesterase inhibition dynamics: potential role of peripheral binding site. Toxicol. 80, 239-248.

Kouloumbos V.N., Tsipi D.F., Hiskia A.E., Nikolic D., van Breemen R.B. 2003. Identification of Photocatalytic degradation products of diazinon in TiO_2 aqueous suspension using GC/MS/MS and LC/MS with quadrupole time-of-flight mass spectrometry. J. Am. Soc.Mass. Spectrom. 14, 803-817.

Koutchma T. 2009. Advances in Ultraviolet Light Technology for Non-thermal Processing of Liquid Foods. Food. Bioprocess. Technol. 2, 138-155.

Krohn J., Hellpointner E., 2002. Environmental fate of imidacloprid. Special edition. Pflanzenschutz Nachrichten Bayer.

Lambropoulou D.A., Konstantinou I.K., Albanis T.A., Fernandez-Alba A.R. 2011. Photocatalytic degradation of the fungicide Fenhexamid in aqueous TiO_2 suspensions: Identification of intermediates products and reaction pathways. Chemosphere 83, 367–378.

Lapertot M., Ebrahimi S., Oller, I., Maldonado M.I., Gernjak W., Malato S., Pulgarin C., 2008. Evaluating Microtox (c) as a tool for biodegradability assessment of partially treated solutions of pesticides using Fe^{3+} and TiO_2 solar photo-assisted processes. Ecotoxicol. Environ. Safe. 69, 546–555.

Lartiges S.B., Garrigues P.P. 1995. Degradation kinetics of organophosphorus and organonitrogen pesticides in different waters under various environmental conditions. Environ Sci. Technol. 29, 1246-1254.

Lavine B.K., Ding T., Jacobs D., 2010. LC–PDA–MS studies of the photochemical degradation of imidacloprid. Anal. Lett. 43, 1812–1821.

Lee H.S., Hur T., Kim S., Kim J.-H., Lee H.I., 2003. Effects of pH and surface modification of TiO_2 with SiO_x on the photocatalytic degradation of a pyrimidine derivative. Catal. Today. 84, 173-180.

Lee H.S., Woo C.S., Youn B.-K., Kim S.Y., Oh S.-T., Sung Y.-E., Lee H.I. 2005. Bandgap modulation of TiO_2 and its effect on the activity in photocatalytic oxidation of 2-isopropyl-6-methyl-4-pyridinol. Top. Catal. 35 (3-4), 255-260.

Lešer V., Drobne D., Vilhar B., Kladnik, A., Žnidaršič, N., Štrus, J. 2008. Epithelial thickness and lipid droplets in the hepatopancreas of *Porcellio scaber* (Crustacea: Isopoda) in different physiological conditions. Zoology, 111, (6), 419-432.

Li P.C.H., Swanson E.J., Gobas F.A.P.C. 2002. Diazionon and its degradation products in agricultural water courses in British Columbia, Canada. Bull. Environ. Contam. Toxicol. 69, 59-65.

Linden A., Gülden M., Martin H-J., Maser E., Seibert H., 2008. Peroxide-induced cell death and lipid peroxidation in C6 glioma cells. Toxicol. In. Vitro. 22, 1371–1376.

Liotta R., Hoff W.S., 1980. Trifluoroperacetic acid – oxidation of aromatic rings. J. Org. Chem. 45, 2887–2890.

Litter M.I., 2005. Introduction to Photochemical Advanced Oxidation Processes for Water Treatment, vol. 2. Springer-Verlag, Berlin. pp. 325-366, Part M.

Liu B., McConnell L.L., Torrents A. 2001. Hydrolysis of chlorpyrifos in natural waters of the Chesapeake Bay. Chemosphere 44, 1315-1323.

Lykkesfeldt J. 2007. Malondialdehyde as biomarker of oxidative damage to lipids caused by smoking. Clin. Chim. Acta 380, 50-58.

Lodevico R.G., Li Q.X. 2002 Determination of total imidacloprid residues in coffee by gas-chromatography-mass spectrometry. Anal. Lett. Vol 35, 2, 315-326.

Maiue-Pierre C., Carpentie P., Martel A.-C., Bougeard S., Cougoule N., Porta P., Lachaize J., Madec F., Aubert M., Faucon J.-P. 2009. Influence of Pesticide Residues on Honey Bee (Hymenoptera: Apidae) Colony Health in France. Environ. Entomol. 38(3), 514-523.

Malato S., Caceres J., Agüera A., Mezcua M., Hernando D., Vial J., Fernandez Alba A.R., 2001. Degradation of imidacloprid in water by photo-fenton and TiO_2 photocatalysis at a solar pilot plant: A comparative study. Environ. Sci. Technol. 35, 4359–4366.

Manson, S.F. 1962. In: The Pyrimidines, Chapter XIII. Brown D.J. (ed.). New York, Wiley, p.464.

Mansour M., Feicht E.A., Behechti A., Scheunert I. 1997. Experimental approaches to studying the photostability of selected pesticides in water and soil, Chemosphere 35, 39–50.

Marin A., Martinez Vidal J.L., Egea Gonzalez F.J., Garrido Frenich A., Glass C.R., Sykes M. 2004. Assessment of potential (inhalation and dermal) and actual exposure to acetamiprid by greenhouse applicators using liquid chromatography–tandem mass spectrometry. J. Chromatogr. B 804, 269–275.

Martínez Galera M., Frenich G.A., Vidal J.L.M., Vázquez P.P. 1998. Resolution of imidacloprid pesticide and its metabolite 6-chloronicotinic acid using cross-sections of spectrochromatograms obtained by high-performance liquid chromatography with diode-array detection. J. Chrom. A. 799, 149-154.

Martínez Vidal J.L., Plaza-Bolaños P., Romero-González R., Garrido-Frenich A. 2009. Determination of pesticide transformation products: A review of extraction and detection methods. J. Chromatogr. A. 1216, 6767-6788.

Matsuda K., Buckingham S.D., Kleiner D., Rauh J.J., Garuso M., Sattelle D.B., 2001. Neonicotinoids: insecticides acting on insect nicotinic acetylcholine receptors. Trends Pharmacol. Sci. 22 (11), 573–580.

Meallier P. Phototransformation of Pesticides in Aqueous Solution. In: P. Boule (ed). The Handbook of Environmental Chemistry, Volume 2, Part L, Environmental Photochemistry, Springer, Berlin 1999, pp. 241-261.

Meleiro Porto A. L., Zelayarán Melgar G., Consiglio Kasemodel M., Nitschke M. 2011. Biodegradation of Pesticides, Pesticides in the Modern World - Pesticides Use and Management, Margarita Stoytcheva (Ed.), ISBN: 978-953-307-459-7, InTech.

Menager M., Pan X, Wong-Wah-Chung P., Sarakha M., 2007. Photochemistry of the pesticide azinphos methyl and its model molecule 1,2,3-benzotriazin-4(3*H*)-one in aqueous solutions: Kinetic and analytical studies J. Photochem. Photobiol. A: Chem. 192 (1), 41-48.

Mikhailopulo K.I., Serchenya T.S., Kiseleva E.P., Chernov Y.G., Tsvetkova T.M., Kovganko N.V., Sviridov O.V. 2008. Interaction of molecules of the neonicotinoid imidacloprid and its structural analogs with human serum albumin. J. Appl. Spectrosc. 75, 857–863.

Millar N.S., Denholm I. 2007. , Nicotinic acetylcholine receptors: targets for commercially important insecticides. Invert Neurosci. 7, 53-66.

Milne G.W.A. 2004. Pesticides: An international guide to 1800 pest control chemicals. Cornwall, MPG Books Ltd., pp 609.

Mouvet C., Jeannot R., Riolland H., Maciag C. 1997. Stability of isoproturon, bentazone, terbuthylazine and alachlor in natural groundwater, surface water and soil water samples stored under laboratory conditions. Chemosphere 35, 1083-1097.

Moza P.N., Hustert K., Feicht E., Kettrup A. 1998. Photolysis of imidacloprid in aqueous solution. Chemosphere 36, 497-502.

Muñoz A., Le Person A., Le Calvé., Mellouki A., Borrás E., Daële V., Vera T. 2011. Studies on atmospheric degradation of diazinon in the EUPHORE simulation chamber. Chemosphere, doi: 10.1016/j.chemosphere.2011.06.044.

Murov S.L., Carmichael, I., Hug, G.L. 1993. Handbook of photochemistry, 2nd ed. Marcel Dekker Inc., 1993, 299–305.

Nauen R., Ebbinghaus-Kintscher U., Schmuck R. 2001. Toxicity and nicotinic acetylcholine receptor interaction of imidacloprid and its metabolites in Apis mellifera (Hymenoptera:Apidae). Pest Manag. Sci. 57 (7), 577–586.

Oh S.-T., Choi J.-S., Lee H.S., Lu L., Kwon H.-H., Song i.K., Kim J.J., Lee H.I. 2007. H_2O-controlled synthesis of TiO_2 with nanosized channel structure through *in situ* esterification and its application to photocatalytic oxidation. J. Mol. Catal. A-Chem. 267, 112-119.

Oller I., Malato S., Sánchez-Pérez J.A. 2011. Combination of Advanced Oxidation Processes and biological treatments for wastewater decontamination—A review. Sci. Total. Environ. 409. 4141–4166.

Palma P., Palma V. L., Fernandes R. M., Soares A. M. V. M., Barbosa I. R. 2008. Acute Toxicity of Atrazine, Endosulfan Sulphate and Chlorpyrifos to *Vibrio fischeri*, *Thamnocephalus platyurus* and *Daphnia magna*, Relative to Their Concentrations in Surface Waters from the Alentejo Region of Portugal. Bull. Environ. Contam. Toxicol. 81, 485–489.

Peña A., Rodríguez-Liébana J.A., Mingorance M.D. 2011. Persistence of two neonicotinoid insecticides in wastewater, and in aqueous solutions of surfactants and dissolved organic matter. Chemosphere 84, 464-470.

Phytosanitary Administration of the Republic of Slovenia, personal communication, 2005.

Phytosanitary Administration of the Republic of Slovenia; FITO-INFO browser (http://spletni2.furs.gov.si/FFS/REGSR/index.htm (7th November, 2011)).

Pomor čebel v Pomurju dobiva nove razsežnosti (http://www.rtvslo.si/okolje/pomor-cebel-v-pomurju-dobiva-nove-razseznosti/256048, 16th May, 2011).

Porter, N.A., Caldwell, S.E., Mills, K.A., 1995. Mechanisms of free radical oxidation of unsaturated lipids. Lipids 30, 2290–2787.

Randhawa M.A., Anjum F.M., Ahmed A., Randhawa M.S. 2007. Filed incurred chlorpyrifos and 3,5,6-trichloro-2-pyridinol residues in fresh and processed vegetables. Food Chem. 103, 1016-1023.

Raina R. and Sun L. 2008. Trace level determination of delected opganophosphorus pesticides and their degradation products in environmental air samples by liquid chromatography-positive ion electro spray tandem mass spectrometry. J. Environ Sci. Heal. B. 43, 323-332.

Ray M.B. Chen J.P., Wang L.K. Pehkonen S.O. 2006. Advanced Oxidation Processes. 2006. In: Wang L.K., Hung Y.T., Shammas N.K. (eds), Handbook of Environmental engineering, Volume 4: Advanced Physicochemical society of chemistry, Cambridge, UK; 105-106.

Redlich D., Shahin N., Ekici P., Friess A., Parlar H. 2007. Kinetical study of the Photoinduced Degradation of Imidacloprid in Aquatic Media. Clean 35 (5), 452-458.

Roberts T., Huston D. 1999. Metabolic Pathways of Agrochemicals, Insecticides and fungicides, part two. The royal society of chemistry, Cambridge, UK, pp. 105-106.

Robertson L.N., Chandler K.J., Stickley B.D.A., Cocco R.F., Ahmetagic M. 1998. Enhanced microbial degradation implicated in rapid loss of chlorpyrifos from the controlled-release formulation suSCon® Blue in soil. Crop. Prot. Vol.17, 1, 29-33.

Sakkas V.A., Arabatzis I.M., Konstantinou I.K., Dimou A.D., Albanis T.A., Falaras P., 2004. Metolachlor photocatalytic degradation using TiO_2 photocatalysts. Appl. Catal., B 49, 195–205.

Sanchez-Hernandez J.C. 2011. Pesticide Biomarkers in Terrestrial Invertebrates, Pesticides in the Modern World - Pests Control and Pesticides Exposure and Toxicity Assessment, Margarita Stoytcheva (Ed.), ISBN: 978-953-307-457-3, InTech.

Sarkar M.A., Biswas P.K., Roy S., Kole R.K., Chowdhury A. 1999. Effect of pH and type of formulation on the persistence of imidacloprid in water. B. Environ. Contam. Tox. 63, 604-609.

Saravi S.S.S., Shokrzadeh M. 2011. Role of Pesticides in Human Life in the Modern Age: A review. In: Pesticides in the Modern World - Risks and Benefits. Stoytcheva M. (ed.). InTech: 4-11.

Saulsbury M.D., Heyliger S.O., Wang K., Round D. 2008. Characterization of chlorpyrifos-induced apoptosis in placental cells. Toxicol. 244, 98-110.

Schippers N., Schwack W. 2008. Photochemistry of imidacloprid in model systems. J. Agric. Food Chem. 56, 8023–8029.

Segura C., Zaror C., Mansilla H.D., Mondaca M.A. 2008. Imidacloprid oxidation by photo-Fenton reaction. J. Haz. Mat. 150, 679–686.

Segura Carretero A., Cruces-Blanco C., Perez Duran S., Fernandez Gutierrez A. 2003. Determination of imidacloprid and its metabolite 6-chloronicotinic acid in greenhouse air by application of micellar electrokinetic capillary chromatography with solid-phase extraction. J. Chromatogr. A 1003, 189–195.

Shemer H., Linden K.G. 2006. Degradation and by-products formation of diazinon in water during UV and UV/H_2O_2 treatment. J. Haz. Mat. B 136, 553-559.

Shemer H., Sharpless C.M., Linden K.G. 2005. Photodegradation of 3,5,6-trichloro-2-pyridinol in aqueous solution. Water Air Soil Poll. 168, 145-155.

Shim W.-B.. M.E Yakovleva, Kyeong-Yeol K., Nam B.-R., Vylegzhanina E.S., Komarov A.A., Eremin S.A., Chung D.-H. 2009. Development of Fluorescence Polarization Immunoassay for the Rapid Detection of 6-Chloronicotinic Acid: Main Metabolite of Neonicotinoid Insecticides. J. Agric. Food Chem., 57, 791–796.

Sinclair C.J. Boxall A.B.A., Parsons S.A., Thomas M.R. 2006. Priorization of Pesticide Environmental Transformation Products in Drinking Water Supplies. . Environ. Sci. Technol. 40, 7283-7289.

Sinclair C.J., Boxall A.B.A. 2009. Ecotoxicity of Transformation Products. In:The Handbook of Environmental Chemistry, Volume 2, Part P, Springer, Berlin 2009, pp. 241-261.

Sinclair C.J., Boxall A.B.A. 2003. Assesing the Ecotoxicity of Pesticide Transformation products. Environ. Sci. Technol. 37, 4617-4625.

Stanek K., Drobne D., Trebše P. 2006. Linkage of biomarkers along levels of biological complexity in juvenile and adult diazinon fed terrestrial isopod (*Porcellio scaber*, Isopoda, Crustacea). Chemosphere 64, 1745-1752.

Stanek K., Gaabrijelčič E., Drobne D., Trebše P. 2003. Inhibition of acetylcholinesterase activity in the terrestrial isopod *Porcellio scaber* as a biomarker of organophosphorus compounds in food. Arh. Hig. Rada. Toksikol. 54, 183-188.

Suchail S., Guez D., Belzunces L.P. 2001. Discrepancy between acute and chronic toxicity induced by imidacloprid and its metabolites in *Apis mellifera*. Environ Toxicol Chem. 20(11), 2482-2486.

TCP Material Safety Data Sheet, Sigma-Aldrich (http://www.sigmaaldrich.com/catalog/DisplayMSDSContent.do).

The Official Gazette of the Republic of Slovenia No. 50/2008.

The Official Gazette of the Republic of Slovenia No. 80/2008.

The Official Gazette of the Republic of Slovenia No. 31/2011.

Tišler T., Jemec A., Mozetič B., Trebše P. 2009. Hazard identification of imidacloprid to aquatic environment. Chemosphere 76, (7), 907-914.

Tomizawa M., Casida J.E. 2005. Neonicotinoid insecticide toxicology: Mechanisms of Selective Action; Annu. Rev. Pharmacol. 45, 247-268.

Topalov A., Abramović B., Molnar-Gabor D., Csanadi J., Arcso O., 2001. Photocatalytic oxidation of the herbicide (4-chloro-2-methylphenoxy)acetic acid (MCPA) over TiO_2. J. Photochem. Photobiol. A 140, 249–253.

Totti S., Fernández M., Ghini S., Picó Y., fini F., Mañes J., Girotti S. 2006. Application of matrix solid phase dispersion to the determination of imidacloprid, carbaryl, aldicarb, and their main metabolites in honeybees by liquid chromatography-mass spectrometry detection. Talanta 69, 724-729.

Valant J., Drobne D., Novak S. 2011. Effect of ingested titanium dioxide nanoparticles on the digestive gland cell membrane of terrestrial isopods. Chemosphere, doi:10.1016/j.chemosphere.2011.11.047.

Velasco-Arjona A., Manclús, Montoya A., Luque de Castro M.D. 1997. Robotic sample pretreatment – immunoassay determination of chlorpyrifos metabolite (TCP) in soil and fruit. Talanta 45, 371-377.

Walker C.H., Hopkin S.P., Sibly R.M., Peakall D.B. 2001. Principles of exotocixology. Second Edition. London. Taylor & Francis.

Wamhoff H., Schneider V. 1999. Photodegradation of imidacloprid. J. Agric. Food Chem. 47, 1730–1734.

Wheatley R.A. 2000. Some recent trends in the analytical chemistry of lipid peroxidation. TrAc Trends. Anal. Chem. 19 (10), 617-628.

Widianarko B., Van Straalen N.1996. Toxicokinetics-based survival analysis in bioassay using nonpersistent chemicals. Environ. Tox. Chem. 15(3), 402-406.

Wikipedia
(http://en.wikipedia.org/wiki/File:Porcellio_scaber_%28AU%29-left_01.jpg, 16th January, 2012).

Zhang Q., Pehkonen S.O. 1999. Oxidation of Diazinon by Aqueous Chlorine: Kinetics, Mechanism and Product Studies. J. Agric. Food. Chem 47, 1760-1766.

Žabar R, Sarakha M., Chung P.W.W., Trebše P. 2011a. Stability of Pesticides' Residues Under Ultraviolet Germicidal Irradiation. Acta. Chim. Slov. Vol.58, 2, 326-332.

Žabar R., Dolenc D., Jeman T., Franko M., Trebše P. 2011b. Photolytic and photocatalytic degradation of 6-chloronicotinic acid. Chemospehere, 85, 861–868.

Žabar R., Rotar M., Trebše P. 2012a in preparation. Acetamiprid oxidation by photo-Fenton oxidation.

Žabar R, Bavcon Kralj M., Komel T., Fabjan J., Trebše P. 2012b, submitted. Photocatalytic degradation with immobilised TiO_2 of three selected neonicotinoid insecticides: imidacloprid, thiamethoxam and clothianidin.

9   ANNEXES

ANNEX A1

Table 25: Leaf weight before and after exposure, faeces mass, body weight of P. scaber *exposed for 14 days (control, 1 µg/g, 10 µg/g, 50 µg/g and 100 µg/g)* **for IMP.**

Note: Pink colour denotes the concentration of used chemical, gray colour denotes dead animals, blue colour denotes eliminated animals with juveniles.

nr.	animal			leaf			faeces
	weight before [mg]	weight after [mg]	WC [mg]	weight before [mg]	weight after [mg]	food consumed [mg]	faeces mass [mg]
control group							
1	39.3	37.6	-1.7	99.7	68.9	30.8	18.0
2	66.1	59.3	-6.8	99.0	77.9	21.1	6.3
3	46.7	55.3	8.6	102.0	32.0	70.0	56.1
4	22.1	24.5	2.4	99.6	71.2	28.4	20.1
5	91.9	87.4	-4.5	98.7	41.9	56.8	40.8
6	39.8	38.4	-1.4	101.7	62.8	38.9	27.1
7	33.9	/	/	102.0	/	/	/
8	21.8	/	/	100.8	/	/	/
9	63.7	65.8	2.1	100.9	36.8	64.1	52.7
10	41.0	35.5	-5.5	102.0	62.7	39.3	29.2
11	53.7	44.4	-9.3	100.7	77.7	23.0	17.5
12	45.0	48.5	3.5	101.2	59.5	41.7	32.9
1 µg IMP/g dry food							
13	34.4	39.0	4.6	100.9	78.2	22.7	19.5
14	57.7	/	/	101.0	/	/	/
15	28.4	27.1	-1.3	98.0	70.0	28.0	17.4
16	38.9	39.1	0.2	101.7	64.2	37.5	25.6
17	36.7	/	/	101.8	/	/	/
18	74.6	78.8	4.2	98.7	37.3	61.4	74.6
19	21.2	24.4	3.2	101.6	55.8	45.8	21.2
20	56.8	53.8	-3.0	100.7	62.9	37.8	56.8
21	87.4	87.8	0.4	101.9	58.5	43.4	87.4
22	30.7	36.5	5.8	101.2	63.6	37.6	30.7
23	26.7	26.7	0.0	102	62.7	39.3	26.7
24	64.0	63.6	-0.4	102	55.6	46.4	64.0
10 µg IMP/g dry food							
25	35.1	37.4	2.3	100.6	77.3	23.3	10.1
26	82.0	/	/	101.6	/	/	/
27	25.1	24.3	-0.8	101	69.4	31.6	25.1
28	26.5	25.0	-1.5	101.3	65.2	36.1	27.8
29	50.9	41.9	-9	98.7	75.6	23.1	17.0
30	36.3	/	/	101.7	/	/	/
31	68.5	64.2	-4.3	100.2	72.0	28.2	18.3
32	45.0	44.4	-0.6	99.9	63.0	36.9	26.2
33	76.8	73.0	-3.8	100.9	59.5	41.4	29.8
34	32.3	34.9	2.6	101.7	72.6	29.1	19.7
35	37.4	38.9	1.5	101.2	60.9	40.3	31.0
36	60.5	61.8	1.3	100.0	57.3	42.7	30.8

.....continuation of Table 25: Leaf weight before and after exposure, faeces mass, body weight of P. scaber *exposed for 14 days (control, 1 μg/g, 10 μg/g, 50 μg/g and 100 μg/g) for IMP.*

	animal			leaf			faeces
nr.	weight before [mg]	weight after [mg]	WC [mg]	weight before [mg]	weight after [mg]	food consumed [mg]	faeces mass [mg]
50 μg IMP/g dry food							
37	32.8	30.1	-2.7	101	77.2	23.8	14.3
38	59.8	59.7	-0.1	100.6	63.2	37.4	27.5
39	23.6	/	/	102.0	/	/	/
40	98.7	58.8	-39.9	101.2	62.1	39.1	27.9
41	55.1	66.3	11.2	98.2	74.8	23.4	18.5
42	36.1	37.2	1.1	101.9	54.7	47.2	36.1
43	41.6	42.6	1.0	100	59.9	40.1	31.7
44	45.0	49.3	4.3	101	52.9	48.1	34.3
45	26.2	30.7	4.5	101.4	73.0	28.4	20.2
46	82.7	88.3	5.6	99.8	34.6	65.2	51.2
47	56.7	54.3	-2.4	98.0	41.1	56.9	45.0
48	61.2	/	/	98.0	/	/	/
100 μg IMP/g dry food							
49	32.1	28.9	-3.2	101.4	86.0	15.4	8.6
50	57.9	/	/	101.4	/	/	/
51	27.1	26.2	-0.9	99.1	63.6	35.5	27.0
52	99.8	95.6	-4.2	100.4	45.5	54.9	45.5
53	40.0	42.6	2.6	100.8	64.8	36.0	25.9
54	26.6	31.0	4.4	101.8	74.6	27.2	15.3
55	80.5	77.6	-2.9	102.0	73.5	28.5	14.4
56	53.9	51.2	-2.7	98.0	55.4	42.6	34.4
57	36.3	/	/	102.0	/	/	/
58	35.8	31.8	-4.0	100.3	61.2	39.1	27.6
59	23.5	/	/	98.0	/	/	/
60	66.6	/	/	101.3	/	/	/

Table 26: Faecal pellets production (in mg/mg fresh body wt./day), consumption rate (in mg leaves/mg fresh body wt./day) and assimilation efficiency (in mg food consumed – mg faeces/mg food consumed) for **P. scaber** *exposed for 14 days (control, 1 µg/g, 10 µg/g, 50 µg/g and 100 µg/g) for IMP.*

Note: Pink colour denotes the concentration of used chemical, gray colour denotes dead animals, blue colour denotes eliminated animals with juveniles.

nr.	FPP (faecal pellets production)	CR (consumption rate)	AE (assimilation efficiency)
control group			
1	0.03419	0.05851	0.41558
2	0.00759	0.02542	0.70142
3	0.07246	0.09042	0.19857
4	0.05860	0.08280	0.29225
5	0.03334	0.04642	0.28169
6	0.05041	0.07236	0.30334
7	/	/	/
8	/	/	/
9	0.05721	0.06958	0.17785
10	0.05875	0.07907	0.2570
11	0.02815	0.03700	0.23913
12	0.04845	0.06141	0.21103
1 µg IMP/g dry food			
13	0.03571	0.04158	0.14097
14	/	/	/
15	0.04586	0.0738	0.37857
16	0.04677	0.06851	0.31733
17	/	/	/
18	0.03988	0.05566	0.28339
19	0.08811	0.13407	0.34279
20	0.02669	0.05019	0.46825
21	0.02677	0.03531	0.24194
22	0.05753	0.07358	0.21809
23	0.07143	0.10514	0.32061
24	0.04200	0.05211	0.19397
10 µg IMP/g dry food			
25	0.01929	0.04450	0.56652
26	/	/	/
27	0.07378	0.09289	0.20570
28	0.07943	0.10314	0.22992
29	0.02898	0.03938	0.26407
30	/	/	/
31	0.02036	0.03138	0.35106
32	0.04215	0.05936	0.28997
33	0.02916	0.04051	0.28019
34	0.04032	0.05956	0.32302
35	0.05692	0.0740	0.23077
36	0.03560	0.04935	0.27869
50 µg IMP/g dry food			
37	0.03393	0.05648	0.39916
38	0.03290	0.04475	0.26471
39	/	/	/
40	0.03389	0.04750	0.28645

.....continuation of Table 26: Faecal pellets production (in mg/mg fresh body wt./day), consumption rate (in mg leaves/mg fresh body wt./day) and assimilation efficiency (in mg food consumed – mg faeces/mg food consumed) for **P. scaber** *exposed for 14 days (control, 1 µg/g, 10 µg/g, 50 µg/g and 100 µg/g) for IMP.*

nr.	FPP (faecal pellets production)	CR (consumption rate)	AE (assimilation efficiency)
41	0.01993	0.02521	0.20940
42	0.06932	0.09063	0.23517
43	0.05315	0.06724	0.20948
44	0.04970	0.06969	0.28690
45	0.04700	0.06608	0.28873
46	0.04142	0.05274	0.21472
47	0.05919	0.07485	0.20914
48	/	/	/
100 µg IMP/g dry food			
49	0.02126	0.03806	0.44156
50	/	/	/
51	0.07361	0.09678	0.23944
52	0.03400	0.04102	0.17122
53	0.04343	0.06036	0.28056
54	0.03525	0.06267	0.43750
55	0.01325	0.02623	0.49474
56	0.04799	0.05943	0.19249
57	/	/	/
58	0.06199	0.08783	0.29412
59	/	/	/
60	/	/	/

Table 27: Calculated values of lipid peroxidation (normalised) and absorbance values (in AU) for MDA-TBA product (535 nm), non-specific turbidity correction (600 nm) and protein content (280 nm) of P. scaber *exposed for 14 days (control, 1 μg/g, 10 μg/g, 50 μg/g and 100 μg/g) for IMP.*

Note: Pink colour denotes the concentration of used chemical, gray colour denotes dead animals, blue colour denotes eliminated animals with juveniles.

nr.	A (535 nm)	A (600 nm)	A (280 nm)	LP (lipid peroxidation)
control group				
1	0.005	0.003	2.266	1.28097
2	0.003	0.002	2.449	0.59262
3	0.001	0.001	2.325	0
4	0.002	0.001	2.467	0.5883
5	0.006	0.004	2.417	1.20094
6	0.002	0.002	2.114	0
7	/	/	/	/
8	/	/	/	/
9	0.007	0.005	2.336	1.24258
10	0.004	0.003	2.249	0.64532
11	0.007	0.003	2.190	2.65084
12	0.006	0.003	2.421	1.79843
1 μg IMP/g dry food				
13	0.007	0.005	2.276	1.27534
14	/	/	/	/
15	0.014	0.010	2.338	2.48304
16	0.004	0.003	2.309	0.62856
17	/	/	/	/
18	0.001	0	2.238	0.6485
19	0.001	-0.001	2.329	1.24632
20	0.005	0.003	2.375	1.22218
21	0.012	0.010	2.316	1.25331
22	0.006	0.004	2.339	1.24099
23	0.003	0.002	2.315	0.62693
24	0.006	0.003	2.349	1.85356
10 μg IMP/g dry food				
25	0.001	0	2.493	0.58216
26	/	/	/	/
27	0	0	2.428	0
28	0.001	0.001	2.379	0
29	0.002	0.001	2.457	0.59069
30	/	/	/	/
31	0.006	0.004	2.505	1.15875
32	0.005	0.003	2.451	1.18428
33	0.007	0.004	2.315	1.88078
34	0.011	0.006	2.556	2.83907
35	0.008	0.005	2.413	1.80439
36	0.002	0.001	2.464	0.58902
50 μg IMP/g dry food				
37	0.003	0.002	2.332	0.62236
38	0.008	0.006	2.425	1.19698
39	/	/	/	/
40	0.006	0.003	2.345	1.85672
41	0.012	0.010	2.238	1.29699

.....continuation of Table 27: Calculated values of lipid peroxidation (normalised) and absorbance values (in AU) for MDA-TBA product (535 nm), non-specific turbidity correction (600 nm) and protein content (280 nm) of P. scaber *exposed for 14 days (control, 1 µg/g, 10 µg/g, 50 µg/g and 100 µg/g) for IMP.*

nr.	A (535 nm)	A (600 nm)	A (280 nm)	LP (lipid peroxidation)
42	0.009	0.008	2.367	0.61315
43	0.009	0.007	2.477	1.17185
44	0.010	0.007	2.594	1.67849
45	0.006	0.002	2.352	2.46826
46	0.009	0.007	2.570	1.12944
47	0.009	0.006	2.483	1.75353
48	/	/	/	/
100 µg IMP/g dry food				
49	0.009	0.007	2.513	1.15506
50	/	/	/	/
51	0.008	0.006	2.399	1.20995
52	0.005	0.003	2.596	1.11813
53	0.009	0.006	2.541	1.71350
54	0.007	0.005	2.320	1.25115
55	0.010	0.007	2.615	1.66501
56	0.003	0.002	2.428	0.59775
57	/	/	/	/
58	0.001	0	2.280	0.63655
59	/	/	/	/
60	/	/	/	/

ANNEX B1

Data for ecotoxicological experiments with *P. scaber* for TCP

Table 28: Leaf weight before and after exposure, faeces mass, body weight of P. scaber *exposed for 14 days (control, 1 µg/g, 10 µg/g, 50 µg/g and 100 µg/g) for TCP.*

Note: Pink colour denotes the concentration of used chemical, gray colour denotes dead animals, blue colour denotes eliminated animals with juveniles.

nr.	animal			leaf			faeces
	weight before [mg]	weight after [mg]	WC [mg]	weight before [mg]	weight after [mg]	food consumed [mg]	faeces mass [mg]
control group							
1	27.7	26.1	-1.6	99.1	77.2	21.9	11.9
2	24.1	22.7	-1.4	99.9	81.9	18.0	4.2
3	38.5	36.3	-2.2	99.5	75.6	23.9	8.2
4	37.8	37.3	-0.5	99.9	73.0	26.9	10.9
5	46.2	42.3	-3.9	99.4	67.4	32.0	10.5
6	65.3	60.8	-4.5	100.0	80.0	20.0	6.0
7	72.4	65.4	-7.0	101.1	85.5	15.6	4.3
8	58.6	/	/	99.5	/	/	/
9	64.3	62.4	-1.9	100.8	69.2	31.6	18.6
10	66.1	63.8	-2.3	98.5	64.0	34.5	19.3
11	50.9	49.3	-1.6	99.8	77.5	22.3	13.7
12	44.5	/	/	100.6	/	/	/
1 µg TCP/g dry food							
13	27.7	28.2	0.5	101.7	73.2	28.5	20.3
14	38.8	40.6	1.8	100.8	66.0	34.8	25.0
15	33.8	28.9	-4.9	100.6	69.6	31.0	24.2
16	38.6	39.7	1.1	100.0	45.8	54.2	43.2
17	81.0	80.0	-1.0	101.3	76.4	24.9	18.2
18	57.2	55.7	-1.5	100.6	66.9	33.7	25.3
19	54.8	47.8	-7.0	100.6	76.3	24.3	16.0
20	60.2	64.7	4.5	101.6	53.4	48.2	35.9
21	62.2	58.4	-3.8	101.6	67.2	34.4	28.6
22	76.4	74.1	-2.3	101.1	80.4	20.7	15.5
23	39.6	40.0	0.4	98.5	54.9	43.6	33.0
24	50.7	/	/	101.9	/	/	/
10 µg TCP/g dry food							
25	27.2	25.5	-1.7	100.8	86.1	14.7	1.0
26	34.9	39.1	4.2	101.7	64.9	36.8	21.5
27	37.8	37.2	-0.6	98.0	55.6	42.4	23.9
28	49.6	48.4	-1.2	101.2	69.5	31.7	23.2
29	56.2	62.7	6.5	102.0	33.2	68.8	60.6
30	64.4	/	/	101.4	/	/	/
31	82.9	76.8	-6.1	102.0	55.7	46.3	35.2
32	56.8	55.1	-1.7	102.0	77.2	24.8	16.8
33	71.6	67.6	-4.0	101.6	48.3	53.3	44.1
34	71.7	75.0	3.3	101.4	39.6	61.8	48.6
35	37.4	38.4	1.0	101.2	70.5	30.7	20.2
36	25.6	26.6	1.0	99.7	75.9	23.8	17.3

.....continuation of Table 28: Leaf weight before and after exposure, faeces mass, body weight of P. scaber *exposed for 14 days (control, 1 µg/g, 10 µg/g, 50 µg/g and 100 µg/g) for TCP.*

	animal			leaf			faeces
nr.	weight before [mg]	weight after [mg]	WC [mg]	weight before [mg]	weight after [mg]	food consumed [mg]	faeces mass [mg]
50 µg TCP/g dry food							
37	22.2	23.1	0.9	101.2	76.7	24.5	17.3
38	38.6	33.0	-5.6	101.3	68.1	33.2	17.2
39	30.5	31.2	0.7	101.7	86.6	15.1	10.3
40	61.7	/	/	100.1	/	/	/
41	54.1	53.2	-0.9	98.8	81.5	17.3	5.1
42	54.5	47.8	-6.7	101.9	/	/	/
43	56.6	55.9	-0.7	99.8	65.8	34.0	18.1
44	116.1	111.3	-4.8	98.0	63.3	34.7	10.7
45	80.5	81.2	0.7	101.2	65.1	36.1	23.0
46	37.1	34.2	-2.9	102.0	81.8	20.2	10.7
47	21.5	/	/	99.3	/	/	/
48	54.6	/	/	101.3	/	/	/
100 µg TCP/g dry food							
49	21.4	20.4	-1.0	98.4	79.5	18.9	10.5
50	35.7	36.2	0.5	101.9	80.1	21.8	6.6
51	47.6	46.8	-0.8	100.9	76.6	24.3	12.1
52	58.9	58.8	-0.1	99.3	65.5	33.8	21.6
53	51.6	47.3	-4.3	101.8	65.3	36.5	20.2
54	82.8	75.5	-7.3	100.7	74.1	26.6	12.6
55	75.3	69.6	-5.7	100.6	57.7	42.9	23.1
56	56.8	55.7	-1.1	99.1	44.0	55.1	40.6
57	62.1	62.4	0.3	100.1	53.5	46.6	30.6
58	77.7	78.0	0.3	101.0	70.7	30.3	13.6
59	26.4	27.7	1.3	101.5	73.7	27.8	14.4
60	37.4	/	/	100.5	/	/	/

Table 29: Faecal pellets production (in mg/mg fresh body wt./day), consumption rate (in mg leaves/mg fresh body wt./day) and assimilation efficiency (in mg food consumed – mg faeces/mg food consumed) for **P. scaber** *exposed for 14 days (control, 1 µg/g, 10 µg/g, 50 µg/g and 100 µg/g) for TCP.*

Note: Pink colour denotes the concentration of used chemical, gray colour denotes dead animals, blue colour denotes eliminated animals with juveniles.

nr.	FPP (faecal pellets production)	CR (consumption rate)	AE (assimilation efficiency)
control group			
1	0.03257	0.05993	0.45662
2	0.01322	0.05664	0.76667
3	0.01614	0.04703	0.65690
4	0.02087	0.05151	0.59480
5	0.01773	0.05404	0.67188
6	0.00705	0.02350	0.70000
7	0.00470	0.01704	0.72436
8	/	/	/
9	0.02129	0.03617	0.41139
10	0.02161	0.03863	0.44058
11	0.01985	0.03231	0.38565
12	/	/	/
1 µg TCP/g dry food			
13	0.05142	0.07219	0.28772
14	0.04398	0.06122	0.28161
15	0.05981	0.07662	0.21935
16	0.07773	0.09752	0.20295
17	0.01625	0.02223	0.26908
18	0.03244	0.04322	0.24926
19	0.02391	0.03631	0.34156
20	0.03963	0.05321	0.25519
21	0.03498	0.04207	0.16860
22	0.01494	0.01995	0.25121
23	0.05893	0.07786	0.24312
24	/	/	/
10 µg TCP/g dry food			
25	0.00280	0.04118	0.93197
26	0.03928	0.06723	0.41576
27	0.04589	0.08141	0.43632
28	0.03424	0.04678	0.26814
29	0.06904	0.07838	0.11919
30	/	/	/
31	0.03274	0.04306	0.23974
32	0.02178	0.03215	0.32258
33	0.04660	0.05632	0.17261
34	0.04629	0.05886	0.21359
35	0.03757	0.05711	0.34202
36	0.04646	0.06391	0.27311
50 µg TCP/g dry food			
37	0.05349	0.07576	0.29388
38	0.03723	0.07186	0.48193
39	0.02358	0.03457	0.31788
40	/	/	/

.....continuation of Table 29: Faecal pellets production (in mg/mg fresh body wt./day), consumption rate (in mg leaves/mg fresh body wt./day) and assimilation efficiency (in mg food consumed – mg faeces/mg food consumed) for **P. scaber** *exposed for 14 days (control, 1 µg/g, 10 µg/g, 50 µg/g and 100 µg/g) for TCP.*

nr.	FPP (faecal pellets production)	CR (consumption rate)	AE (assimilation efficiency)
41	0.00685	0.02323	0.70520
42	/	/	/
43	0.02313	0.04344	0.46765
44	0.00687	0.02227	0.69164
45	0.02023	0.03176	0.36288
46	0.02235	0.04219	0.47030
47	/	/	/
48	/	/	/
100 µg TCP/g dry food			
49	0.03676	0.06618	0.44444
50	0.01302	0.04301	0.69725
51	0.01847	0.03709	0.50206
52	0.02624	0.04106	0.36095
53	0.03050	0.05512	0.44658
54	0.01192	0.02517	0.52632
55	0.02371	0.04403	0.46154
56	0.05206	0.07066	0.26316
57	0.03503	0.05334	0.34335
58	0.01245	0.02775	0.55116
59	0.03713	0.07169	0.48201
60	/	/	/

Table 30: Calculated values of lipid peroxidation (normalised) and absorbance values (in AU) for MDA-TBA product (535 nm), non-specific turbidity correction (600 nm) and protein content (280 nm) of P. scaber *exposed for 14 days (control, 1 µg/g, 10 µg/g, 50 µg/g and 100 µg/g) for IMP.*

Note: Pink colour denotes the concentration of used chemical, gray colour denotes dead animals, blue colour denotes eliminated animals with juveniles.

nr.	A (535 nm)	A (600 nm)	A (280 nm)	LP (lipid peroxidation)
control group				
1	0.003	0.001	1.818	1.50713
2	0.001	0	2.018	0.67888
3	0.002	0.001	2.194	0.62442
4	0	0	2.018	0
5	0.003	0.001	1.905	1.43830
6	0.001	0	2.013	0.68057
7	0.002	0	2.080	1.31729
8	/	/	/	/
9	0.003	0.001	2.252	1.21668
10	0.004	0.003	2.173	0.63046
11	0.005	0.002	2.156	1.90628
12	/	/	/	/
1 µg TCP/g dry food				
13	0.002	0.001	1.910	0.71727
14	0.005	0.002	2.016	2.03866
15	0.003	0.001	1.643	1.66766
16	0.006	0.003	1.543	2.66360
17	0.005	0.003	1.359	2.01616
18	0.006	0.002	1.656	3.30913
19	0.005	0.007	1.872	1.46365
20	0.003	0.001	1.639	1.67173
21	0.004	0.002	1.582	1.73196
22	0.003	0.001	1.590	1.72324
23	0.002	0.002	1.180	0
24	/	/	/	/
10 µg TCP/g dry food				
25	0.009	0.004	2.0130	3.40283
26	/	/	/	/
27	0.003	0.001	1.822	1.50382
28	0.007	0.002	2.267	3.02157
29	0.012	0.003	1.576	7.82349
30	/	/	/	/
31	0.007	0.002	1.891	3.62237
32	0.005	0.001	1.473	3.72024
33	0.003	0.001	0.950	2.88417
34	0.004	0.001	1.757	2.33918
35	0.010	0.004	1.143	7.19149
36	0.006	0.003	1.401	2.93357
50 µg TCP/g dry food				
37	0.003	0.001	1.419	1.93091
38	0.006	0.002	1.428	3.83748
39	0.003	0.001	1.650	1.66058
40	/	/	/	/
41	0.004	0.002	1.184	2.31415

nr.	A (535 nm)	A (600 nm)	A (280 nm)	LP (lipid peroxidation)
42	/	/	/	/
43	0.005	0.002	1.719	2.39089
44	0.006	0.002	1.814	3.02090
45	0.001	0.001	1.934	0
46	0.006	0.004	1.861	1.47230
47	/	/	/	/
48	/	/	/	/
100 µg TCP/g dry food				
49	0.004	0.002	2.044	1.34049
50	0.003	0.002	1.643	0.83383
51	0.011	0.003	1.575	6.08880
52	0.004	0.003	1.957	0.70004
53	0.005	0.003	2.018	1.35776
54	0.001	0.001	1.664	0
55	0.006	0.005	1.553	0.88215
56	0.011	0.004	1.804	4.55647
57	0.011	0.005	1.721	4.77900
58	0.005	0.002	1.719	2.39089
59	0.005	0.002	1.665	2.46843
60	/	/	/	/

ANNEX C1

Data for ecotoxicological experiments with *P. scaber* for 6CNA experiment.

Table 31: Leaf weight before and after exposure, faeces mass, body weight of P. scaber *exposed for 14 days (control, 1 μg/g, 10 μg/g, 50 μg/g and 100 μg/g) for 6CNA experiment.*

Note: Pink colour denotes the concentration of used chemical, gray colour denotes dead animals, blue colour denotes eliminated animals with juveniles.

nr.	weight before [mg]	weight after [mg]	WC [mg]	weight before [mg]	weight after [mg]	food consumed [mg]	faeces mass [mg]
	animal			**leaf**			**faeces**
	control group						
1	108.6	91.4	-17.2	98.4	65.0	33.4	29.3
2	27.5	27.0	-0.5	98.7	76.2	22.5	15.5
3	45.0	42.6	-2.4	100.6	80.5	20.1	11.5
4	22.6	/	/	101.2	/		/
5	39.6	38.9	-0.7	101.2	86.4	14.8	7.2
6	29.6	27.8	-1.8	100.6	72.1	28.5	18.3
7	33.4	34.5	1.1	100.3	75.8	24.5	12.8
8	27.5	25.1	-2.4	100.6	88.6	12.0	0.5
9	61.2	62.5	1.3	101.4	86.4	15.0	5.5
10	32.7	28.6	-4.1	101.3	72.4	28.9	17.2
11	26.3	27.1	0.8	101.8	71.6	30.2	12.4
12	33.5	34.0	0.5	101.0	75.0	26.0	14.6
	1 μg 6CNA/g dry food						
13	31.4	30.2	-1.2	101.6	80.8	20.8	8.3
14	85.1	87.7	2.6	100.5	66.5	34.0	19.6
15	20.7	20.5	-0.2	101.4	84.4	17.0	6.3
16	58.9	/	/	98.4	/	/	/
17	29.9	29.3	-0.6	100.5	63.6	36.9	24.2
18	25.0	24.7	-0.3	98.9	83.6	15.3	10.8
19	31.5	30.9	-0.6	101.6	88.2	13.4	7.1
20	38.4	36.9	-1.5	101.7	62.8	38.9	27.6
21	37.9	37.7	-0.2	99.2	69.6	29.6	20.2
22	40.3	/	/	99.9	/		
23	21.1	20.9	-0.2	102.0	74.5	27.5	13.3
24	33.9	33.4	-0.5	101.7	72.1	29.6	14.9
	10 μg 6CNA/g dry food						
25	33.7	/		101.4	/	/	/
226	51.7	56.3	4.6	102.0	92.7	9.3	1.2
27	26.0	25.7	-0.3	100.9	81.4	19.5	10.4
28	51.2	52.7	1.5	100.8	52.7	48.1	28.9
29	28.9	/	/	101.0	/	/	/
30	21.0	24.7	3.7	102.0	59.9	42.1	25.9
31	24.4	27.7	3.3	101.4	72.7	28.7	15.8
32	50.3	/	/	101.1	/	/	/
33	32.5	33.0	0.5	99.6	81.2	18.4	7.3
34	40.1	39.7	-0.4	101.4	72.7	28.7	16.4
35	28.1	28.0	-0.1	99.1	78.0	21.1	13.9
36	36.5	35.1	-1.4	100.5	71.3	29.2	16.0

.....continuation of Table 31: Leaf weight before and after exposure, faeces mass, body weight of P. scaber *exposed for 14 days (control, 1 μg/g, 10 μg/g, 50 μg/g and 100 μg/g) for 6CNA experiment.*

	animal			leaf			faeces
nr.	weight before [mg]	weight after [mg]	WC [mg]	weight before [mg]	weight after [mg]	WC [mg]	faeces mass [mg]
50 μg 6CNA/g dry food							
37	44.8	40.4	-4.4	98.0	81.1	16.9	11.4
38	26.5	22.5	-4.0	101	86.4	14.6	6.1
39	40.2	34.3	-5.9	101	82.7	18.3	7.6
40	22.5	18.9	-3.6	101.7	83.3	18.4	9.1
41	44.7	49.3	4.6	100.3	60.1	40.2	28.6
42	26.0	25.0	-1.0	102.0	85.8	16.2	7.3
43	24.4	31.8	7.4	98.1	69.4	28.7	19.2
44	74.0	67.3	-6.7	99.7	87.1	12.6	3.2
45	28.0	32.5	4.5	99.5	65.3	34.2	25.2
46	49.9	/	/	101.2	/	/	/
47	26.9	25.0	-1.9	101.1	79.4	21.7	14.0
48	33.3	30.1	-3.2	99.8	68.3	31.5	18.2
100 μg 6CNA/g dry food							
49	67.2	70.5	3.3	100.2	70.5	29.7	17.9
50	35.4	33.6	-1.8	99.7	84.1	15.6	3.7
51	24.8	29.5	4.7	101.9	48.7	53.2	38.3
52	27.8	/	/	98.2	/	/	/
53	36.4	37.9	1.5	101.2	67.8	33.4	24.7
54	32.8	31.3	-1.5	101.1	83.3	17.8	4.4
55	32.2	30.8	-1.4	100.4	81.9	18.5	8.6
56	35.9	35.5	-0.4	98.6	57.1	41.5	28.6
57	44.6	48.6	4.0	99.3	59.0	40.3	27.9
58	29.5	28.9	-0.6	99.6	65.0	34.6	26.2
59	30.2	/	/	101.0	/	/	/
60	23.1	22.0	-1.1	100.5	73.5	27.0	1.02

Table 32: Faecal pellets production (in mg/mg fresh body wt./day), consumption rate (in mg leaves/mg fresh body wt./day) and assimilation efficiency (in mg food consumed – mg faeces/mg food consumed) for **P. scaber** *exposed for 14 days (control, 1 µg/g, 10 µg/g, 50 µg/g and 100 µg/g) for 6CNA experiment.*

Note: Pink colour denotes the concentration of used chemical, gray colour denotes dead animals, blue colour denotes eliminated animals with juveniles.

nr.	FPP (faecal pellets production)	CR (consumption rate)	AE (assimilation efficiency)
control group			
1	0.02209	0.02610	0.12275
2	0.04101	0.05952	0.31111
3	0.01928	0.03370	0.42786
4	/	/	/
5	0.01322	0.02718	0.51351
6	0.04702	0.07323	0.35789
7	0.02650	0.05072	0.47755
8	0.00142	0.03415	0.95833
9	0.00629	0.01714	0.63333
10	0.04296	0.07218	0.40484
11	0.03268	0.07960	0.58940
12	0.03067	0.05462	0.43846
1 µg 6CNA/g dry food			
13	0.01963	0.04920	0.60096
14	0.01596	0.01043	0.42353
15	0.02195	0.05923	0.62941
16	/	/	/
17	0.05900	0.08996	0.34417
18	0.03123	0.04425	0.29412
19	0.01641	0.03098	0.47015
20	0.05343	0.07530	0.29049
21	0.03827	0.05608	0.31757
22	/	/	/
23	0.04545	0.09398	0.51636
24	0.03186	0.06330	0.49662
10 µg 6CNA/g dry food			
25	/	/	/
26	0.00152	0.01180	0.87097
27	0.02890	0.05420	0.46667
28	0.03917	0.06519	0.39917
29	/	/	/
30	0.07490	0.12175	0.38480
31	0.04074	0.07401	0.44948
32	/	/	/
33	0.01580	0.03983	0.60326
34	0.02951	0.05164	0.42857
35	0.03546	0.05383	0.34123
36	0.03256	0.05942	0.45205
50 µg 6CNA/g dry food			
37	0.02016	0.02988	0.32544
38	0.01937	0.04635	0.58219
39	0.01583	0.03811	0.58470
40	0.03439	0.06954	0.50543

.....continuation of Table 32: Faecal pellets production (in mg/mg fresh body wt./day), consumption rate (in mg leaves/mg fresh body wt./day) and assimilation efficiency (in mg food consumed – mg faeces/mg food consumed) for **P. scaber** *exposed for 14 days (control, 1 μg/g, 10 μg/g, 50 μg/g and 100 μg/g) for 6CNA experiment.*

nr.	FPP (faecal pellets production)	CR (consumption rate)	AE (assimilation efficiency)
41	0.04144	0.05824	0.28856
42	0.02086	0.04629	0.54938
43	0.04313	0.06447	0.33101
44	0.00340	0.01337	0.74603
45	0.05538	0.07516	0.26316
46			
47	0.04000	0.06200	0.35484
48	0.04319	0.07475	0.42222
100 μg 6CNA/g dry food			
49	0.01814	0.03009	0.39731
50	0.00787	0.03316	0.76282
51	0.09274	0.12881	0.28008
52	/	/	/
53	0.04655	0.06295	0.26048
54	0.01004	0.04062	0.75281
55	0.01994	0.04290	0.53514
56	0.05755	0.08350	0.31084
57	0.04101	0.05923	0.30769
58	0.06476	0.08552	0.24277
59	/	/	/
60	0.03896	0.08766	0.55556

Table 33: Calculated values of lipid peroxidation (normalised) and absorbance values (in AU) for MDA-TBA product (535 nm), non-specific turbidity correction (600 nm) and protein content (280 nm) of P. scaber *exposed for 14 days (control, 1 µg/g, 10 µg/g, 50 µg/g and 100 µg/g) for 6CNA experiment.*

Note: Pink colour denotes the concentration of used chemical, gray colour denotes dead animals, blue colour denotes eliminated animals with juveniles.

nr.	A (535 nm)	A (600 nm)	A (280 nm)	LP (lipid peroxidation)
control group				
1	/	/	/	/
2	0.004	-0.002	0.094	0.90244
3	0.004	0.001	0.041	1.03451
4	/	/	/	/
5	0.022	0.001	0.147	2.21211
6	0.007	0.002	0.041	1.72418
7	0.015	0.002	0.204	0.90097
8	0.006	0.001	0.213	0.46464
9	/	/	/	/
10	0.007	0	0.168	0.58909
11	0.007	0.002	0.102	0.69305
	0.004	0.002	0.059	0.47926
1 µg 6CNA/g dry food				
13	0.002	-0.003	0.153	0.46204
14	0.024	0.003	0.135	2.19929
15	0.020	0.003	0.170	1.41383
16	/	/	/	/
17	0.012	0.003	0.139	0.91543
18	0.006	-0.002	0.297	0.38083
19	0.008	0.004	0.261	0.21668
20	0.006	-0.001	0.251	0.39429
21	0.013	-0.001	0.513	0.38584
22	/	/	/	/
23	0.016	0.003	0.141	1.30353
24	0.019	0.001	0.249	1.02204
10 µg 6CNA/g dry food				
25	/	/	/	/
26	0.032	0.005	0.188	2.03050
27	0.009	0.002	0.126	0.78546
28	0.031	0	0.124	3.53457
29	/	/	/	/
30	0	-0.002	0.105	0.26930
31	0.005	-0.002	0.143	0.69208
32	/	/	/	/
33	0	-0.002	0.129	0.21920
34	0.002	-0.002	0.270	0.20946
35	0.012	0.003	0.129	0.98639
36	0.011	0.001	0.118	1.19816
50 µg 6CNA/g dry food				
37	0.007	0	0.172	0.57539
38	0.002	-0.001	0.070	0.60593
39	0.012	-0.001	0.125	1.47038
40	0.001	-0.002	0.192	0.22091
41	0.004	-0.001	0.239	0.29578

.....continuation of Table 33: Calculated values of lipid peroxidation (normalised) and absorbance values (in AU) for MDA-TBA product (535 nm), non-specific turbidity correction (600 nm) and protein content (280 nm) of P. scaber *exposed for 14 days (control, 1 μg/g, 10 μg/g, 50 μg/g and 100 μg/g) for 6CNA experiment.*

nr.	A (535 nm)	A (600 nm)	A (280 nm)	LP (lipid peroxidation)
42	0.013	-0.002	0.261	0.81254
43	0.025	0.015	0.230	0.61471
44	0.054	0.015	0.103	5.35333
45	0.032	0.005	0.122	3.12896
46	/	/	/	/
47	0.014	0.004	0.191	0.74022
48	0.015	0.003	0.209	0.81177
100 μg 6CNA/g dry food				
49	0.012	0.002	0.019	7.44120
50	0.039	0.004	0.090	5.49822
51	0.032	0.002	0.102	4.15832
52	/	/	/	/
53	0	-0.002	0.168	0.16831
54	0.007	0	0.110	0.89971
55	0.001	-0.002	0.172	0.24660
56	0.013	0	0.260	0.70691
57	0.035	-0.002	0.114	4.58874
58	0.009	0.002	0.092	1.07574
59	/	/	/	/
60	0.027	0.003	0.152	2.23236